Microwave mild hyperthermia applicators for chemo-thermotherapy of liver

By

Mustafa Asili

A Dissertation
Submitted to the Faculty of
Mississippi State University
in Partial Fulfillment of the Requirements
for the Degree of Doctor of Philosophy
in Electrical and Computer Engineering
in the Department of Electrical and Computer Engineering

Mississippi State, Mississippi

August 2016

Microwave mild hyperthermia applicators for chemo-thermotherapy of liver

By

Mustafa Asili

Approved:

_____

J. Patrick Donohoe
(Major Professor)

_____

Erdem Topsakal
(Director of Dissertation)

_____

Nicolas H. Younan
(Committee Member)

_____

John E. Ball
(Committee Member)

_____

James E. Fowler
(Graduate Coordinator)

_____

Jason M. Keith
Dean
Bagley College of Engineering

Name: Mustafa Asili

Date of Degree: August 12, 2016

Institution: Mississippi State University

Major Field: Electrical and Computer Engineering

Director of Dissertation: Erdem Topsakal

Title of Study: Microwave mild hyperthermia applicators for chemo-thermotherapy of liver

Pages in Study 100

Candidate for Degree of Doctor of Philosophy

Increasing demands for hyperthermia (HT) as an adjuvant therapy is caused from the contributions of thermal therapy to the traditional treatments. Latest improvements in hyperthermia make it popular among thermal therapies to cure cancer in any organ or body parts. HT takes advantage of EM radiation inside the tumor that provides temperature and blood perfusion increment that helps radiation therapy and chemotherapy to be more efficient. Therefore, some advantages makes HT preferred when compared to similar treatments. Being noninvasive and painless with an efficient cooling system, and helping to shorten the application period and session number of conventional treatments are most important advantages of HT. However, existing HT systems require high input power per elements on the applicators and long application time. Designing conformal and patient specific applicators with mild application can solve this issue. Moreover, mild HT application can make cancer treatment cheaper and more accessible.

The main goal in this study is to design conformal HT applicators through optimization for liver and provide a patient specific and cost-effective local hyperthermia

treatment that can be widely used in local clinical cancer treatment centers without expensive applicators.

DEDICATION

To my son, wife, and parents

ACKNOWLEDGEMENTS

I would like to express my deepest appreciation to Dr. Erdem Topsakal for his guidance and effort to encourage and support during my graduate studies. I would like to thank Dr. J. Patrick Donohoe for his contributions and sharing the responsibility of supporting and advising me after Dr. Topsakal left. I would also like to thank Dr. Nicolas H. Younan and Dr. John E. Ball for serving on my committee.

TABLE OF CONTENTS

LIST OF TABLES

LIST OF FIGURES

CHAPTER I

INTRODUCTION

1.1 A Brief Overview

Principles of electromagnetics (EM) and antennas have been used in medical treatments for many years. Promising results have kept scientists investigating the advantages and effects of EM in medicine. Thermal therapies especially require extensive application of EM and antennas. Directed EM waves are used to heat cancerous cells in the tissue. In this dissertation, I design microwave (MW) antenna arrays for hyperthermia applicators to heat the tissue and enable thermal treatment.

Existing hyperthermia systems use bulky whole body applicators. There is no available applicator for a specific organs like breast, the liver etc. Current systems also require a shielded room because of high input power per element on the applicator thus increasing treatment cost. Therefore, there is an increasing demand for local hyperthermia applicators that are aimed at a specific organ instead of whole body.

For this purpose, I am designing a MW mild-hyperthermia applicator for the liver. This applicator requires low input power for each MW antenna on the applicator that eliminates higher costs. It is small and conformal, somehing that also decreases the cost of the treatment, and increases the efficiency of the input power by focusing on the specified organ.

My main goal is to provide a patient specific and cost-effective local hyperthermia treatment that can be widely used in local clinical cancer treatment centers without expensive applicators.

1.2 Thermal Therapies

Nowadays, discovering a non-invasive and economical cure is the main challenge in medicine for cancer treatment. Applications of electromagnetics in medicine are gaining more importance. Technologies related to electromagnetics such as monitoring and imaging have already been used for decades. Thermal therapy is one of the most intensive areas as an application of electromagnetics and antennas in medicine. Recently, the diagnosis and treatment techniques for cancer have improved greatly because the most common threat for human health is rapidly growing malignant tumors [1, 2]. The traditional treatments of cancer cells are chemotherapy (CT), radiation therapy (RT) and surgery; however, all of these treatments have strong side effects and clinical limitations. Thus, researchers are in need of adjuvant therapy to decrease the side effects and duration of the treatments. At this point, thermal treatments such as ablation and hyperthermia can be considered as the best adjuvant therapies.

1.2.1 Ablation

The main description of tumor ablation is to exterminate the cancerous tissue by applying any clinical treatment techniques. However, the disadvantages and invasive nature of current techniques make the doctors and researchers search for adjunctive treatment. For instance, some tumors cannot be cleaned off completely with surgical resection due to the placement of the cancerous cells inside the organ. This results in

leaving a part of the tumor inside the body and may lead to further growth of the unhealthy cells. Today, thermal therapies – ablation and hyperthermia – are popular as an adjunct method. There are quite convincing developments that show the advantages and simplicity of thermal therapies. One of the main purposes of thermal therapies is not to damage normal tissue while killing the unhealthy one.

Thermal ablation is one of the types of thermal therapies. It can be defined as destroying tumor cells using electromagnetic (EM) energy or heat. There are many ablation modalities mentioned in literature. Cyroablation, laser ablation, ultrasound ablation, radiofrequency (RF) ablation, and MW ablation are some of these techniques. Recently applied ablation techniques already meet the desired criteria. MW ablation, which is a minimally invasive method, eliminates the disadvantages of other techniques and is in the limelight. Moreover, it is open to improvements by new clinical trials and experiments. Early results of this technique can be obtained in [4,5] and show that the success of the treatment depends on the size of the tumor.

Before MW ablation, RF was used for the same purpose due to its simplicity and effectiveness [22]. The disadvantages of this technique are high input power levels and ground pad requirement to allow AC current moving in a complete circuit. While applying RF ablation, tissue is considered as a circuit component; however, it is not perfect in terms of conduction. Therefore, RF ablation causes resistive heating. Since resistive heating only affects the superficial tissue, temperature can be increased by conductive heating in deep tissue tumors [25]. During the application, degradation in water content causes death in tissue due to coagulation necrosis at high temperatures

(>50°C) [10, 15]. Figure 1.1 shows what the simplified system looks like with applicator, ground pad, and generator [104] for RF ablation.

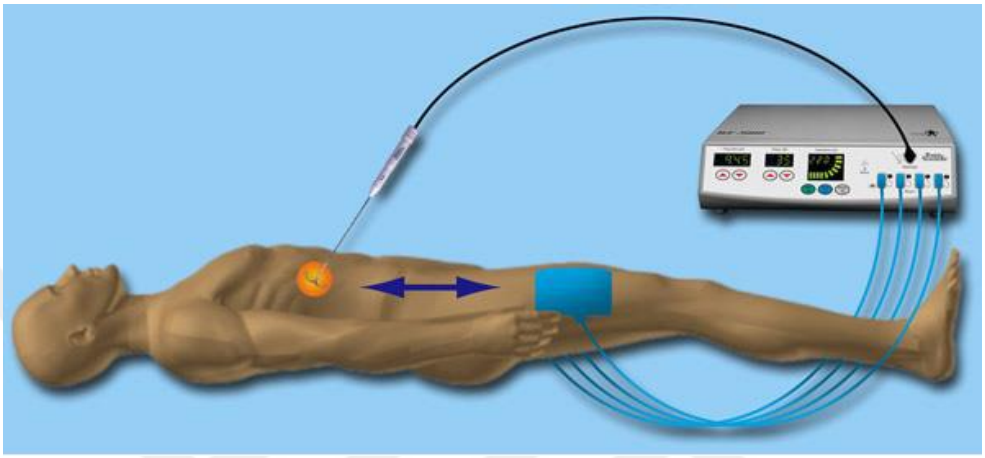

Figure 1.1 Simplified RF ablation system

RF ablation may be superior to the previous techniques, but it also has some disadvantages associated with the procedure. A single probe can be used due to the nature of the procedure (electric current conduction). This means that the ablation zone cannot be increased with multiple probes. Moreover, application of electrical current can result in heating of tissue. This causes changes in cells including protein denaturation and water loss. Therefore, the tissue becomes more resistant to the current. Water loss causes this impedance increment that limits ablation zone size after 100 °C (Figure 1.2) [3, 27, 28, 29]. Thus, monitoring tissue impedance during the treatment is used to indicate the completion of ablation. Furthermore, one of the most important problems is skin burns due to the ground pad. These undesired results have shifted attention from RF to MW ablation.

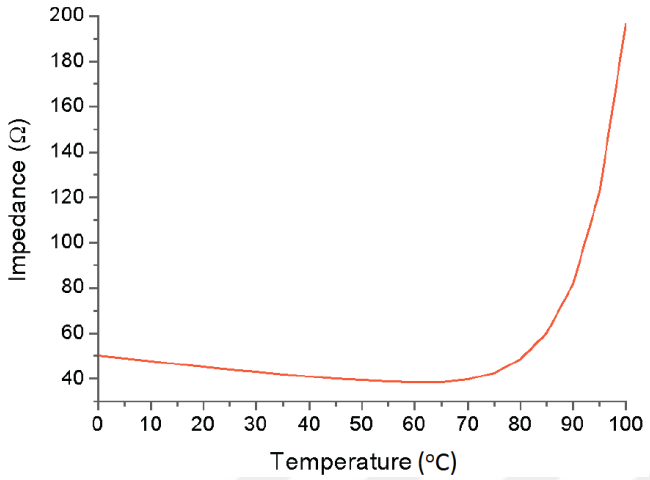

Figure 1.2 Change in impedance with increasing temperature

MW ablation emerged as an alternative method to eliminate the disadvantages of RF ablation. It relies on the propagation of EM energy instead of the flow of electrical current which helps to minimize the pain. Moreover, the nature of EM waves provides rapid uniform heating with energy focused inside the target tissue. The first clinical application of MW ablation was performed in Japan in 1990s [4]. In the United States, the first MW ablation operation was perfomed a decade later at 915 MHz [31]. The Federal Communications Commission (FCC) allowed for only two frequency bands for ablation applications (915 MHz and 2.4 GHz).

The main advantages of MW ablation are providing adjustable ablation zone by manipulating the amplitude and phase of the input power and using multiple probes unlike RF ablation. Furthermore, it does not require a grounding pad which causes skin burns. The probes (MW applicator) are directly applied to the target to create an ablation zone in surrounding tissue. Regular MW ablation equipment and the sample application

from University of California can be seen in the Figure 1.3 [1] and Figure 1.4 [33] respectively. The system includes probes, generators and monitoring equipment.

Figure 1.3 MW ablation system a) probes, b) applicators connected to signal source

Figure 1.4 MW ablation in UC, San Diego, 2009

MW ablation is superior to RF ablation. It provides larger zones with higher temperature at deeper tissue. MW ablation also requires less input power as it is less

dependent on tissue conductivity. Moreover, multiple probe usage is available for this method to increase the ablation zone. Figure 1.5 shows the difference between temperature increase when RF and MW ablation is applied with 200W and 60W input power, respectively. Figure 1.2 and Figure 1.5 indicate that since RF ablation is based on the flow of electrical current, when the impedance increases, the system behavior tend to that of an open circuit. Therefore, temperature increase is not possible inside the tissue after a certain time. However, MW ablation provides continuous temperature increase, since it depends on the propagation of EM waves [123].

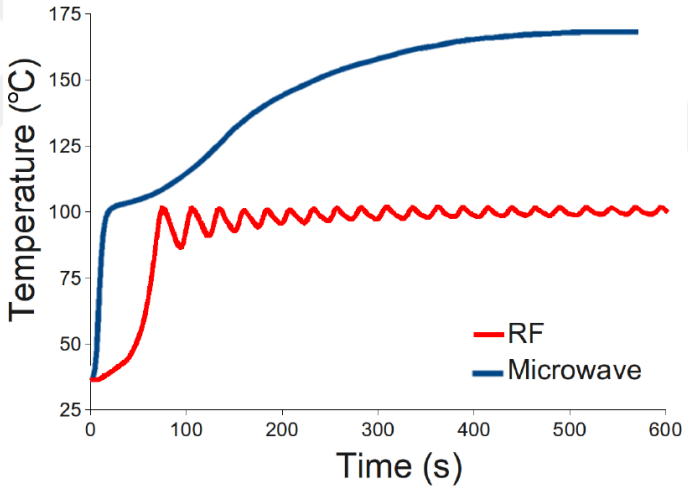

Figure 1.5 Temperature vs Time during RF and MW ablation

Although current MW ablation systems provide better results than RF ablation systems, they have an important problem: the narrow band nature of the antennas used in the applicator. Generally, slot and/or dipole antennas (narrow band antennas) are used for the probes (Figure 1.6). Therefore, while temperature increases, dielectric properties of the tissue change due to water loss. Since the antenna is designed and optimized

according to the specific dielectric properties that affects the operating frequency, this change shifts resonation frequency of the antenna and causes undesired power reflection from the load. Moreover, the stalk of the probe causes tail heating due to power reflection and mismatch (Figure 1.7 [122] – 1.9).

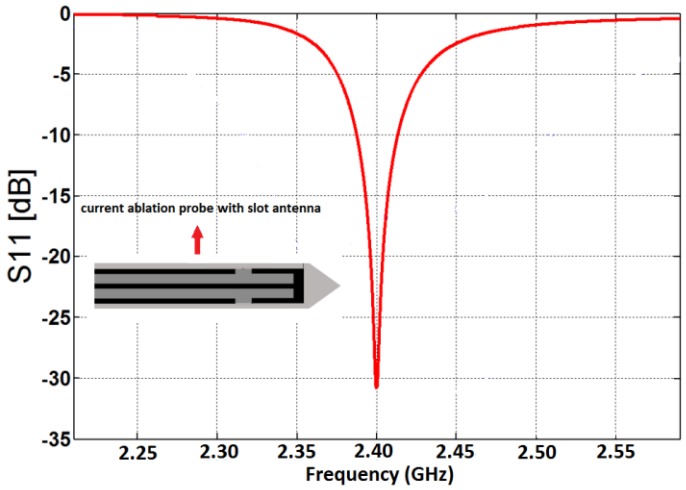

Figure 1.6 S_{11} of a narrow band slot antenna

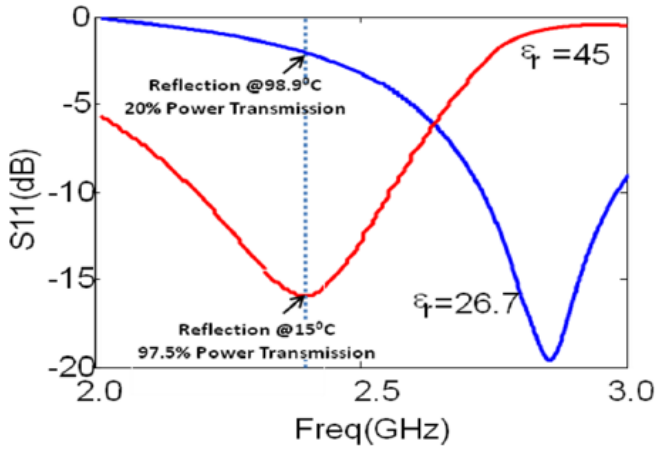

Figure 1.7 Effect of heat on power transmission at 2.4 GHz (red: normal, blue: shifted)

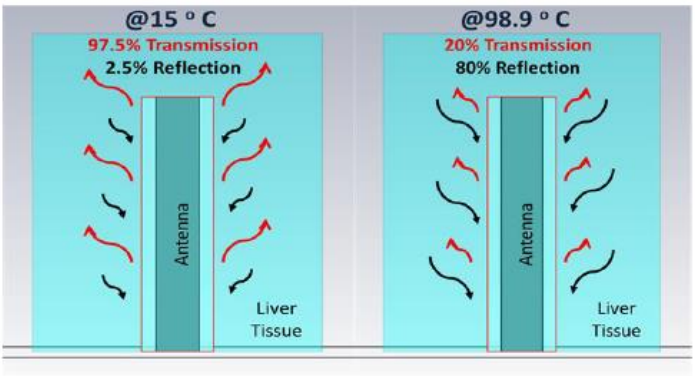

Figure 1.8 Power transmission while heating up the liver tissue

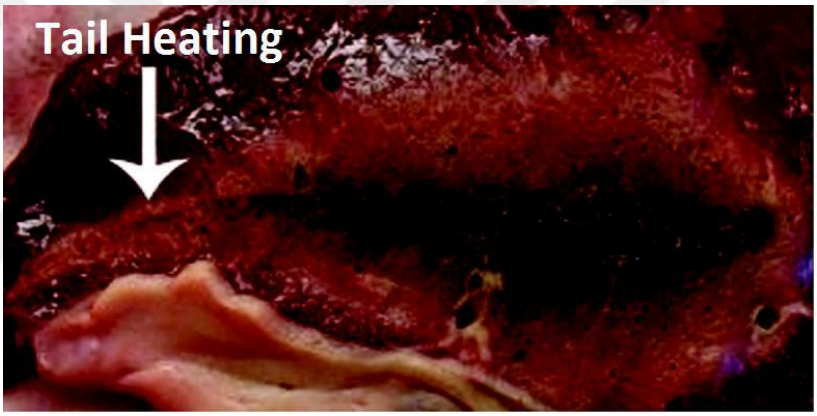

Figure 1.9 Tail heating during RF ablation

In order to overcome the frequency shift and the power reflection problem, I designed a wide band MW antenna for ablation applicator. In this way, even with frequency shifts, power transmission levels are satisfactory (at least 95% transmission) to continue the treament. The fabricated ablation probe and its reflection coefficient value can be seen in Figure 1.10. Experiment setup and *ex-vivo* experiment results of our probe can also be seen in Figure 1.11 and Figure 1.12 – 1.13, respectively.

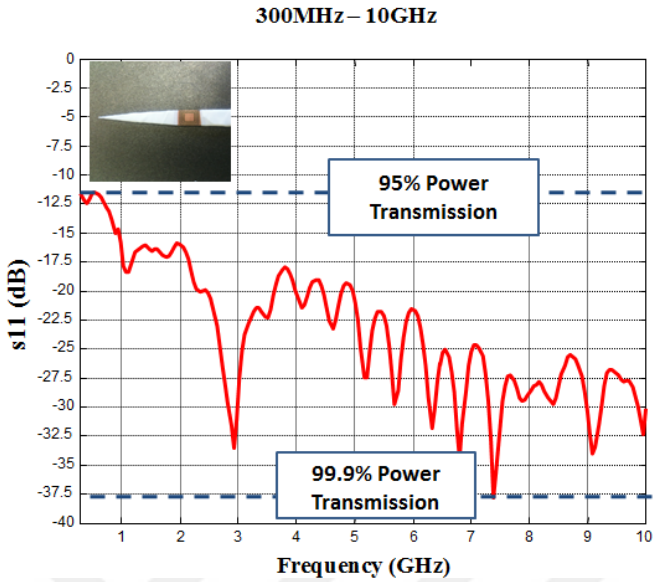

Figure 1.10 Reflection coefficient (S_{11}) of the fabricated wide band probe (300 MHz – 10 GHz)

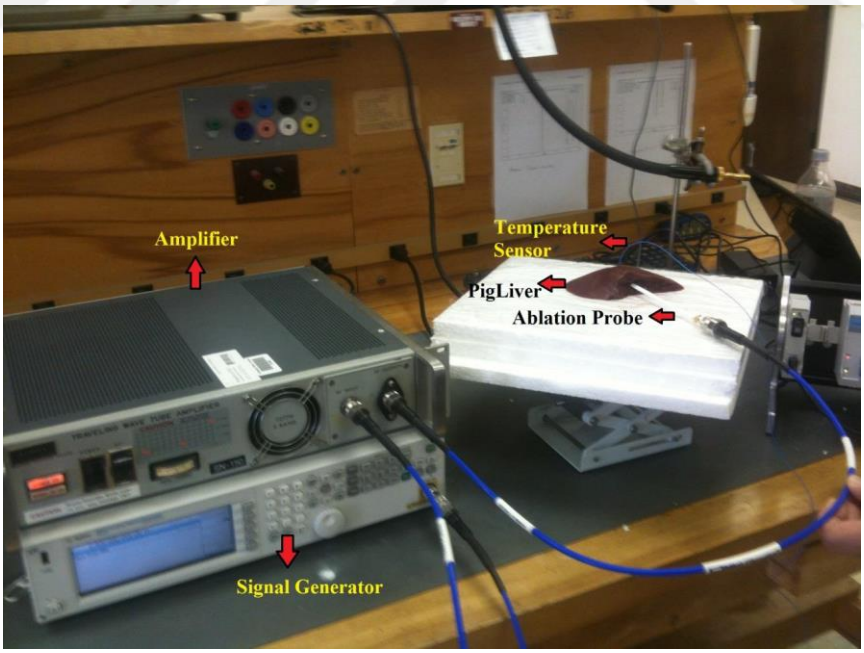

Figure 1.11 Experiment setup for MW ablation

Figure 1.12 2.4 GHz MW ablation result in porcine liver

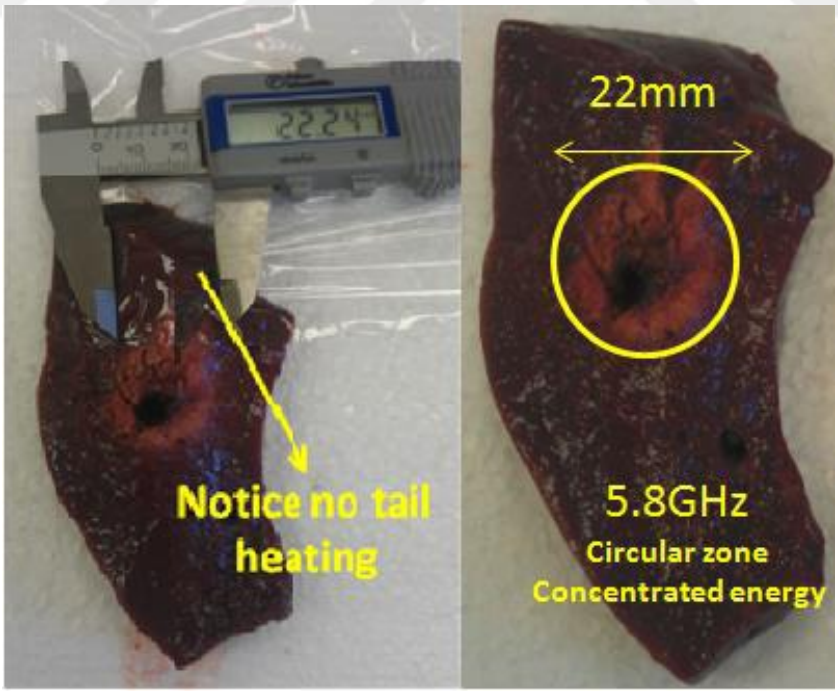

Figure 1.13 5.8 GHz MW ablation result in porcine liver

1.2.2 Hyperthermia

Hyperthermia (HT), a medical treatment technique of cancer [6-8], heats the malignant cells inside the tissue by using EM energy at radio or MW frequencies with sufficient input power (~100W) to cure the tumor. Frequencies used for treatment are mostly 2.4 GHz and 915 MHz (HT1 8-15). Thermal therapies aim to kill tumor cells without damaging the healthy cells. Current HT and ablation techniques are minimally invasive. The difference between ablation and HT is that the applicator of HT is placed on the surface of the body instead of directly applied to the tumor.

There are three hyperthermia types: local hyperthermia (LH), regional hyperthermia (RH), and whole body hyperthermia (WBH). LH is used to heat a small area of any organ with directed energy, and RH is applied for large areas on the body. LH is generally used to treat the tumors close to the surface (skin), while RH is applied to large body parts like breasts, arms and feet. WBH is the process of heating the entire body. For all types of hyperthermia treatments, microwave (MW) or RF antennas are used to deposit EM waves into the cancerous cells.

In the early history of HT, tissue temperature could be elevated 20 ^{o}C above body temperature. This means that tissue temperature could go up to 60 ^{o}C, which destroys healthy cells, too. HT studies on animals began in the early 1900's [9-12]. Studies done by Muller [46] and Warren [47] are known as the earliest clinical applications of hyperthermia in 1910 and 1935, respectively. Relatively low temperatures, which can selectively damage cancer cells, were also used during these years [13]. This research shows the preliminary effect of thermal therapy on the treatment of cancer when combined with conventional treatments. Further studies have proven the efficiency and

positive effect of HT as an adjuvant therapy on many cancer types [17-45]. According to all experiments, tests, and studies, researchers investigated that HT causes apoptosis above 45 °C. More recent studies show that heating tissue more than 45 °C and holding this temperature for approximately 60 minutes can damage cancerous cells significantly with minimal side effects [14-17]. At this temperature, tumor cells cannot tolerate the exposure to heat in contrast to benign cells because of low blood flow volume and vascularization in tumors [18]. For HT, there are two important parameters, blood flow and thermo-tolerance, that need to be considered to determine the heat distribution inside the tissue. Thermo-tolerance should be considered when multiple HT fraction is needed because heat sensitivity of the tissue may not return the normal levels before 72 hours [10]. Therefore, it is required to wait long enough before the second dose of the therapy is delivered. The second parameter, blood flow, is the most important one in determining the temperature distribution. Temperature distribution varies between healthy cells and cancerous cells. Studies show that blood perfusion rate in tumors is lower than the normal tissue [19].

It is impossible to achieve high temperature value (> 45°C) without destroying healthy tissue. Thus, it was discovered that HT can be used more efficiently if it is considered as an adjuvant therapy. For adjuvant therapy (mild HT), input power and other high cost requirements can be reduced significantly. Scientists researched and confirmed that HT increases the patients' response to conventional treatments (RT and CT), and enhances tumor perfusion [80-95]. There are many studies and clinical trials done to show the result of combined (RT+HT or CT+RT) therapies for many cancer

types [82, 72, 90, 96]. In that way, the size of HT systems and applicators can be minimized.

The effect of HT on radiation sensitivity and drug delivery was demonstrated by clinical studies in [20-26]. Moreover, according to recent studies, the combination of hyperthermia and traditional treatments enhances the outcome of the therapy in terms of survival rate and complete response [17, 27-37]. Some animal studies on heat-triggered release by using HT can be found in [38, 39] to show the impact of the treatment. In [40], animal studies show the importance of the temperature rise achieved in the tumor in analyzing the success of HT. For the combination of CT and HT, Figure 1.14 [103] shows the effect of HT on the increase in survival rate. Similarly, there is a change in complete response as shown in Figure 1.15 [103] when HT is used as an adjunct therapy with RT [32]. In addition, the recurrence of cancer due to microscopic carcinoma may be prevented during surgical process by heating the tissue before the surgery [28, 41-45].

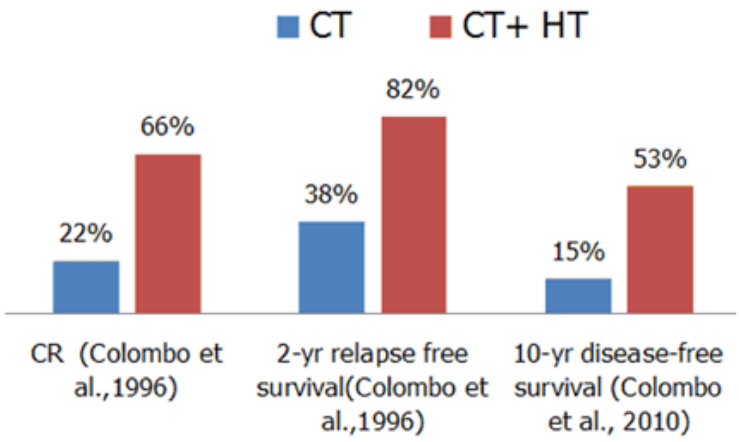

Figure 1.14 Clinical trials for survival rate when CT combined with HT

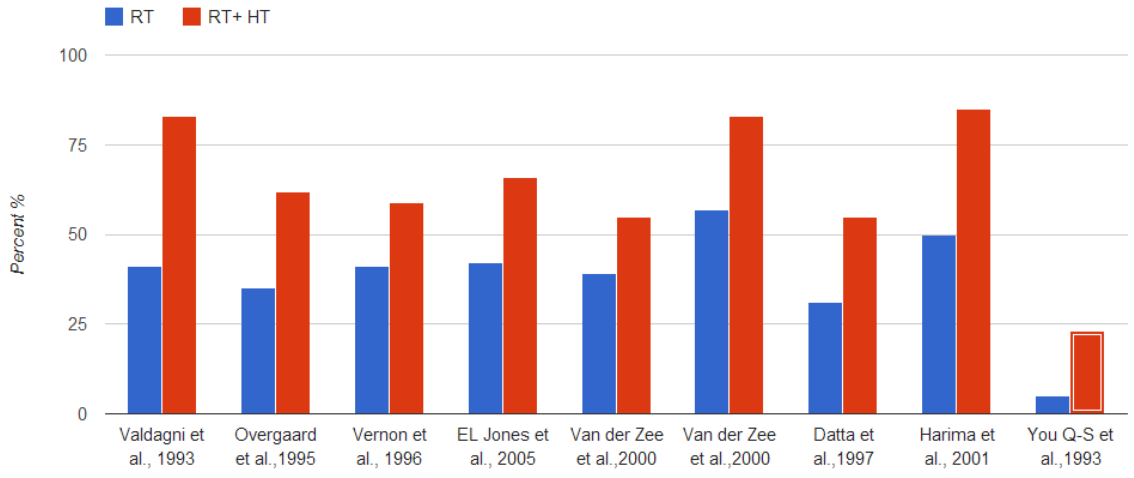

Figure 1.15 Clinical trials for complete response when RT combined with HT

In modern superficial and local HT, the microwave frequency is important because of its penetration ability for deep tissue tumors. Local HT focuses on only heating the tumor. It may be used on any part or organ of the body such as the breast, liver, arm, or head. For both local and surface microwave (MW) HT, electromagnetic energy is deposited through MW antennas [65]. Current HT applicators (BSD-2000 hyperthermia systems- Figure 1.16) uses dipole arrays for energy radiation [66, 67]. Operating frequencies of HT systems range between 0.1 – 2.45 GHz which includes ISM bands with applied power up to 100 Watts [66, 68-79].

Figure 1.16 Commercially available BSD-2000 HT system

Although there are many clinical applications of hyperthermia, uniform heating of an organ or a part of the body and short time applications are still problems [31]. Doctors want to apply this process during the waiting period before chemotherapy and radiation therapy sessions. The fundamental needs of physicians and clinics include less expensive equipment, a specific applicator design process, and short application period lower than 20 minutes. Therefore, research must concentrate on the combinations of antenna arrays with proper low input power for each element in order to get better uniform heating pattern inside the tissue. Another problem is to minimize the size of the equipment and make them patient specific. For this purpose, I designed two different applicators with a different configuration of the MW antennas.

The antenna designed in [100] is used to create the flexible antenna applicator shown in Figure 1.17. It was designed on FR4 substrate, and includes 18 MW antennas. However, for this application, the antenna is fabricated on flexible material (PDMS) and was tested in air and on human breast-mimicking gels (Figure 1.18) that contain skin, fat and fibroglandular layers. As it is seen in Figure 1.20, it resonates at 450 MHz on breast tissue well below -10dB, but does not in air. Figure 1.19 shows the test bench including

the signal generator, amplifier, temperature sensors and the computer used to monitor the temperature changes. The experiment results are also provided in Table 1.1.

The second applicator is designed considering the breast shape. Thus, it is fabricated to be conformal for better fit on realistic shapes of breast mimicking gels. Similarly, PDMS is used as the substrate, but it includes 9 MW elements. The operating frequency of the antennas shifted unexpectedly (Figure 1.24) which may be caused by the shape of the applicator or the fabrication process. This applicator was fabricated by a colleague at Stanford Medical School, so there was no opportunity to modify the fabrication process. Breast mimicking gels used for the measurements, experiment setup, return loss of the antenna, and measurement results are shown in Figure 1.21 – Fig. 24 and Table 1.2, respectively.

Figure 1.17 Microwave antenna applicator printed on a flexible material (PDMS)

Figure 1.18 Breast mimicking gels

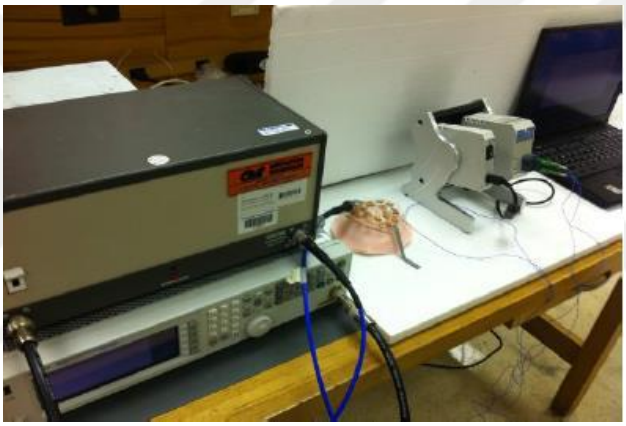

Figure 1.19 Experiment setup for the first HT applicator

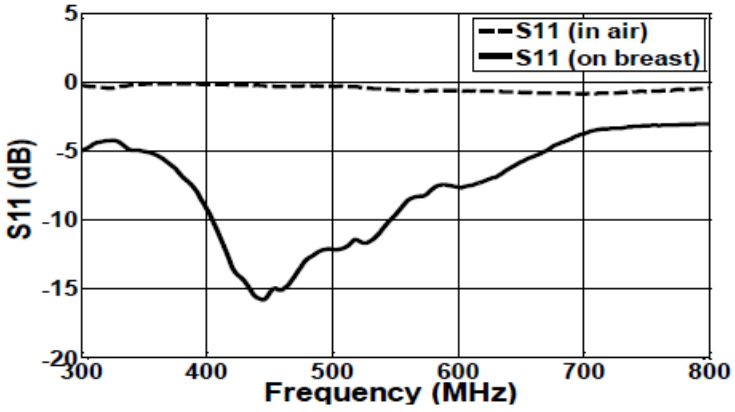

Figure 1.20 S_{11} of the MW antenna on the applicator

Table 1.1 Experiment results for the breast hyperthermia

	1 cm	2.5 cm	4 cm
1W	90 sec / 19 min / 3°C	10 min / 30 min / 1°C	10 min / 25 min / 0.15°C
2W	83 sec / 19 min / 3°C	10 min / 34 min / 1.55°C	10 min / 32 min / 0.313°C
3W	79 sec / 19 min / 3°C	10 min / 49 min / 2.025°C	10 min / 37 min / 0.385°C
4W	66 sec / 19 min / 3°C	10 min / 63 min / 2.4°C	10 min / 48 min / 1°C
5W	60 sec / 19 min / 3°C	10 min / 67 min / 2.644°C	10 min / 60 min / 1.28°C
	duratin of application / cooling time / increment in celcius degree		

According to measurements of the antenna S11 value, tests are performed at 450 MHz and 1.6 GHz for flat and conformal applicators, respectively, and results are shown in Table 1.2 Sufficient temperature increase can be achieved with 2.5W or 5W in 10 minutes in tumors close to the skin's surface. Efficiency of the applicator for deeper tumors can also be improved by utilizing all the antennas on the applicator and increasing the input power with proper equipment and amplifiers. The design process of the applicators will be discussed in the Chapter 3.

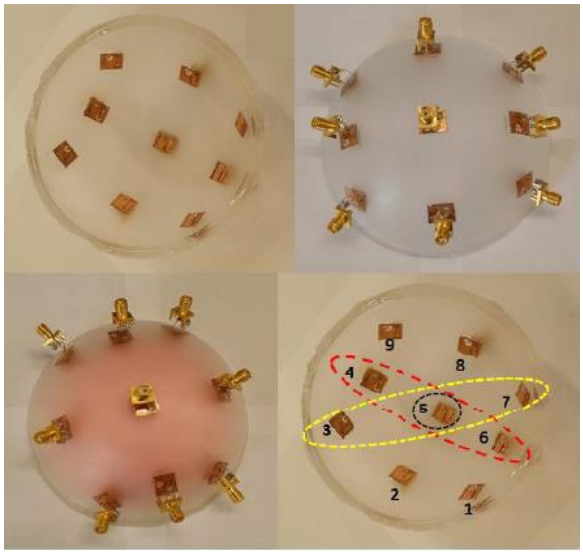

Figure 1.21 Conformal MW HT applicator

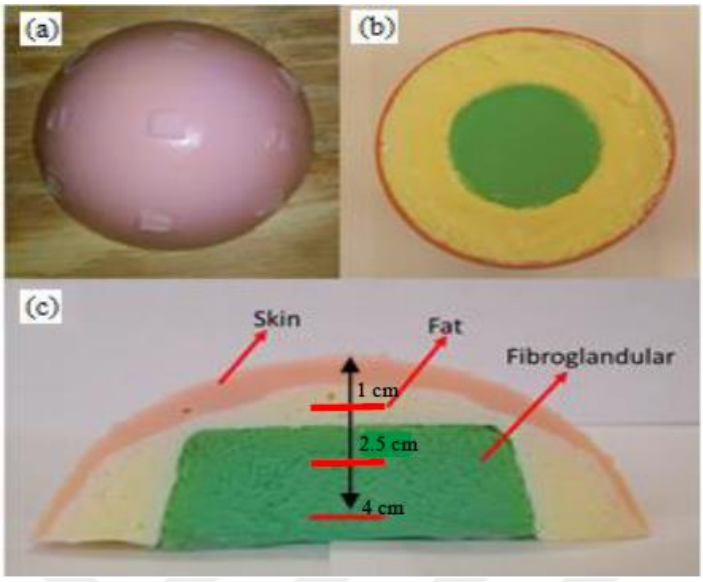

Figure 1.22 Breast mimicking gels used for conformal HT applicator measurements

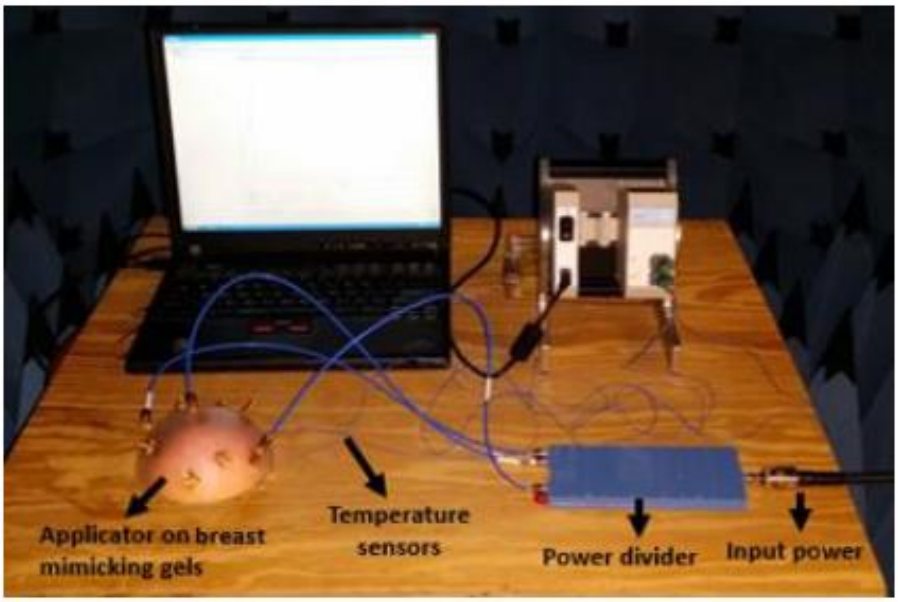

Figure 1.23 Experiment setup for the conformal HT applicator

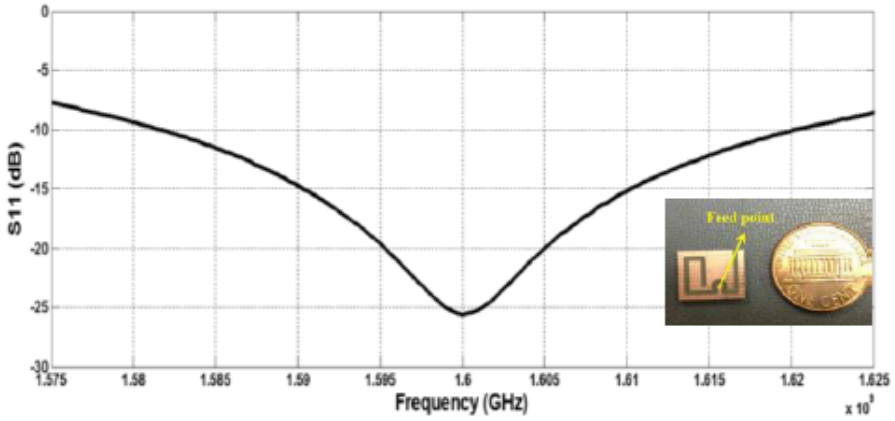

Figure 1.24 S_{11} of the MW antenna on the conformal HT applicator

Table 1.2 Experiment results for the conformal HT applicator

Depth	Antennas	1W	2.5W
1 cm	4, 5, 6	3°C (8min 39s)	3°C (7min 40s)
2.5 cm	4, 5, 6	0.146°C (10min)	0.197°C (10min)
4 cm	4, 5, 6	0.112°C (10min)	0.125°C (10min)

Depth	Antennas	10W input
2.5cm	5	0.872°C (10min)
4cm	5	0.419°C (10min)

In this study, new applicators at 915 MHz and 2.4 GHz were designed for further investigation to meet the demands of doctors and eliminate the disadvantages of current systems. The applicators are designed for liver mild hyperthermia. The applicator was formed with a flexible laminate with high dielectric constant (ε_r=10.2). There are 12 MW antennas located on the substrate. Details of the design process are discussed in Chapter 3.

CHAPTER II

OPTIMIZATION

Optimization is a method that requires mathematical procedures to find maximum or minimum values of a function to resolve the problems. In engineering, it is almost impossible to find a perfect solution. Thus, we seek to determine a solution which converges in an optimal way. This convergence can be done by the trial and error technique (manual method). However, an effective optimization algorithm can search for the best solutions/iterations automatically.

First, a brief description of the general procedure of optimization used in this study is presented. The optimization goal is defined by the objective function which includes the minimum or maximum of the fitness function. The value of the fitness function reflects the optimality of the solution.

Although there are many optimization methods, evolutionary algorithms (EAs) are common techniques used for EM applications. EAs eliminate insufficient solutions and continue iterations with satisfying solutions using natural selection. EAs include evolutionary programming (EP) and GA. Generally EP differs from GA in two ways. First, EP does not use crossover, thus GA provides more diversity. Second, there are no constraints on the representation of EP. For this reason, GA is choosen for this study [120]. Moreover, GA has been applied to many different applications in electromagnetics and engineering since it was introduced [105 – 107].

2.1 Genetic Algorithm (GA)

A genetic algorithm (GA) is a heuristic method which modifies a randomly created population of potential solutions that converge to a local minimum. This step is called initialization. In GA, strings are generally represented in binary numbers. The process starts after the initiation of the population according to fitness value.

GA requires some definitions for understanding the process of the algorithm. First of all, GA is based on the natural selection idea, so it includes biological terms. Chromosomes are the individuals used to generate a population, and each bit in the chromosome is called a gene (Figure 2.1). After the generation of population occurs, the algorithm goes through the following operators: selection, crossover, and mutation.

The selection operator keeps the members of the population if the chromosomes have sufficient fitness values according to the simulation results; otherwise, they are discarded. The sufficiency of each candidate is determined by comparing each calculated value with a preset threshold (temperature interval). Then, the randomly selected pairs of these candidates are used to generate new children, and the mutation operator takes place for diversity if the new generation has identical members. In short, the selection is the operator used to select two individuals for the next operator (crossover). These two individuals are called parents. For the selection procedure, it is important to keep all generated new seed in the population to provide diversity. The selection method used is the roulette wheel selection (RWS) out of several methods mentioned in [99]. This method classifies each chromosome in different groups according to its fitness value, and creates the next generation. The best fit chromosomes will be in the same group. Others will be seperated in three to five different groups from the best fit to the least fit. This

helps to have more members included in the routine, even if they have a lower fitness value. It means that less fit chromosomes can still provide a good result when paired with another chromosome during the optimization.

As previously mentioned, GA uses operators in the routine, including the crossover operator used to create a new and unique generation by pairing parents' genes. Crossover is an operator to create a new individual by mating selected ones by RWS, and a new individual is called an offspring (Figure 2.2). There are two ways to combine two different parents: cutting the chromosomes into two or three pieces from random points. For 2-piece parents, one part from one parent is combined with the second part from another one. For 3-piece parents, two ends of chromosomes are from one parent are combined with the middle part from another parent to generate a new offspring. The rest of the chromosomes are also used to generate another child. In both scenarios, the number of genes remains constant for the new traits, too. Actually, there is no difference between these two options in terms of efficiency. It helps to create better individuals by recombining the selected parents.

The last operator, mutation, generally has very low user-defined probability. It is used to modify offspring by switching the bits, so the diversity can be increased (Figure 2.3). Mutation also occurs to modify the genes if there is duplicate members. This operator takes place until the required population size is achieved depending on the problem type. Termination of the optimization (GA) occurs when initially set criteria are met. It randomly selects a gene from one of the chromosomes and replaces it with another randomly generated gene. If GA is binary-coded, replacing the genes means switching the value from zero to one or vice versa. The frequency of use of this operator is user

defined and normally varies from 1% to 20% [107]. Although the steps explained in GA seem easy, each operator must go through the entire computational process.

Figure 2.1 Gene, chromosome, and population representations

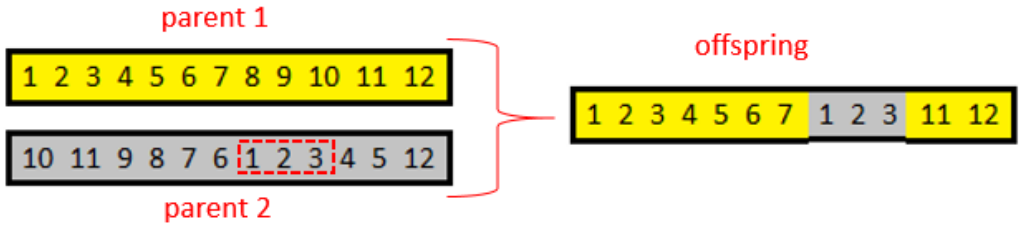

Figure 2.2 Crossover operator

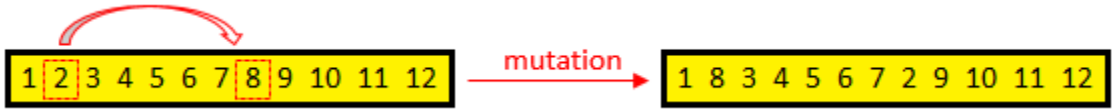

Figure 2.3 Mutation operator

In our case, the problem is finding the minimum input power and optimum phase of the antennas on the microwave HT applicator to provide uniform heat distribution over the tissue volume of interest. The goal of applying GA in our application is to optimize the temperature inside the liver with antennas on pre-defined geometry as a HT applicator. It can be considered as facility-location problems in the literature [97], [98]. P-median problem is known as the most popular facility-location problem and has many applications in engineering [97]. In many electromagnetic applications such as antenna design and optimizations, genetic algorithm (GA) have been applied successfully [101, 102]. Therefore, GA is used to solve the problem at hand. In this study, the location of the MW antennas is fixed before the optimization process begins. Thus, the problem has two antenna variables effecting the the goal (temperature) in the target tissue (liver). These variables are the amplitudes and phased of the MW antennas. After the initialization step, the algorithm runs and progresses to obtain the best values for the variables. For the HT applicator, 12 MW antennas are to be driven optimally to provide a uniform field and the best heating pattern inside the tissue.

GA is implemented in Python which controls the commercially available EM simulation tool CST MWS, providing an automated system. Therefore, no adjustments to the geometry or any simulation settings in CST MWS are required once the optimization process is started. Matlab can also be used as an additional software to skip the opening pop-up window when CST MWS is first run.

CST MWS can be controlled via the Visual BASIC for Application (VBA) scripting language. Thus, the connection of CST MWS and Python requires a VBA interface. When the optimization is started, the GA implemented in Python runs and

writes the fitness value to the text file. Then, it calls VBA to execute a VBA script that includes commands for CST MWS to apply the optimization results to the simulation file. After changes are made to the file, the CST MWS simulation runs and gathers the results, and the results are saved in a text file by VBA script again. Python then takes the control back and compares the results. If the maximum iteration or the goal is achieved, it terminates the loop and saves the results, and gives the best values for the amplitude and phase of the MW antennas on the HT applicators. Flowcharts for connection of both software and the working principle is provided in Figure 2.4 and Figure 2.5, respectively.

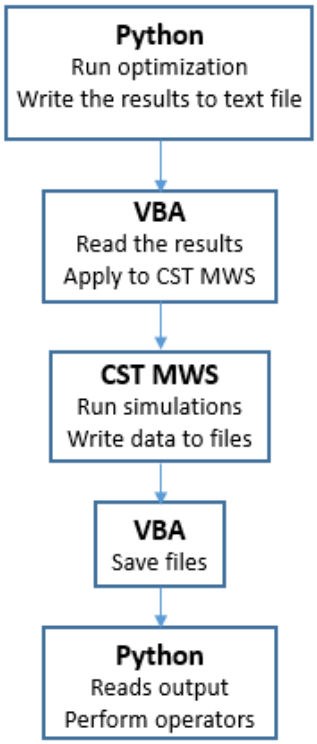

Figure 2.4 Flowchart for connection of Python, CST MWS and VBA

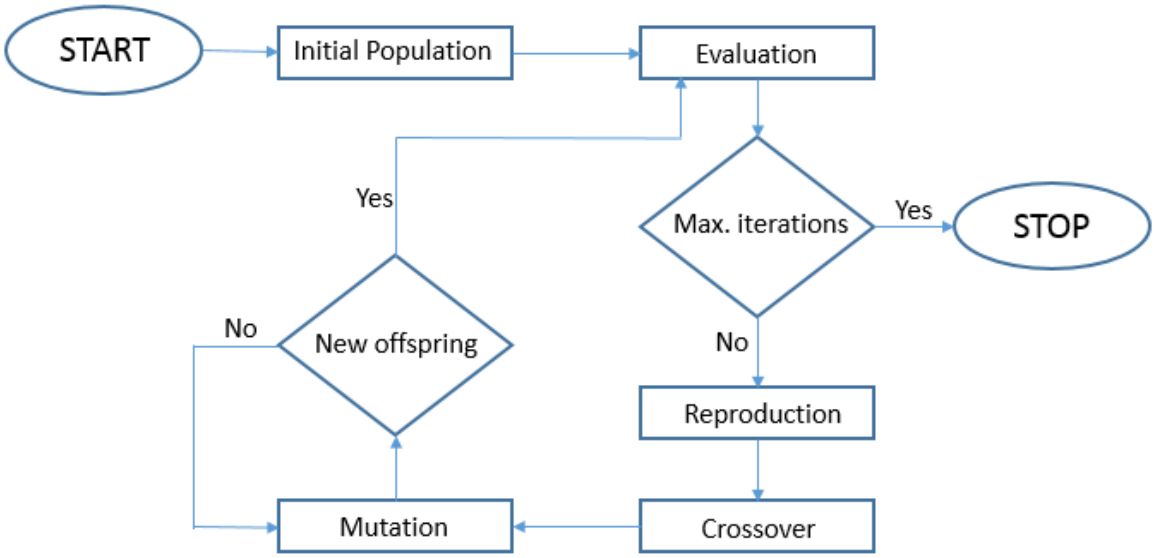

Figure 2.5 Working principle flowchart

2.2 Code Structure

Scripting for GA could be a challenge for this study due to the communication between the software. Launching the EM simulator sometimes causes an error because of misconnection between CST MWS and Python or Matlab. Matlab can be a better choice in terms of controlling other commercial software. However, scripting in Python is easier, so both schemes were tested. Using Python, variables of like population size, length of the string (chromosome), minimum and maximum temperature limitations, etc. were defined. Then a loop was created to determine the bits (genes) in the string. The population is formed with an individual created in the previous loop. After that, the population is used to obtain the first result from CST MWS. Saved results are compared and classified from the best to the worst in different groups with various probability in order to be included in the GA operators. The best solutions will have the highest

probability. Then operators begin to take place. First of all, the selection operator picks two chromosomes for the crossover stage using the roulette wheel selection method. Selected chromosomes are colligated by the crossover operator. It divides both chromosomes from a random point, and creates new offspring with its complement from another individual. After the crossover, the mutation operator is implemented if the user defined probability is met. These processes are repeated until the population capacity is filled. This routine runs to satisfy the demands of the user. Thus, it continues until satisfactory results are obtained or a manually defined iteration number is reached. The required results are saved in a text file during the optimization. A sample structure of the optimization script is provided in the following paragraphs.

For chromosome (individual) definition in the following script can be used.

```
def individual(length, min, max):'Create a member of the population.'
   ind= random.sample(xrange(1,max),length)
   return ind
```

In order to form the initial population, the following script can be used.

```
def population(count, length, min, max):
   """
   Create a number of individuals (i.e. a population).
   count: the number of individuals in the population
   length: the number of values per individual
   min: the minimum possible value in an individual's list of values
   max: the maximum possible value in an individual's list of values
   """
```

```
pop= [ individual(length, min, max) for x in xrange(count) ]
```

Then CST calculates the results (fitness), and the selection operator runs. Before the selection operator runs, results are grouped in different colors (from worst to best).

```
red=[]      #probability 10% 0.0 - 0.1
green=[]    #probability 10% 0.1 - 0.2
blue=[]     #probability 30% 0.2 - 0.5
black=[]    #probability 50% 0.5 - 1.0
random_prob1= random.random()
# first random number to determine which color we will use to crossover, second number is picked with the same method
if random_prob1 < 0.1:
    i=random.randrange(1,len(red),2)
    Ind1=red[i-1]
    Ind1_order=red[i]
if random_prob1 < 0.2:
    i=random.randrange(1,len(green),2)
    Ind1=green[i-1]
    Ind1_order=green[i]
if random_prob1 < 0.5:
    i=random.randrange(1,len(blue),2)
    Ind1=blue[i-1]
    Ind1_order=blue[i]
if random_prob1 < 0.1:
```

```
i=random.randrange(1,len(black),2)
Ind1=black[i-1]
Ind1_order=black[i]
```

Then, crossover takes place and a new individual is created until the population size reached.

```
cross_point=randint(3,9) #random crossover point
pop= population (i_count, i_length, i_min, i_max)
Ind1_string= pop[Ind1_order-1] #get first randomly selected individual
Ind2_string=pop[Ind2_order-1] #get second individual
Ind1_cross= Ind1_string[:cross_point] # keep the positions before the crossover point
Ind2_cross= Ind2_string[cross_point:] # keep the positions after the crossover point
crossed = Ind1_cross + Ind2_cross # crossed individuals are combined
```

Finally, the mutation operator is used to provide diversity according to the user defined probability.

CHAPTER III

MICROWAVE ANTENNA DESIGNS, SIMULATIONS, AND RESULTS

3.1 Microwave Antennas

For HT applications, many antennas – waveguide, horn, spiral patch, micro-strip patch antennas, and antenna arrays – are studied in order to provide the best penetration [47-50]. Some of the studies focus on the selective tissue heating for tumors [51-54], while others concentrate on uniform heating of the whole organ that has multiple tumors [55]. During these studies, the operating frequency of the antennas is also analyzed to understand the characteristics of the specific absorption rate (SAR) based on frequency ranges [56-58]. Since the penetration depth and the size of the heating zone increase with decreasing frequency, the position and the size of the tumor need to be considered to make a decision for operating frequency. This means that superficial tumors within the near-field region can be heated at higher frequencies [27]. Furthermore, the phase of the antenna excitation may also affect the heating pattern. That is, a modification of the heating zone can be achieved by manipulating the phase [59]. Due to multiple controllable parameters such as number of microwave sources and excitation phase, antenna arrays can be used to treat large tumors and create custom heating zone by adjusting the phases.

Designinh an antenna for a HT treatment is a challenge due to the impact of electromagnetic radiation on the human body. During the design and the simulation steps,

tissue properties and the environmental conditions are significant factors included to obtain the most accurate computational results. When the antenna contacts with the body, the resonating frequency and radiation characteristics are affected. Hence, previous research regarding modeling living tissue help researchers to create more realistic models to design an antenna without *in vivo* measurements. The published studies about dielectric properties of human [60 – 63] and animal tissue [108 – 110] make preliminary data possible for applications of antennas in medicine. Dielectric properties of the tissue is also related to SAR, e.g. conductivity and relative permittivity. Remarkable differences in the dielectric properties of normal tissue and tumors at microwave frequencies are clearly demonstrated in [46], and the low blood flow volume in tumors have lead to the development of microwave HT.

In 2012, a small antenna was designed operating at MedRadio (401 – 406 MHz) and ISM (433 – 435 MHz) bands [100]. The geometry of the antenna is shown in Figure 3.1. FR4 substrate was used for the published design.

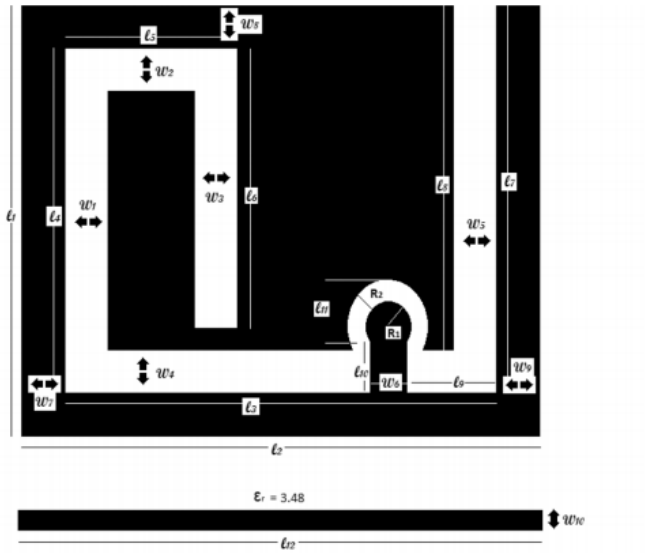

Dimensions		ℓ1	ℓ2	ℓ3	ℓ4	ℓ5	ℓ6	ℓ7
mm		10	12	10	8	4	6.5	9
ℓ8	ℓ9	ℓ10	ℓ11	ℓ12	W1=W2=W3=W4=W5			
8	3.3	1.08	1.135	12	1			
W6	W7=W8=W9		W10	W11	R1	R2		
0.61	1		1.52	1.52	1.22	2.92		

Figure 3.1 Antenna geometry and dimensions

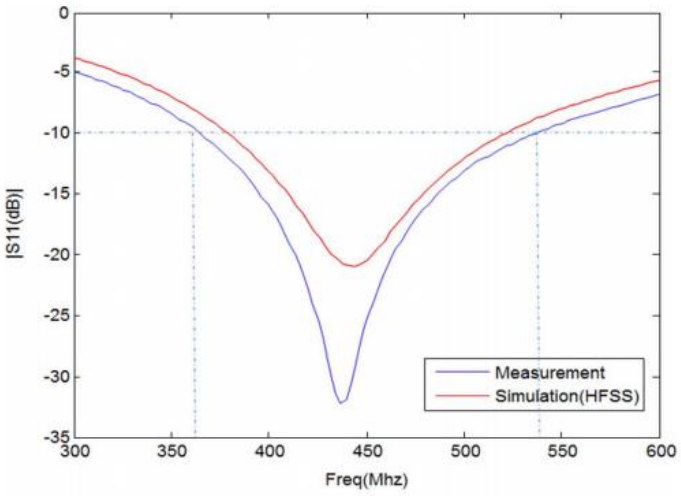

Figure 3.2 S_{11} of the published MW antenna

In 2014, another triple band (Figure 3.4) serpentine antenna was designed for medical purposes. The antenna design and the dimensions can be seen in Figure 3.3.

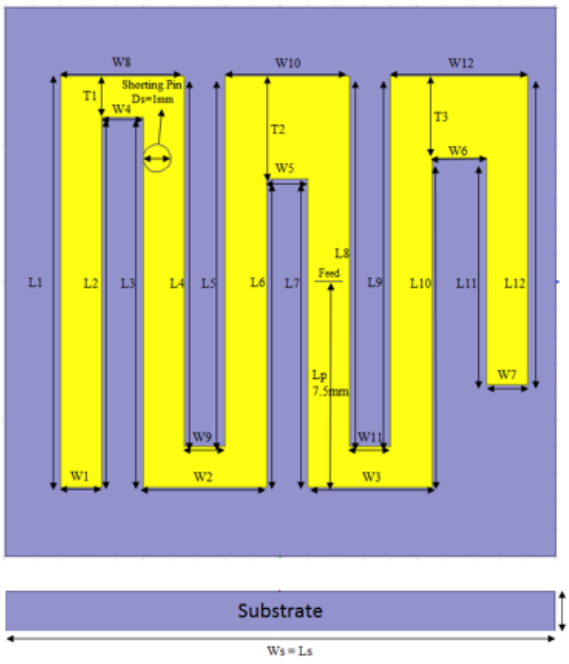

Antenna Dimensions (mm)			
W1	4.5	L1	15
W2	4.5	L2	13.5
W3	4.5	L3	13.5
W4	1.5	L4	13.5
W5	1.5	L5	13.5
W6	2	L6	11.25
W7	1.5	L7	11.25
W8	4.5	L8	13.5
W9	4.5	L9	13.5
W10	4.5	L10	12
W11	1.5	L11	8.25
W12	5	L12	11.25
Ls	20	T1	1.5
Ws	20	T2	3.75
h	1.5	T3	3

Figure 3.3 Triple band antenna geometry and dimensions

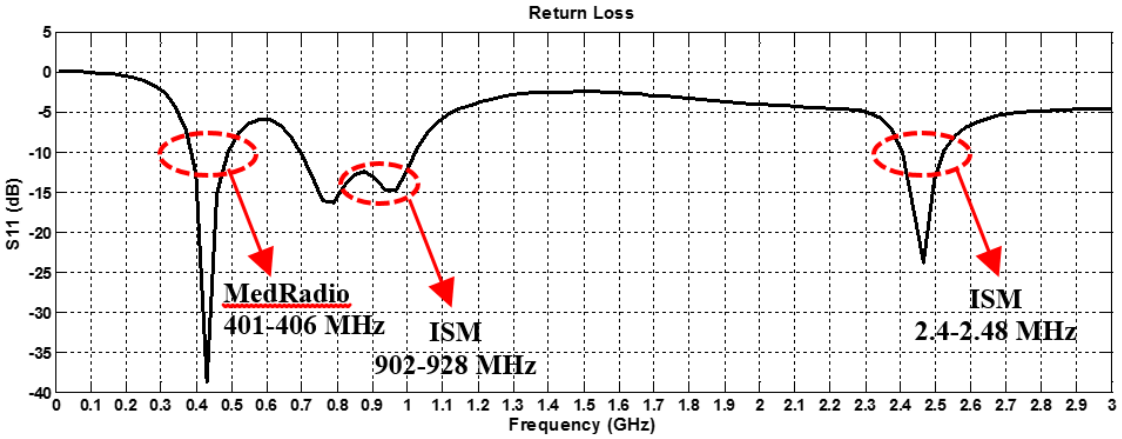

Figure 3.4 S_{11} of triple band serpentine antenna

These antennas can be used for any purpose on the human body. Thus, the first antenna is used in an array to create applicators for hyperthermia of the breast. PDMS, a flexible transparent material, is used as the substrate for each of the applicators. One of the applicators is demonstrated in Figure 3.5 [63]. 18 small MW antennas were arranged along two concentric circles in a radial manner and integrated in a circle-shaped flexible PDMS sheet. Each small antenna was made of two parts of machined copper foils, on which copper wires were soldered as the feed lines. This applicator was fabricated and tested but did not provide an accurate conformal fit to the human breast or mimicking gels. Thus, a better conformal shaped design was produced. The conformal design has 9 MW antennas placed symmetrically on the applicator for uniform SAR distribution. The designed and fabricated conformal MW antenna applicator is shown in Figure 3.6 [64].

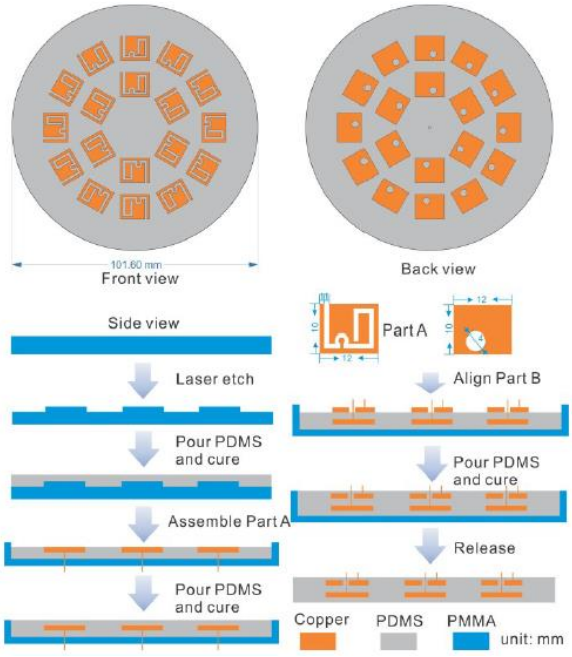

Figure 3.5 Design and fabrication of the flexible antenna applicator

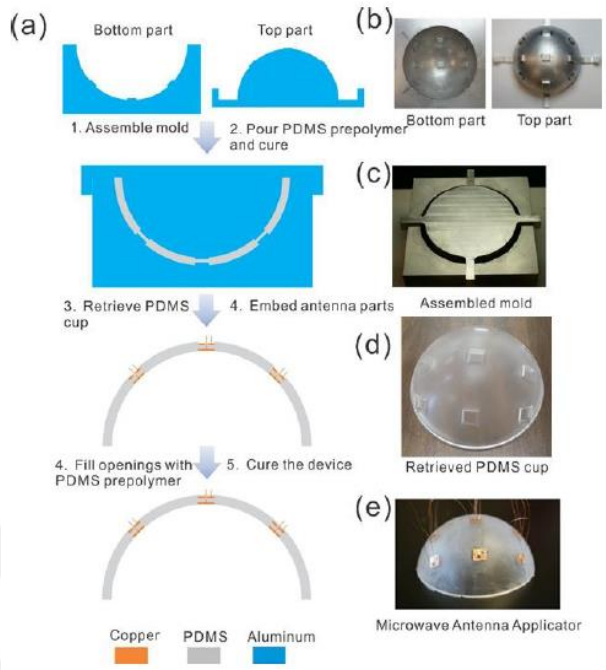

Figure 3.6 Fabrication procedure of the flexible microwave antenna applicator

(a) Schematics of fabrication, (b) top and bottom parts of the aluminum mold, (c) assembled mold, (d) retrieved PDMS cup, (e) final microwave antenna applicator

The patch antenna is one of the most popular antenna types that can be used as implantable device or thermotherapy applicator. It requires a simple rectangular-shaped dielectric material with a conducting patch and a ground plane. As a hyperthermia applicator, the ground plane decreases the radiation away from the body. Various feeding techniques are available for patch antennas which makes them attractive for applicator design given the required feeding network design.

Two edge-fed patch antennas are designed for this mild HT application at 915 MHz and 2.4 GHz. The dimensions of the patch antennas are calculated and designed using the following equation [121]:

$$W = \frac{c}{2f_r}\sqrt{\frac{2}{\varepsilon_r+1}} \tag{3.1}$$

where W is the width, c is the speed of light, f_r is the resonant frequency, and ε_r is the dielectric constant of the substrate. The antenna length is increased by ΔL due to fringing. It is calculated using the following equation:

$$\frac{\Delta L}{h} = 0.412 \frac{(\varepsilon_{reff}+0.3)\left(\frac{W}{h}+0.264\right)}{(\varepsilon_{reff}-0.258)\left(\frac{W}{h}+0.8\right)} \tag{3.2}$$

where L is the length, ε_{reff} is efective dielectric constant, and h is the thickness of the substrate. The effective dielectric constant of the substrate and the length of the patch are also calculated using the following equations.

$$\varepsilon_{reff} = \frac{\varepsilon_r+1}{2} + \frac{\varepsilon_r-1}{2}\left[1+12\frac{h}{W}\right]^{-1/2} \quad for \ {}^{W}/_{h} > 1 \tag{3.3}$$

$$L = \frac{c}{2f_r\sqrt{\varepsilon_r}} - 2\Delta L \tag{3.4}$$

Each antenna geometry is shown in Figure 3.7 and Figure 3.8 for 915 MHz and 2.4 GHz HT applicators, respectively.

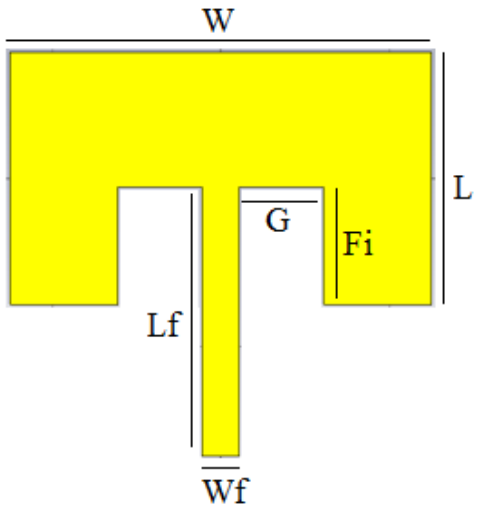

Figure 3.7 915 MHz MW antenna geometry

Table 3.1 915 MHZ MW Antenna Dimensions

Dimensions for 915 MHz MW Antenna (mm)			
W	16.9	**Lf**	10
L	13.85	**Fi**	8.97
G	3.2	**Wf**	2.42

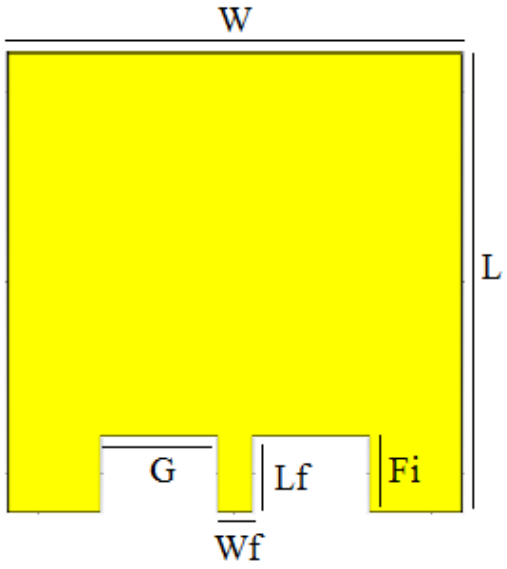

Figure 3.8 2.4 GHz MW antenna geometry

Table 3.2 2.4 GHz MW Antenna Dimensions

Dimensions for 2.4 GHz MW Antenna (mm)			
W	24.27	**Lf**	10
L	17.25	**Fi**	3.92
G	4.63	**Wf**	1.7

The return losses of the 915 MHz and 2.4 GHz MW antennas for the initial design and reflection coefficient after the optimization are shown in Figure 3.9 – 3.12, respectively.

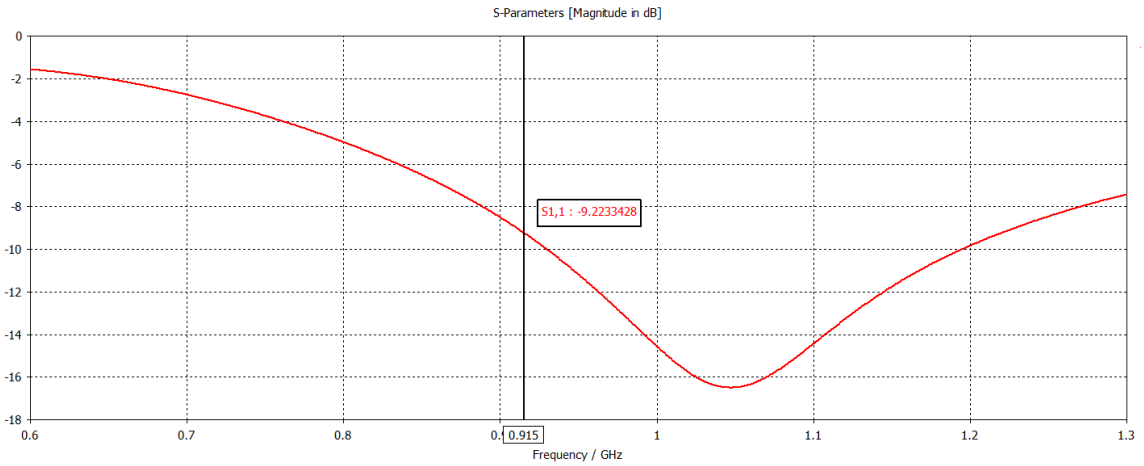

Figure 3.9 915 MHz MW antenna reflection coefficient before the optimization

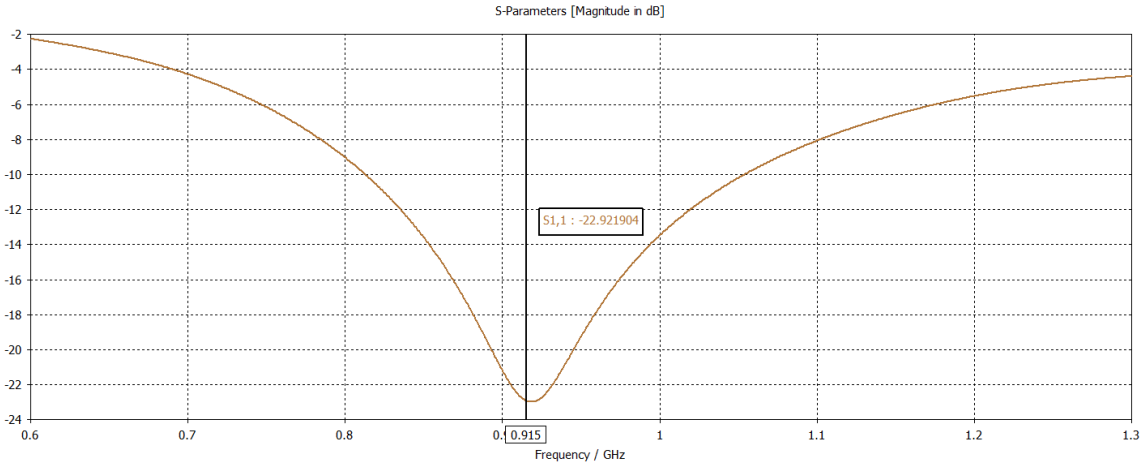

Figure 3.10 915 MHz MW antenna reflection coefficient after the optimization

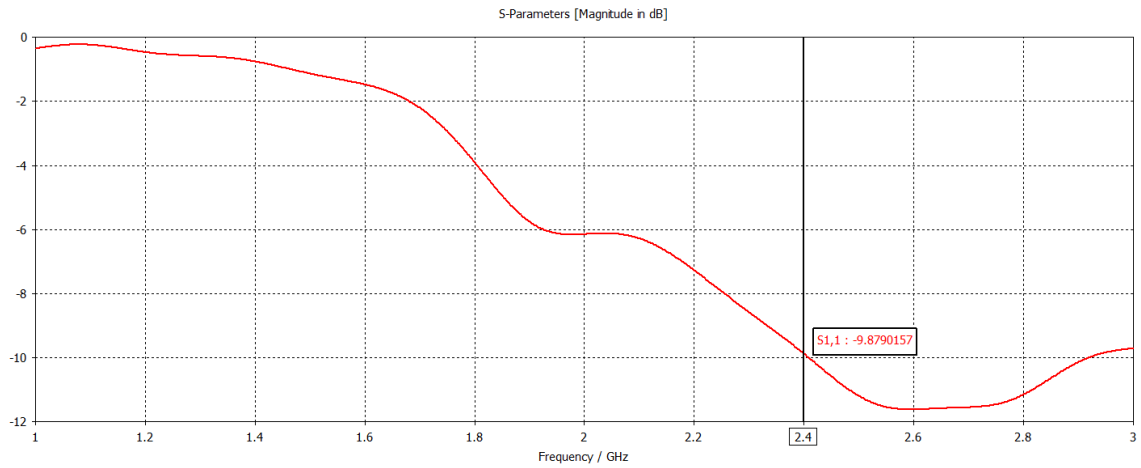

Figure 3.11 2.4 GHz MW antenna reflection coefficient before the optimization

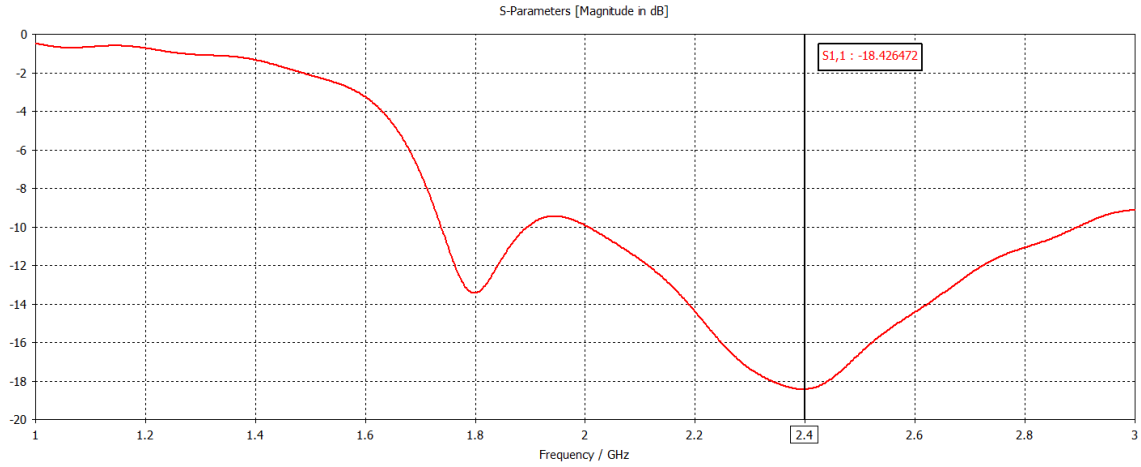

Figure 3.12 2.4 GHz - antenna reflection coefficient after the optimization

3.2 Microwave Antenna Arrays

After the design and optimization of the patch antennas at 915 MHz and 2.4 GHz on human tissue, two different applicators were created for each frequency. A predefined size for the applicators was assumed by considering the substrate used in the fabrication process and the size of the optimized patch antennas, resulting in 12 elements for each

HT applicator and a 4-input feeding network with a 4-output external power divider. The applicator elements are equally spaced, where the coupling between the antennas is minimized as much as possible. For this purpose, the coupling criterion is set lower than -30 dB. The constructed HT applicator, the return losses of MW antennas, and the coupling simulation results are shown in Figure 3.13, Figure 3.14, and Figure 3.15 for the frequency of 915 MHz, respectively. The feeding network is also shown on the applicator, where the feeding network design is discussed in what follows.

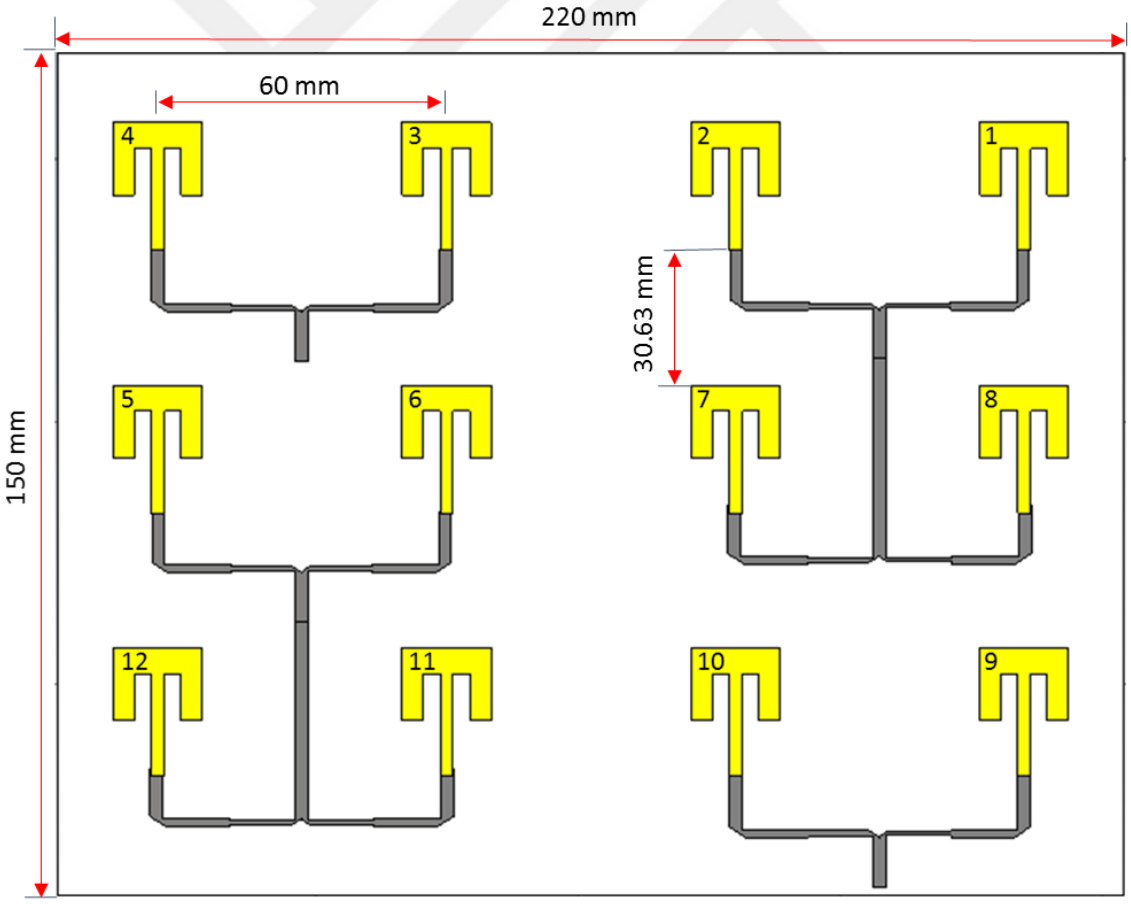

Figure 3.13 MW antenna array for 915 MHz mild HT applicator

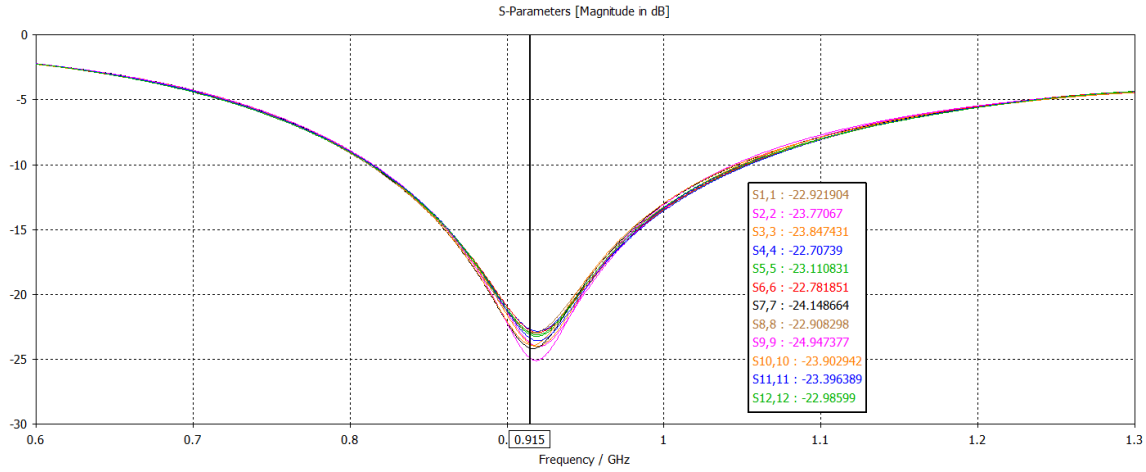

Figure 3.14 S parameters of each element for 915 MHz MW antenna array

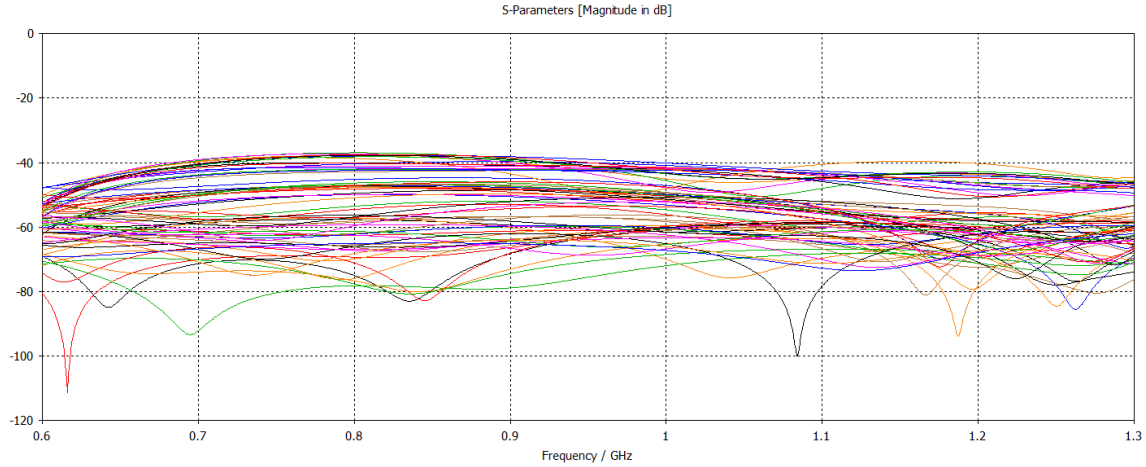

Figure 3.15 Coupling simulations between the elements for 915 MHz MW antenna array

The same design procedures are applied to create the 2.4 GHz mild HT applicator. The array geometry and simulation results are also shown in Figure 3.16, Figure 3.17, and Figure 3.18, respectively.

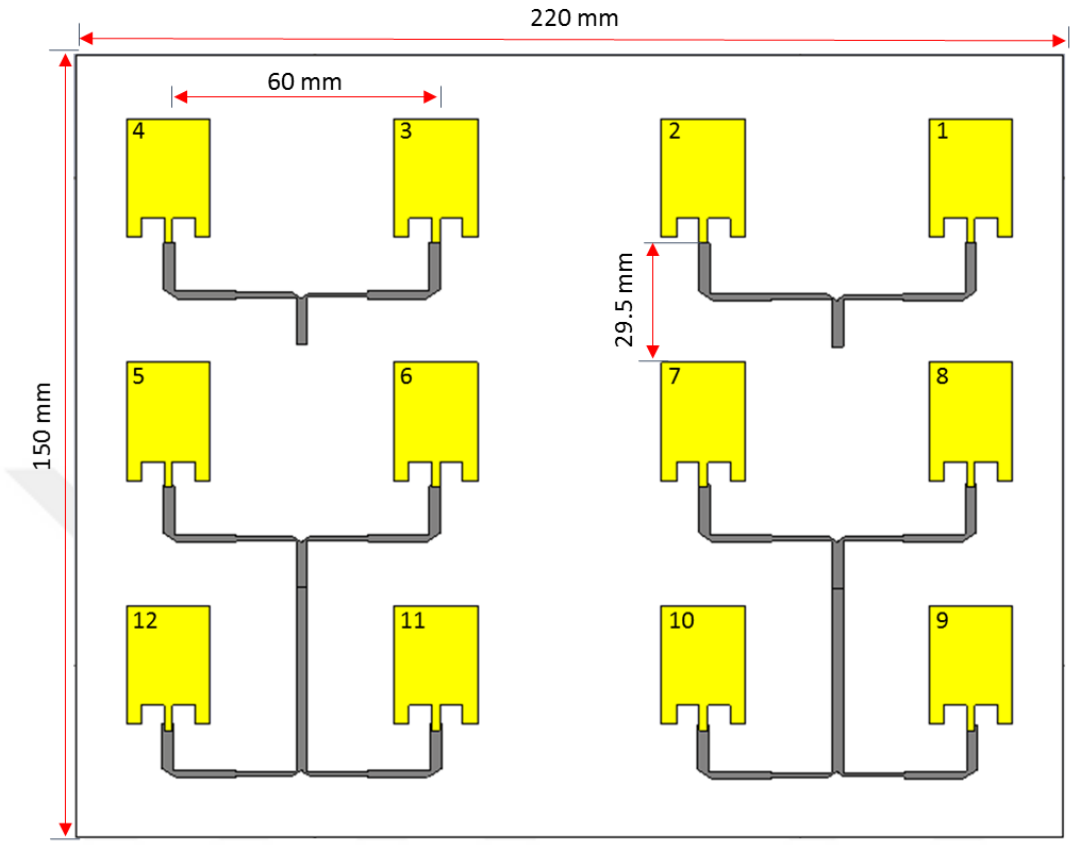

Figure 3.16 MW antenna array for 2.4 GHz mild HT applicator

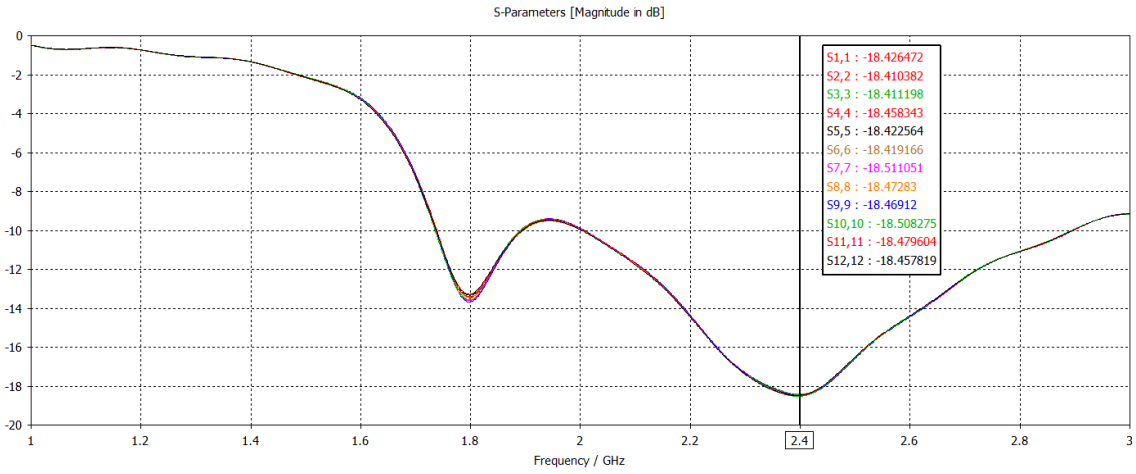

Figure 3.17 S parameters of the elements for 2.4 GHz MW antenna array

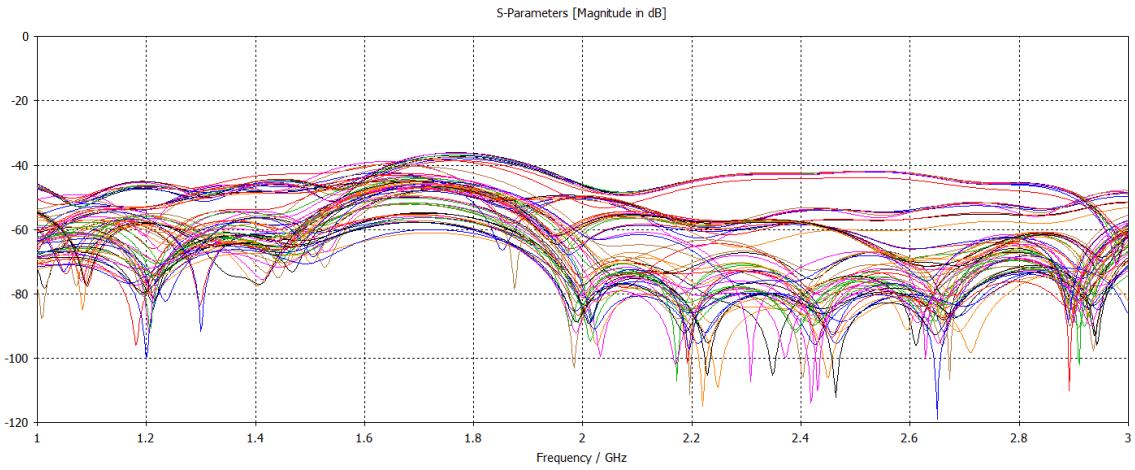

Figure 3.18 Coupling simulations between the elements for 2.4 GHz MW antenna array

3.3 Feeding Network

Fabrication of a microstrip (MS) feeding network can be done by simple techniques such as milling and etching. However, discontinuities at the corners may be a challenge because of abrupt changes in dimensions and parasitic reactances. This causes a additional attenuation which reduces the MS circuit efficiency due to mismatches. One of the easiest way to minimize these effects is to use mitered conductors (Figure 3.19) instead of complex circuits and stubs.

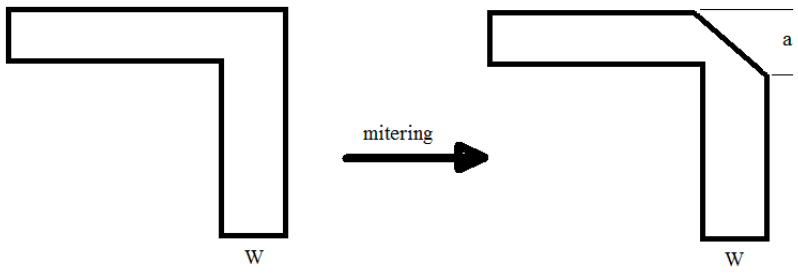

Figure 3.19 Bent and mitered conductor

The mitering technique can eliminate the parasitic reactances due to sharp bends, T-junctions, and discontinuities. This technique helps to decrease the capacitance at the point of discontinuity. It can be applied for any bend angle. Practically, the length of the miter is determined as a=1.8W [111] where W is the width of the MS transmission line (TL). All antennas are designed for 50 Ω TL connection. Thus, W is defined as the width of the 50 Ω TL and can be calculated by using the following equations [111]:

$$\frac{W}{h} = \begin{cases} \frac{8e^A}{e^{2A}-2} & for \quad \frac{W}{h} < 2 \\ \frac{2}{\pi}\left[B - 1 - \ln(2B-1) + \frac{\varepsilon_r - 1}{2\varepsilon_r}\left(\ln(B-1) + 0.39 - \frac{0.61}{\varepsilon_r}\right)\right] & for \quad \frac{W}{h} > 2 \end{cases} \tag{3.5}$$

where

$$A = \frac{Z_0}{60}\sqrt{\frac{\varepsilon_r + 1}{2}} + \frac{\varepsilon_r - 1}{\varepsilon_r + 1}\left(0.23 + \frac{0.11}{\varepsilon_r}\right) \tag{3.6}$$

$$B = \frac{377\pi}{2Z_0\sqrt{\varepsilon_r}} \tag{3.7}$$

and *h* is the thickness of the substrate.

The whole feeding network is printed on a Rogers 3010 flexible substrate. However, the external power dividers are printed on regular FR4 substrate to reduce the cost of the fabrication. Dielectric constants of the flexible and FR4 substrates are 10.2 and 4.28, respectively. The higher relative permittivity allows for smaller MS circuits and antennas.

3.3.1 Basic Power Divider

A common power divider is used for the feeding network and the external dividers. A basic T-junction power divider is shown in Figure 3.20. As indicated in the figure, Z_0, Z_1, and Z_2 represent the characteristic impedances of the TLs connected to

output of the power divider. P_0, P_1, and P_2 are the power levels at Port 1, Port 2, and Port 3, respectively.

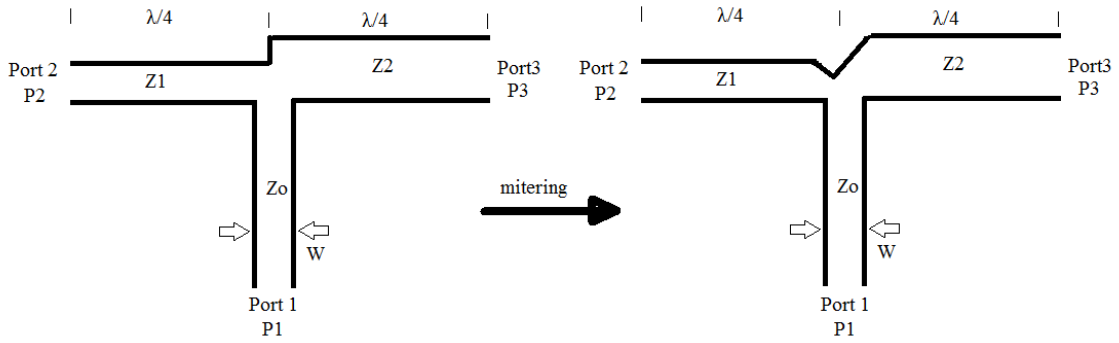

Figure 3.20 Basic and mitered T-split power divider

Power levels are related to each other such that

$$P_1 = P_2 + P_3 \tag{3.8}$$

$$P_2 = \frac{1}{1+K^2} P_1 \tag{3.9}$$

$$P_3 = \frac{K^2}{1+K^2} P_1 \tag{3.10}$$

where K^2 is the power ratio and determined by designer.

The relationship between power levels and characteristic impedances of the TL are defined with the following equations:

$$\frac{Z_2}{Z_1} = \frac{P_2}{P_3} = K^2 \tag{3.11}$$

$$\frac{Z_2}{Z_0} = \frac{P_1}{P_3} = K^2 + 1 \tag{3.12}$$

$$Z_2 = (K^2 + 1)Z_0 \tag{3.13}$$

$$Z_1 = \frac{K^2+1}{K^2} Z_0 \tag{3.14}$$

Also, the length of each arm of the power divider is equal to one quarter wavelength:

$$\lambda = \frac{c}{f\sqrt{\varepsilon_{reff}}} \tag{3.15}$$

where ε_{reff} is effective relative permittivity, c is speed of light, and f is the frequency.

$$\varepsilon_{reff} = \frac{\varepsilon_r+1}{2} + \frac{\varepsilon_r-1}{2}\left(\frac{1}{\sqrt{1+12\left(\frac{1}{W/h}\right)}}\right) \tag{3.16}$$

3.3.2 Designed Feeding Network

For the mild HT applicator, a microstrip feeding network was designed on the applicator. Moreover, another external power divider is needed for each applicator (915 MHz and 2.4 GHz) due to lack of space on the applicator to place all of the power dividers. The HT applicator has 4 inputs, and external power divider has 4 outputs. The following figures (Figure 3.21 – 3.52) show the geometry, dimensions and simulation results of the designed dividers on the applicators and the external power dividers for the frequency of 915 MHz and 2.4 GHz. In the graphs, the S parameters describe the relationship between the ports. S_{21} defines the power transferred from port 1 to port 2, and S_{31} represents the power transferred from port 1 to port 3. Therefore, the ratio of the powers at these ports can be calculated according to the s-parameters. The generalized two – port system is shown in Figure 3.21. It is assumed that all ports are terminated in the 50 ohm reference impedance.

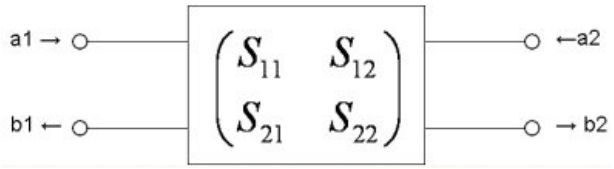

Figure 3.21 Generalized two – port network

$$S_{11} = {}^{b_1}/_{a_1} \tag{3.17}$$

$$S_{12} = {}^{b_1}/_{a_2} \tag{3.18}$$

$$S_{21} = {}^{b_2}/_{a_1} \tag{3.19}$$

$$S_{22} = {}^{b_2}/_{a_2} \tag{3.20}$$

$$\begin{bmatrix} b_1 \\ b_2 \end{bmatrix} = \begin{bmatrix} S_{11} & S_{12} \\ S_{21} & S_{21} \end{bmatrix} \text{x} \begin{bmatrix} a_1 \\ b_1 \end{bmatrix} \tag{3.21}$$

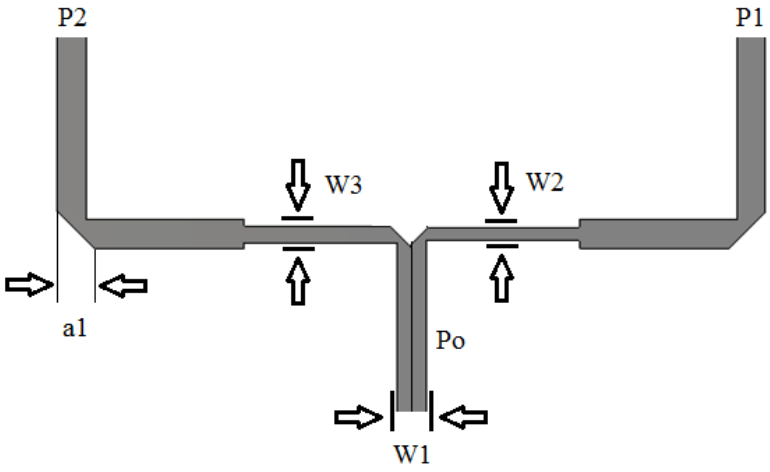

P2/P1	1.6
W1	1.41
W2	0.41
W3	0.8
a	2.53

Figure 3.22 MS power divider used between antenna #1 and #2 at 915 MHz

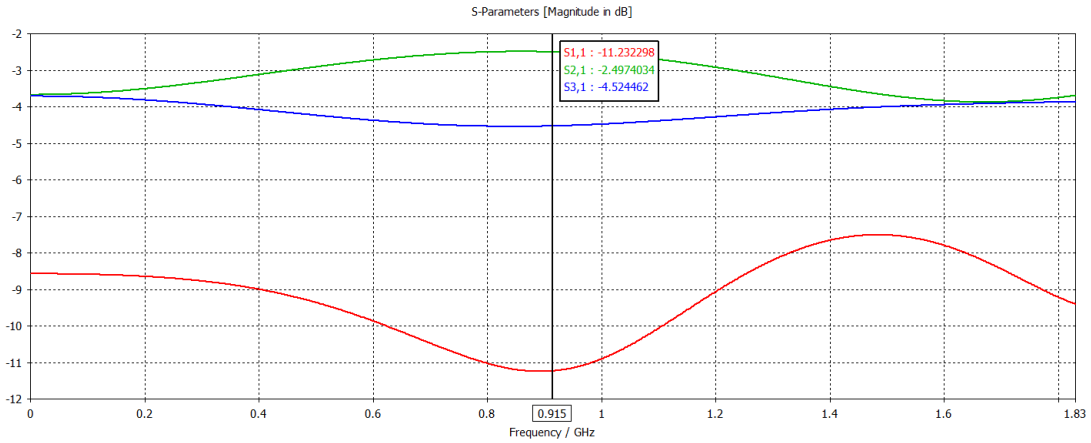

Figure 3.23 S parameters of the divider used between antenna #1 and #2 at 915 MHz

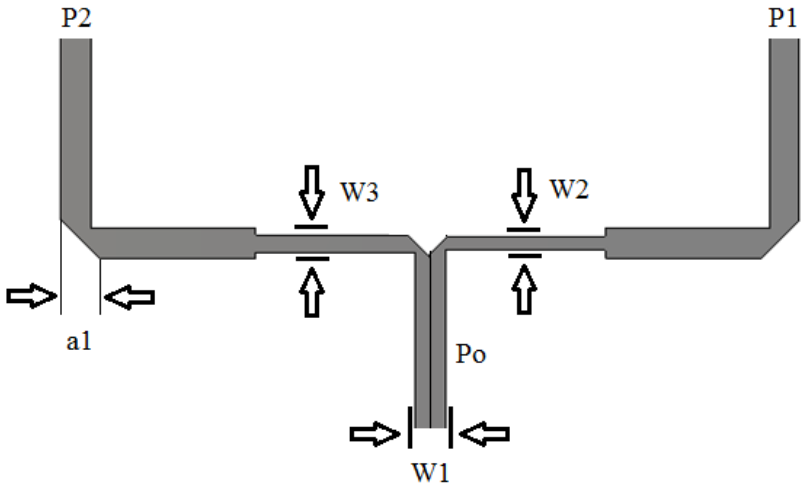

P2/P1	1.29
W1	1.41
W2	0.5
W3	0.72
a	2.53

Figure 3.24 MS power divider used between antenna #3 and #4 at 915 MHz

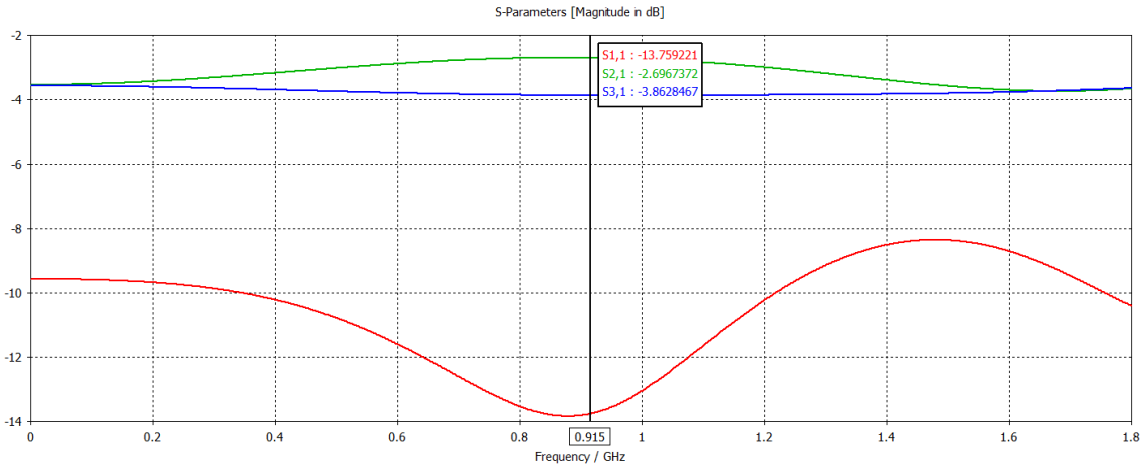

Figure 3.25 S parameters of the divider used between antenna #3 and #4 at 915 MHz

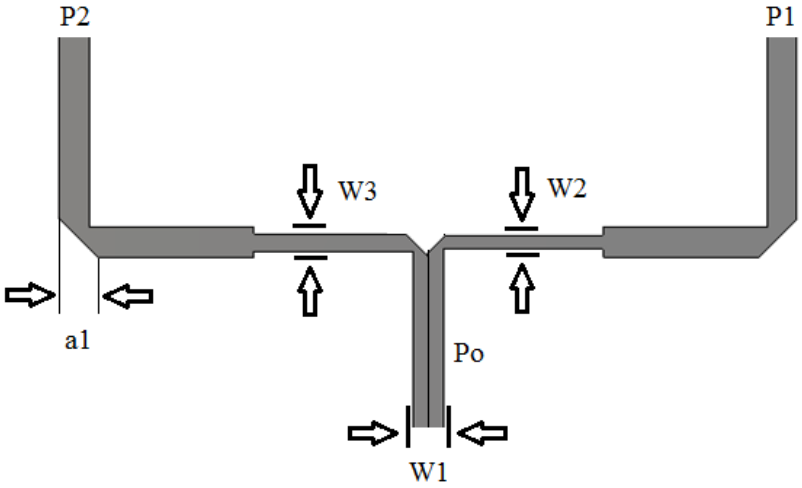

P2/P1	1.29
W1	1.41
W2	0.5
W3	0.72
a1	2.53

Figure 3.26 MS power divider used between antenna #5 and #6 at 915 MHz

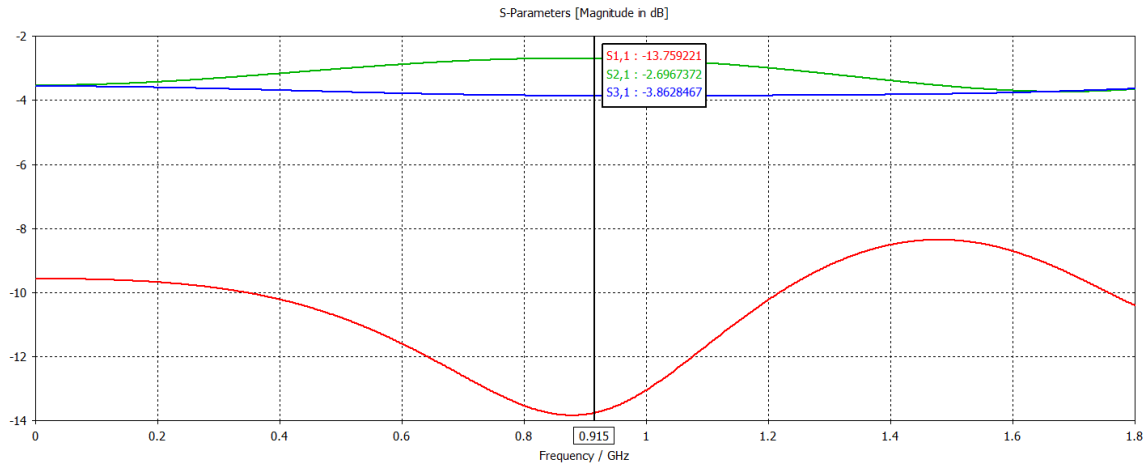

Figure 3.27 S parameters of the divider used between antenna #5 and #6 at 915 MHz

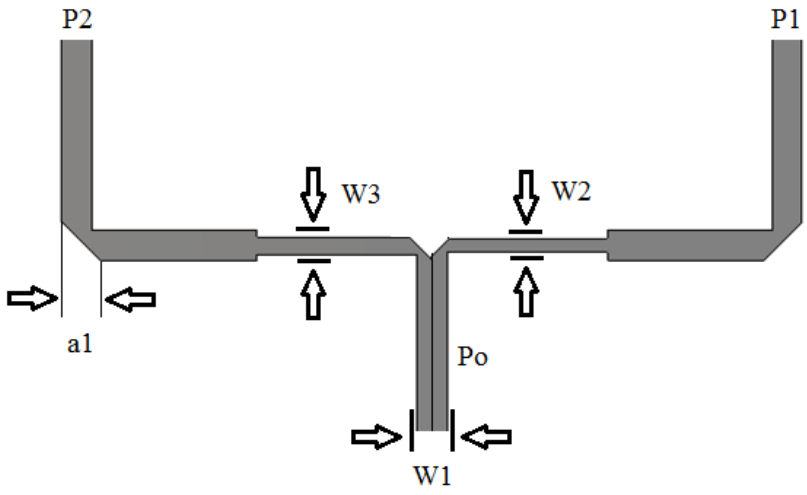

P2/P1	1.6
W1	1.41
W2	0.41
W3	0.8
a	2.53

Figure 3.28 MS power divider used between antenna #7 and #8 at 915 MHz

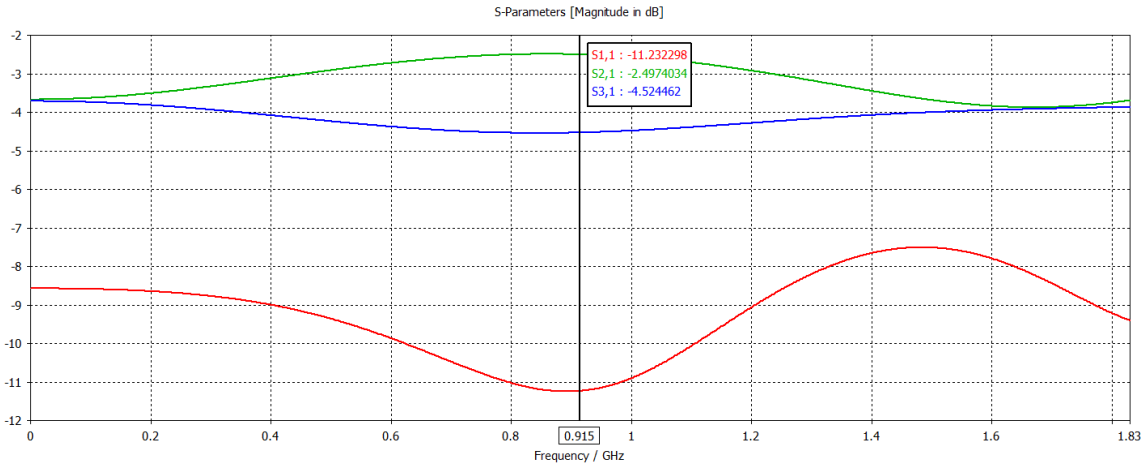

Figure 3.29 S parameters of the divider used between antenna #7 and #8 at 915 MHz

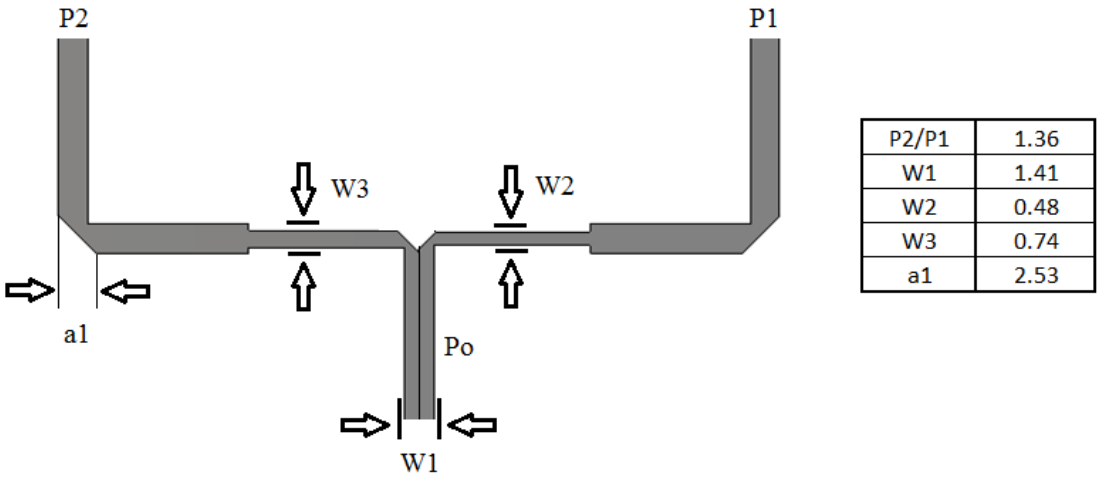

P2/P1	1.36
W1	1.41
W2	0.48
W3	0.74
a1	2.53

Figure 3.30 MS power divider used between antenna #9 and #10 at 915 MHz

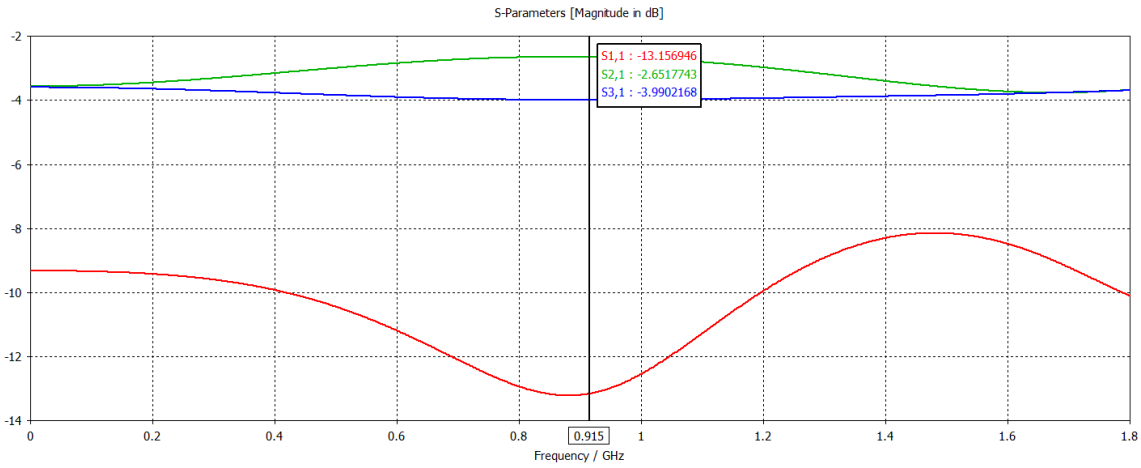

Figure 3.31 S parameters of the divider used between antenna #9 and #10 at 915 MHz

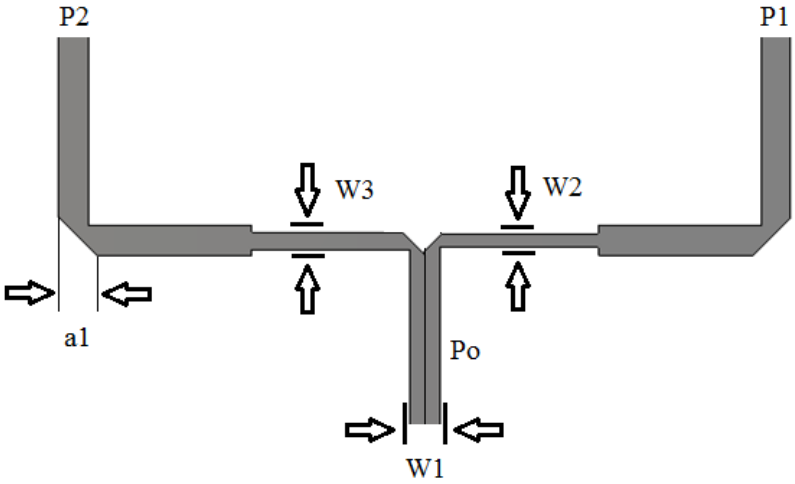

P2/P1	1
W1	1.41
W2	0.61
W3	0.61
a	2.53

Figure 3.32 MS power divider used between antenna #11 and #12 at 915 MHz

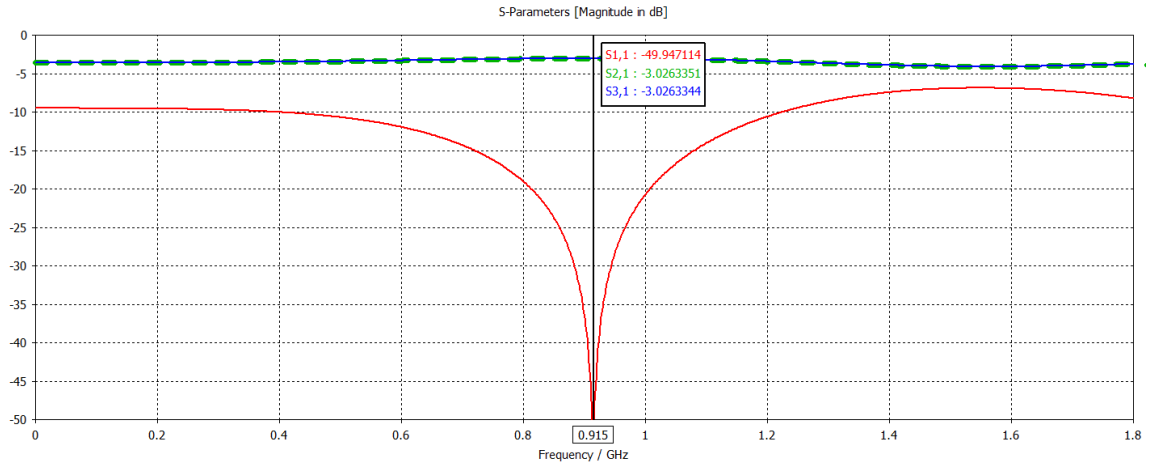

Figure 3.33 S parameters of the divider used between antenna #11 and #12 at 915 MHz

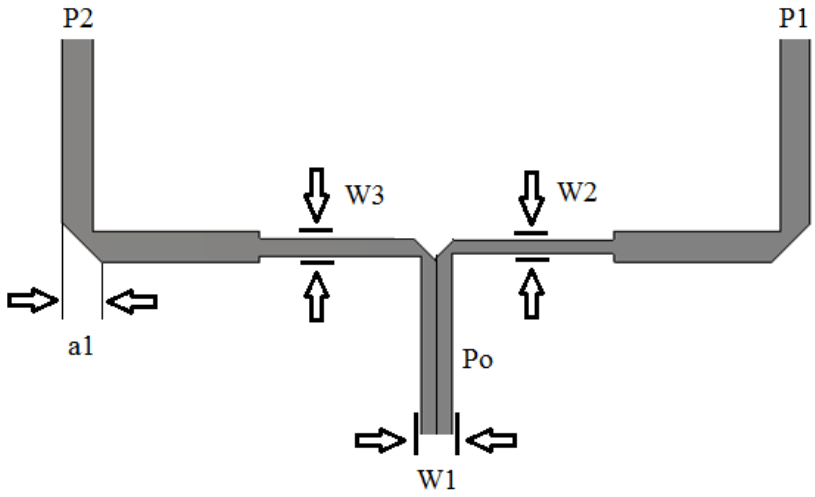

P2/P1	1.21
W1	1.41
W2	0.53
W3	0.69
a	2.53

Figure 3.34 MS power divider used between antenna #1 and #2 at 2.4 GHz

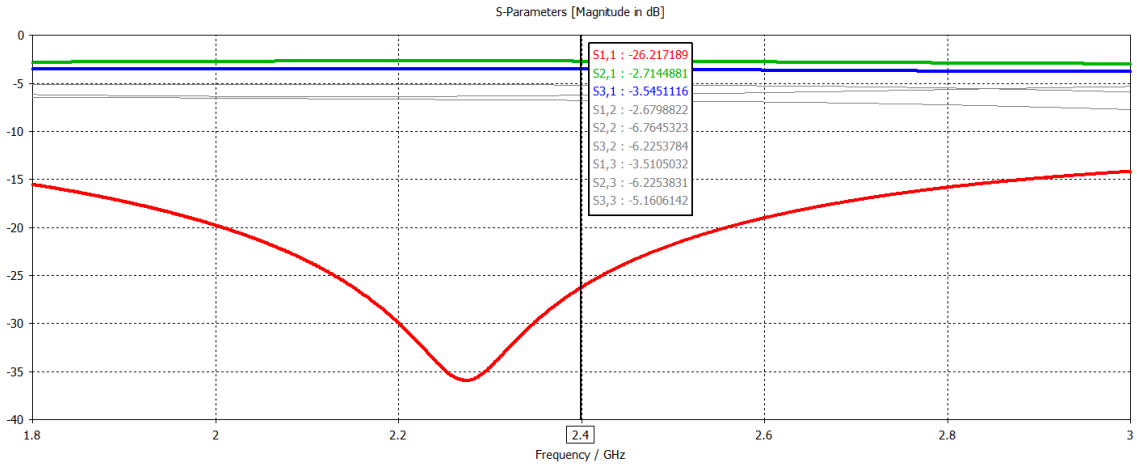

Figure 3.35 S parameters of the divider used between antenna #1 and #2 at 2.4 GHz

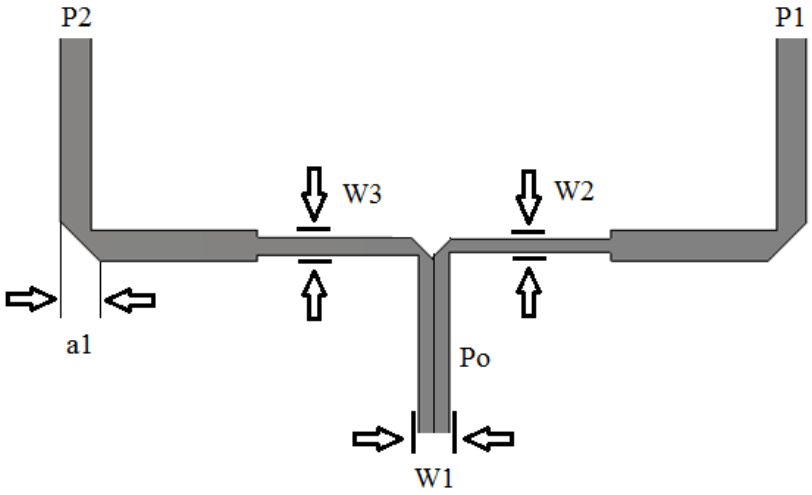

P2/P1	1.23
W1	1.41
W2	0.52
W3	0.7
a1	2.53

Figure 3.36 MS power divider used between antenna #3 and #4 at 2.4 GHz

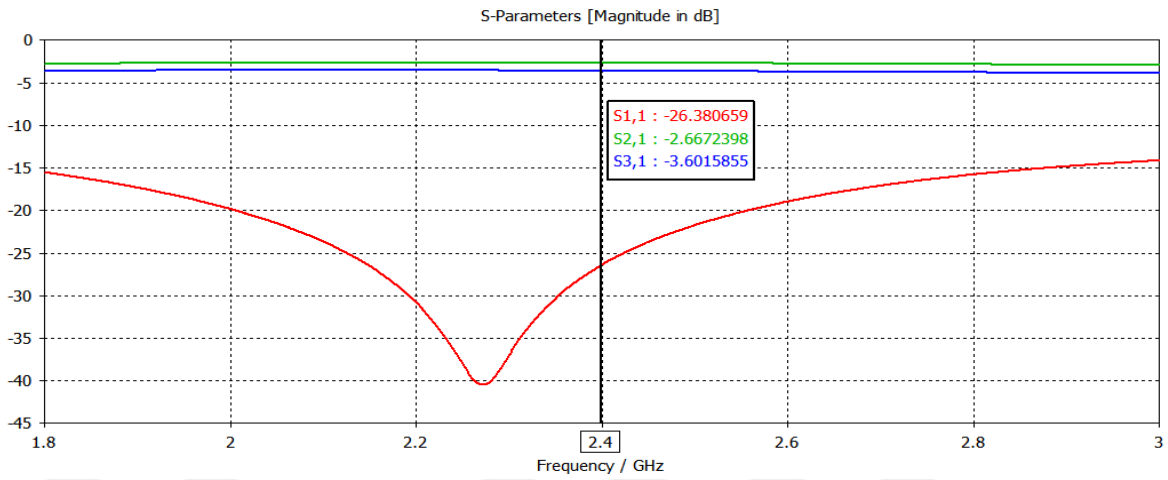

Figure 3.37 S parameters of the divider used between antenna #3 and #4 at 2.4 GHz

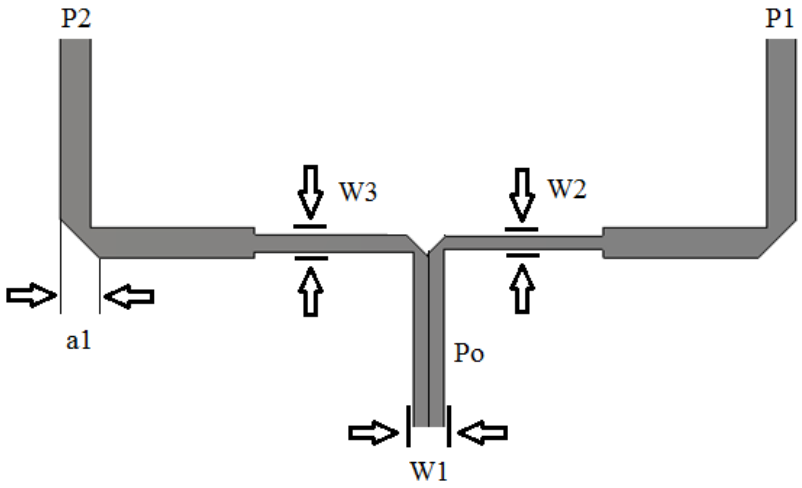

P1/P2	1.1
W1	1.41
W2	0.65
W3	0.57
a1	2.53

Figure 3.38 MS power divider used between antenna #5 and #6 at 2.4 GHz

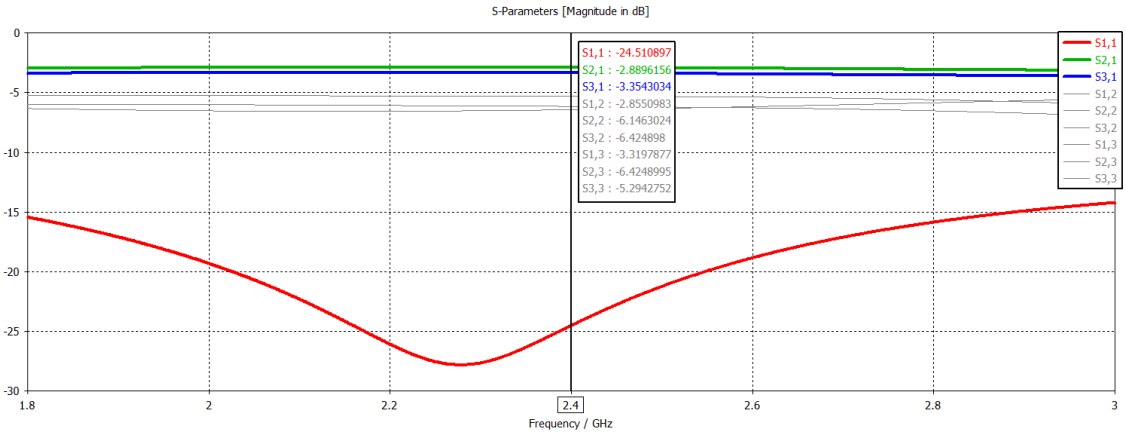

Figure 3.39 S parameters of the divider used between antenna #5 and #6 at 2.4 GHz

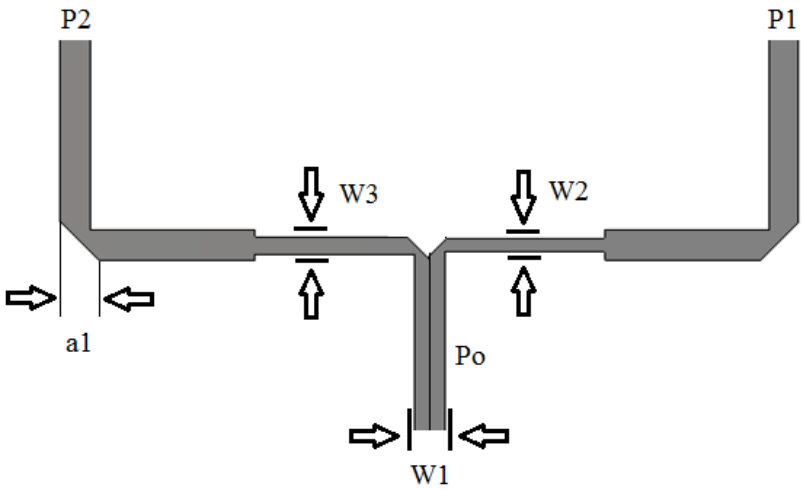

P1/P2	1.42
W1	1.41
W2	0.75
W3	0.46
a1	2.53

Figure 3.40 MS power divider used between antenna #7 and #8 at 2.4 GHz

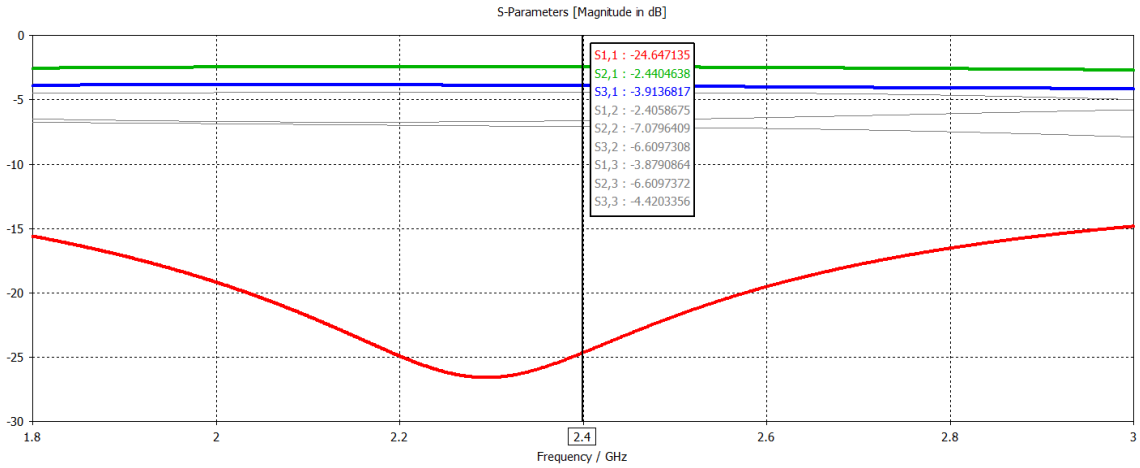

Figure 3.41 S parameters of the divider used between antenna #7 and #8 at 2.4 GHz

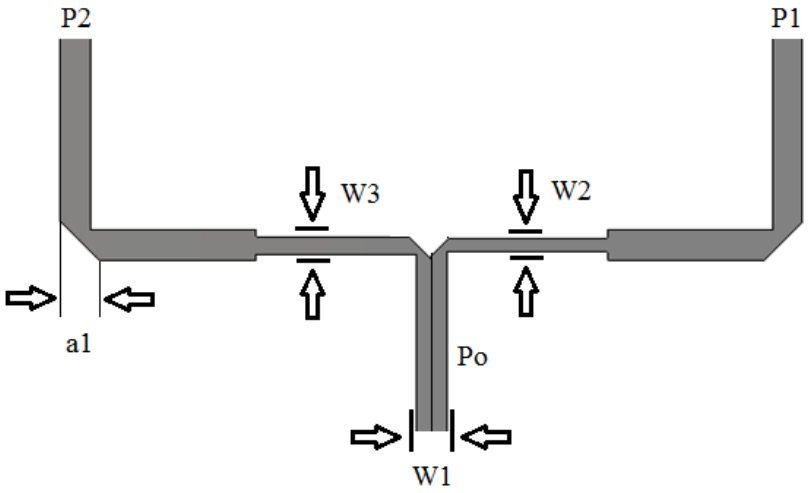

P1/P2	1.16
W1	1.41
W2	0.67
W3	0.55
a1	2.53

Figure 3.42 MS power divider used between antenna #9 and #10 at 2.4 GHz

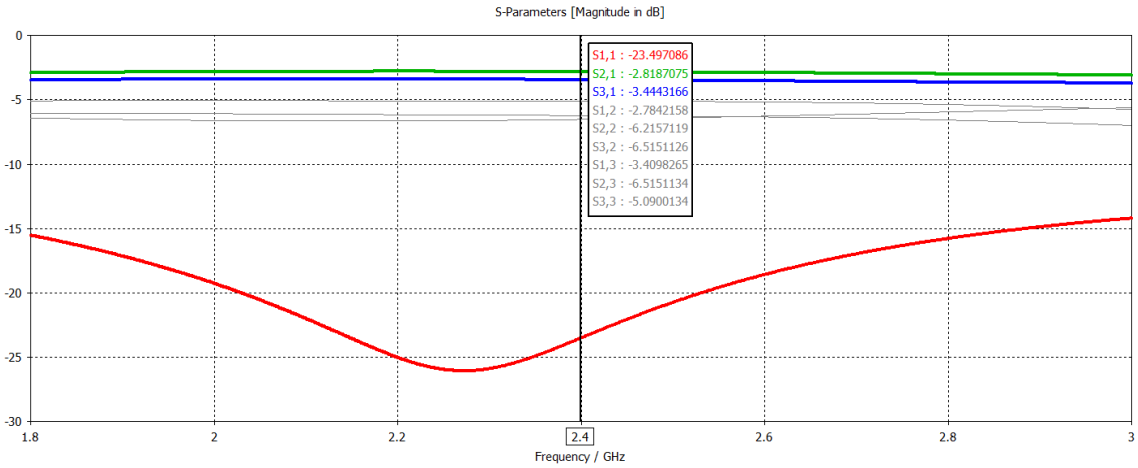

Figure 3.43 S parameters of the divider used between antenna #9 and #10 at 2.4 GHz

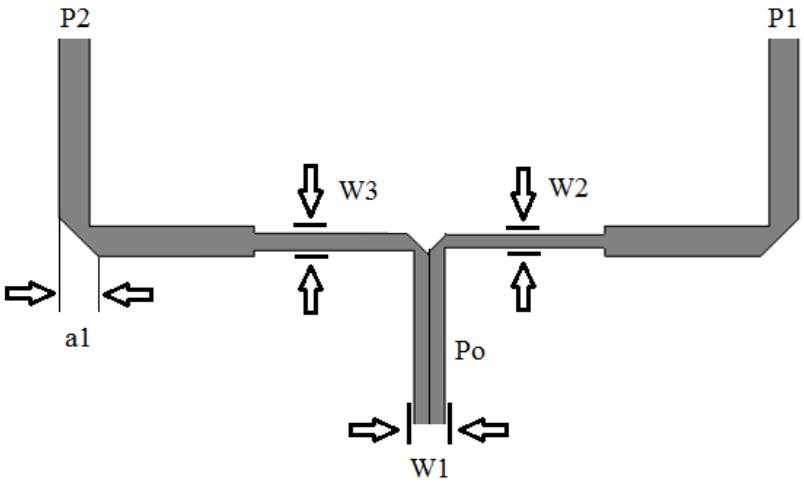

P1/P2	1.38
W1	1.41
W2	0.75
W3	0.47
a1	2.53

Figure 3.44 MS power divider used between antenna #11 and #12 at 2.4 GHz

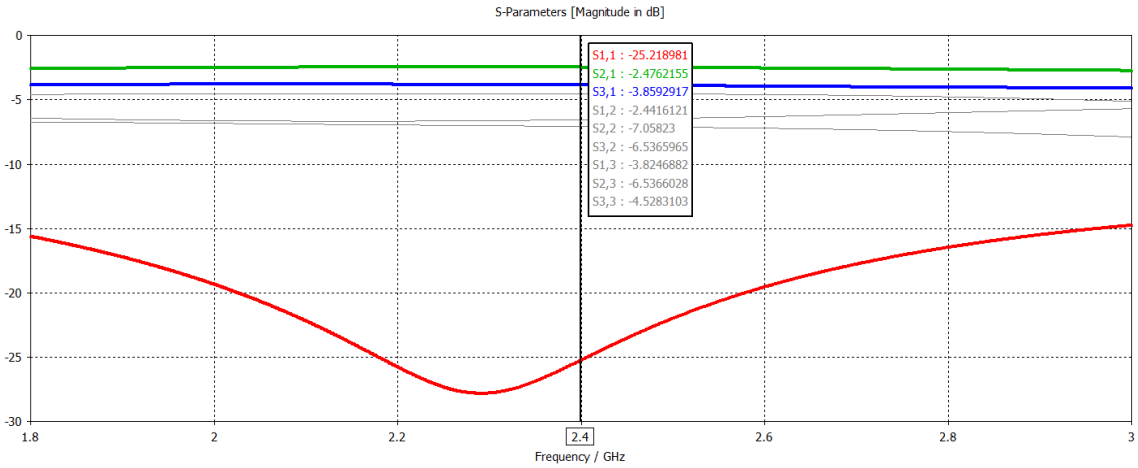

Figure 3.45 S parameters of the divider used between antenna #11 and #12 at 2.4 GHz

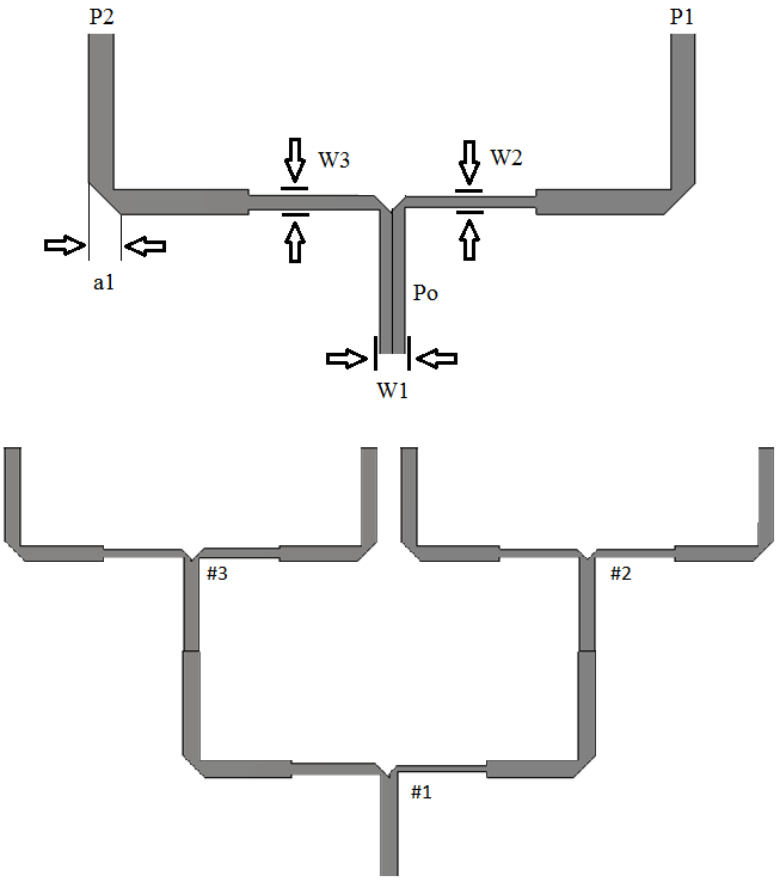

#1

P2/P1	1
W1	1.41
W2	0.61
W3	0.61
a1	2.53

#2

P2/P1	2
W1	1.41
W2	0.3
W3	1
a	2.53

#3

P2/P1	1.7
W1	1.41
W2	0.36
W3	0.95
a	2.53

Figure 3.46 External power divider for 915 MHz

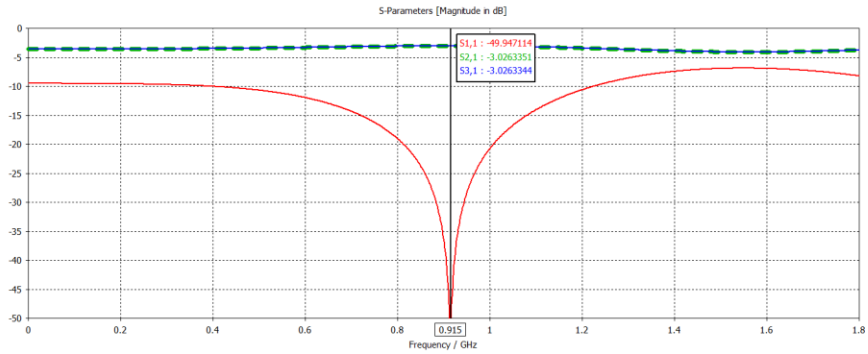

Figure 3.47 S parameters of #1 of 915 MHz external divider

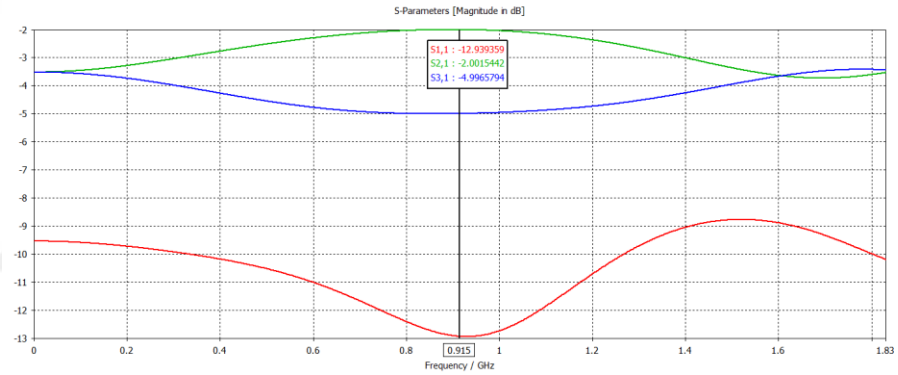

Figure 3.48 S parameters of #2 of 915 MHz external divider

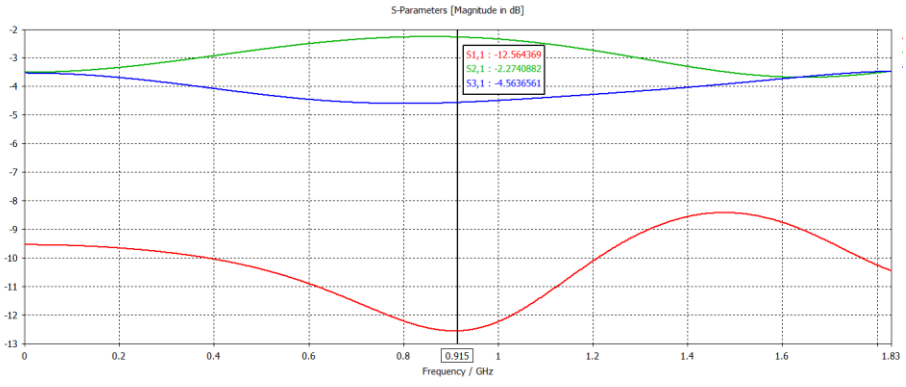

Figure 3.49 S parameters of #3 of 915 MHz external divider

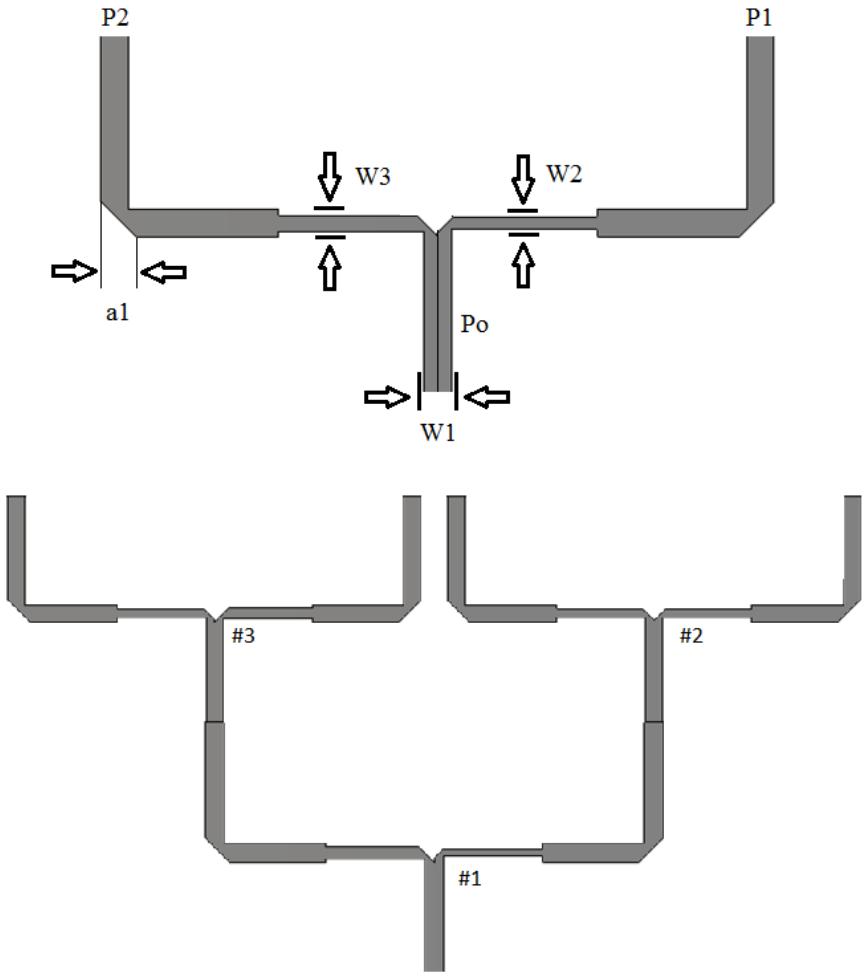

#1

P2/P1	1.84
W1	3.12
W2	1.18
W3	2.15
a	5.62

#2

P2/P1	1
W1	3.12
W2	1.66
W3	1.66
a	5.62

#3

P2/P1	1.2
W1	3.12
W2	1.5
W3	2
a	5.62

Figure 3.50 External power divider for 2.4 GHz

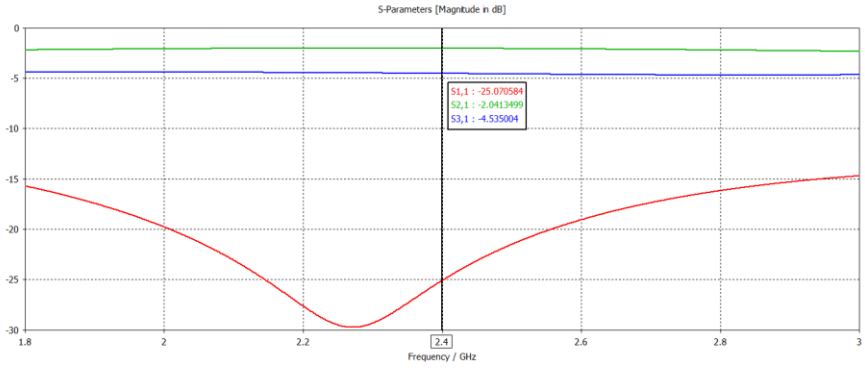

Figure 3.51 S parameters of #1 of 2.4 GHz external divider

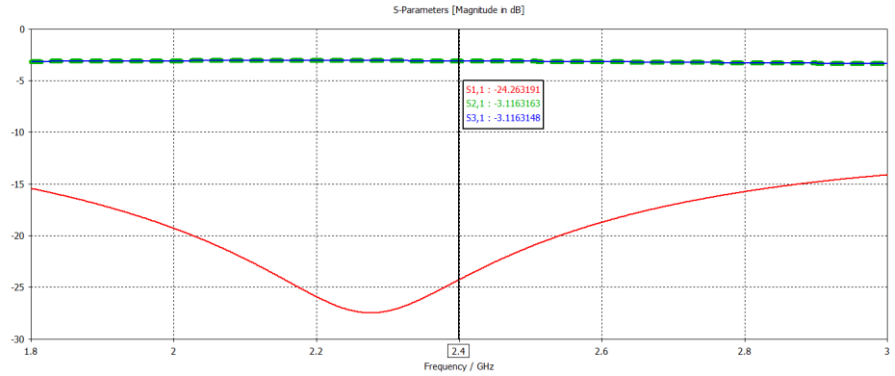

Figure 3.52 S parameters of #2 of 2.4 GHz external divider

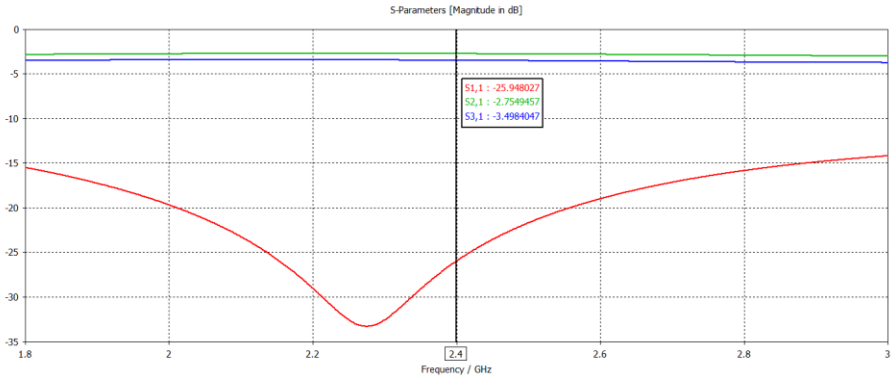

Figure 3.53 S parameters of #3 of 2.4 GHz external divider

Optimization of the applicator designs includes the selection of the operating frequency and the MW antenna array designs. The process should also include temperature optimization. In the software (CST MWS), the power losses in the materials and SAR are converted into temperature by the thermal solver. SAR gives the power absorption over a unit or specific volume. The following equations, including the bioheat equation, are used to calculate SAR and temperaure in CST:

$$SAR = \int \frac{\sigma(r)|E(r)|}{\rho(r)} dr \tag{3.22}$$

$$C\rho \frac{\partial T}{\partial t} = \nabla k \nabla T + \rho(SAR) + A - B(T - T_b) \tag{3.23}$$

$$B = C_b W_b \tag{3.24}$$

where

σ : electric conductivity of the material (S/m);

ρ : material density (kg/m^3);

C_b : specific heat of the blood (J/kg. ºC);

W_b : blood perfusion coefficient (W/K/m^3);

k : coefficient of heat conductivity (W/m. ºC);

T_b : blood temperature (ºC).

The bioheat equation includes the effects of blood perfusion and SAR, and results in temperature value.

The determination of the operating frequency is a very important design parameter, affecting the size of the applicator, the penetration depth, the application duration, and more. For this purpose, two patch antennas were designed for two different frequencies on a simplified human model including skin and fat layers, and a liver extracted from human MRI images which was imported into CST MWS for simulations. The liver in Avizo, and the simplified model in CST MWS can be seen in the following figures (Figure 3.53 – 3.54). Also, the dielectric properties, permittivity and conductivity, of each tissue type are provided in Figure 3.55 – 3.57.

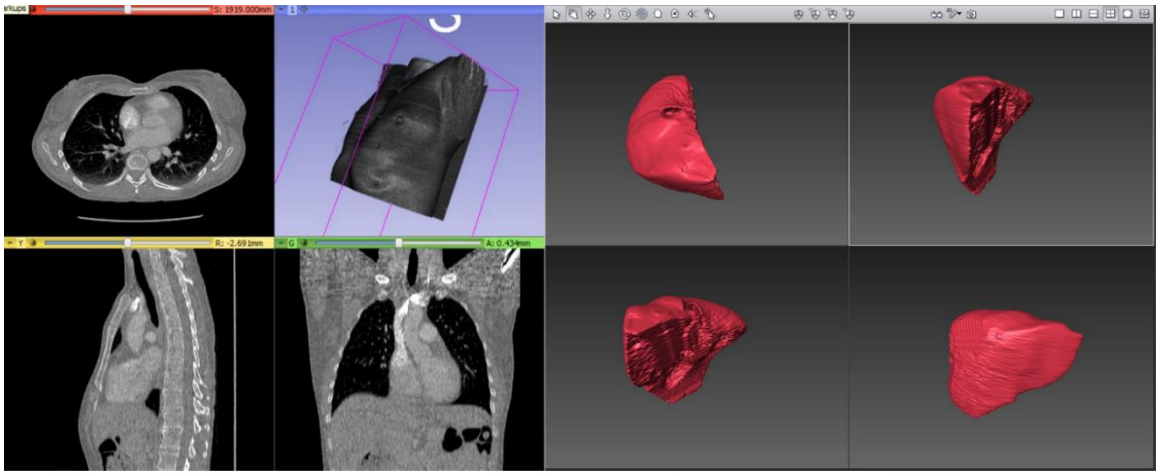

Figure 3.54 Liver extracted from MRI images via Avizo 8.1

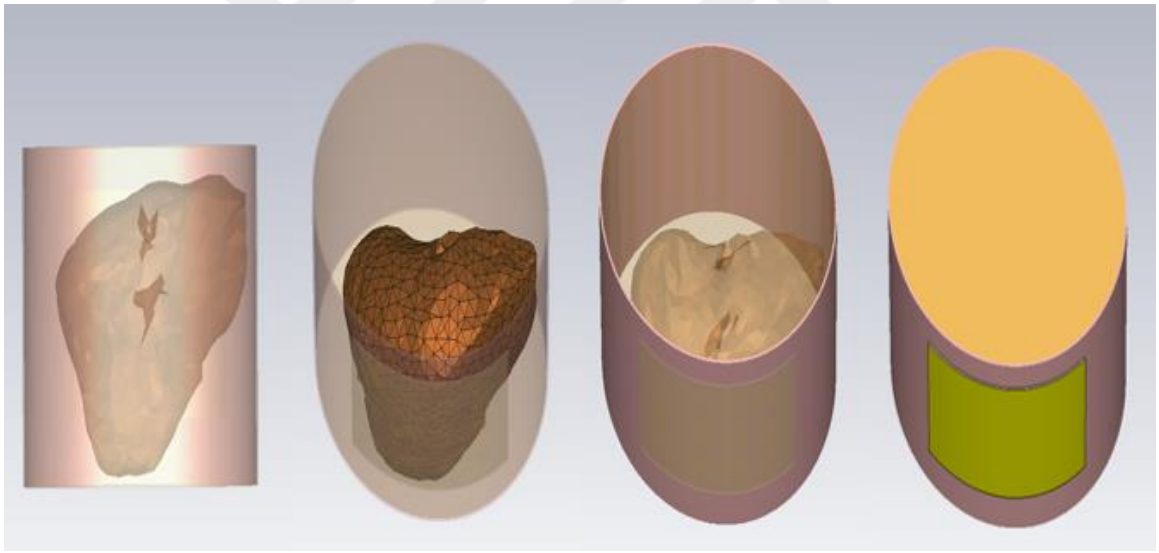

Figure 3.55 Simplified human model in CST MWS for EM and thermal simulations

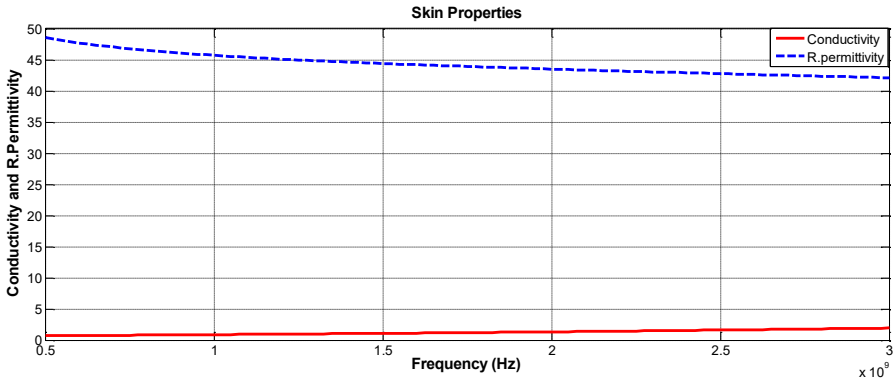

Figure 3.56 Dielectric properties of skin

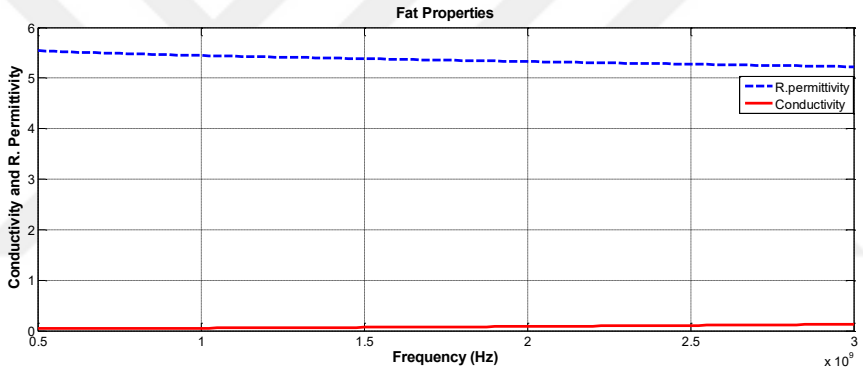

Figure 3.57 Dielectric properties of fat

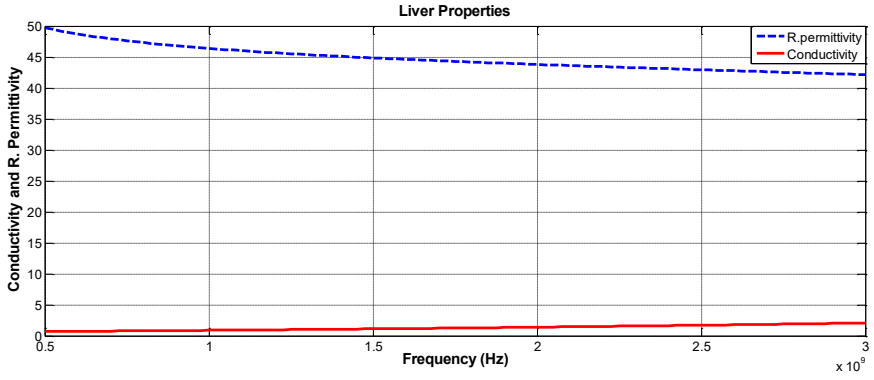

Figure 3.58 Dielectric properties of liver

3.4 Results

The simulations are perfomed by Computer Simulation Technology (CST) Microwave Studio (MWS) that has complete technology for EM field and thermal simulations. After all required elements of the system are designed, built, and optimized (applicators, feeding network, and simplified human model), they were combined for complete simulations. First of all, the EM solver of CST is used to calculate fields and losses, and simulates the behaviour of the EM field. After the EM simulations are completed and power loss is calculated inside the tissue, it is time to convert this data into temperature using the thermal solver of CST. These simulations are quite time consuming if a commercially available whole human body model (HUGO) is used. Therefore, I utilized a simplified model as shown in Figure 3.54. A single iteration for this simplified modal requires more than 30 minutes to complete on a standard personal computer. Depending on the population size of the optimization routine and specifications of the computer system, a complete numerical solution with optimization may take up to 2 months. The computer system used for this research has the following system specifications:

- Processor: i7 @ 2.60 GHz
- Memory (RAM): 32 GB
- System type: 64-bit operating system.

The simulation and experiment results for the applicator designs are shown in the following sections. Experimental measurements were undertaken to demonstrate the consistency and connection of the numerical results with real life application.

3.4.1 Simulation Results

The mild HT applicator optimization process focuses on the amplitude and phase of the input power for each antenna element on the applicator. In the GA, the antenna dimensions (length, width, feeding length, and length of the power divider vertical arms) are adjusted for each iteration. The lengths and widths of the two horizontal arms have fixed values. The overal size of the applicators are also fixed depending on the plates (substrates) used in milling machine. The steps of the optimization proces are shown in Figures 3.58 – 3.61 to demonstrate the number of iterations and changes in the variables. Table 3.3 indicates the optimized amplitudes and phases for the antenna input powers. The effects of the phase (< 0.1 °C) on the temperature increase can be neglected according to results compared for constant phase (0°) and optimized applicators.

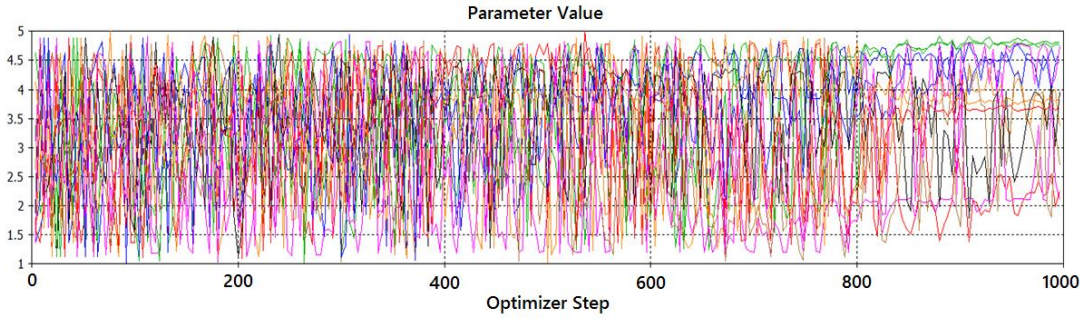

Figure 3.59 Amplitude optimization steps for the mild HT applicator at 915 MHz

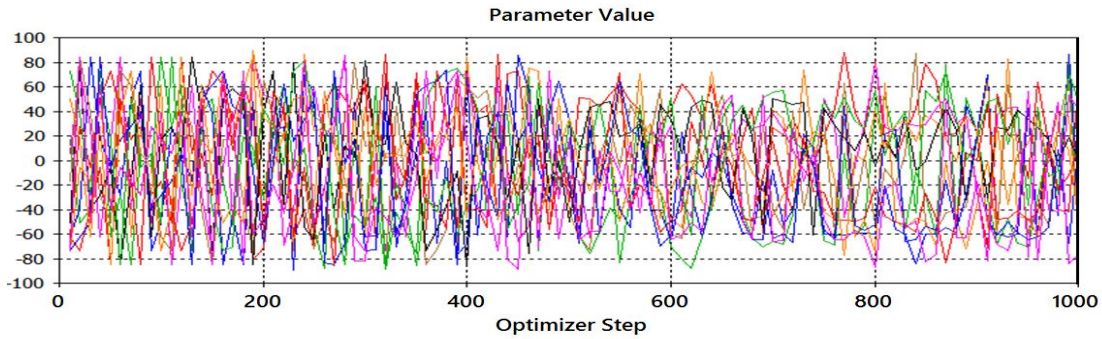

Figure 3.60 Phase optimization steps for the mild HT applicator at 915 MHz

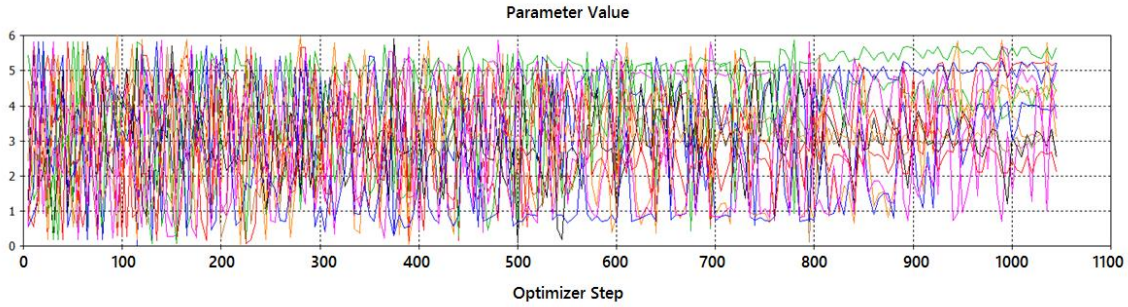

Figure 3.61 Amplitude optimization steps for the mild HT applicator at 2.4 GHz

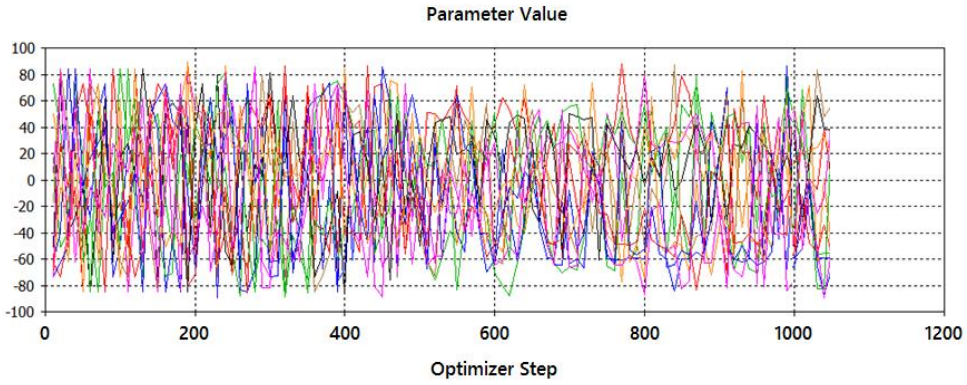

Figure 3.62 Phase optimization steps for the mild HT applicator at 2.4 GHz

Table 3.3 Optimized amplitude and phase of the input power for each antenna

	Amplitude (Watt)		Phase (Degree)	
	915 MHz	2.4 GHz	915 MHz	2.4 GHz
Antenna1	2.5	5.2	2.5	-4.2
Antenna2	4	4.3	68.7	-15.2
Antenna3	4.5	5.25	57.3	18
Antenna4	3.5	4.25	75.3	-11.1
Antenna5	2.5	4.7	-53.4	27.7
Antenna6	2.75	4.3	-24.6	50.1
Antenna7	4	3.3	-75.4	27.4
Antenna8	3.75	3.7	16.6	10.6
Antenna9	4.5	4.5	-17.9	-63.4
Antenna10	4.75	4	31	53.7
Antenna11	3.5	5	20	-6.1
Antenna12	4.75	5.5	54.7	19.6

Both EM and thermal simulations are required to determine the temperature increase inside the tissue. The required electric field characteristics are obtained first for the mild HT applications at 915 MHz and 2.4 GHz, which are then used in the thermal solver to obtain the SAR graphs and temperature distributions. The electric field results are taken at the end of the 10th minute of the mild HT application. Three different views are presented (side, top, and front) as color maps for the liver model. Then, the SAR results are determined from the 'Post Processing' menu in CST MWS. The temperature distributions are found using the Multi Physics Studio (MPS) component of CST. The temperature variation is observed for 20 points inside the liver during the 10 minute duration of the mild HT application. The thermal results are sampled at the beginning of the application and at 100, 200, 400, and 600 seconds. The following figures (Figure 3.62 – 3.80) show the E-field and SAR results at 600 seconds and the transient increase of the tissue temperature of the mild HT applications for 915 MHz and 2.4 GHz.

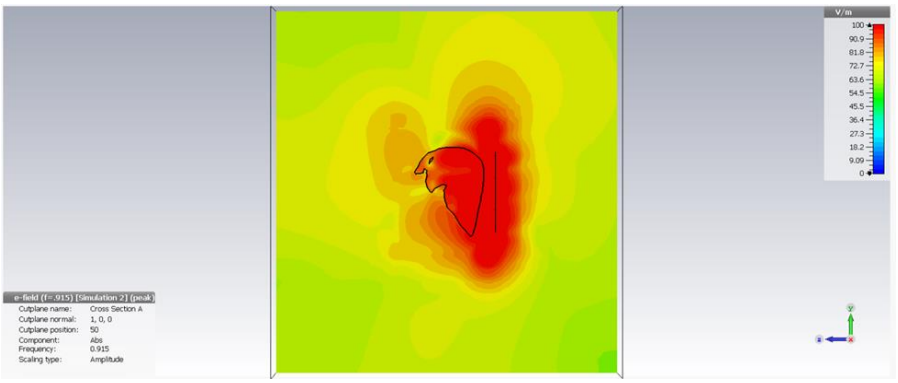

Figure 3.63 E-field simulation results of 915 MHz mild HT application (side view)

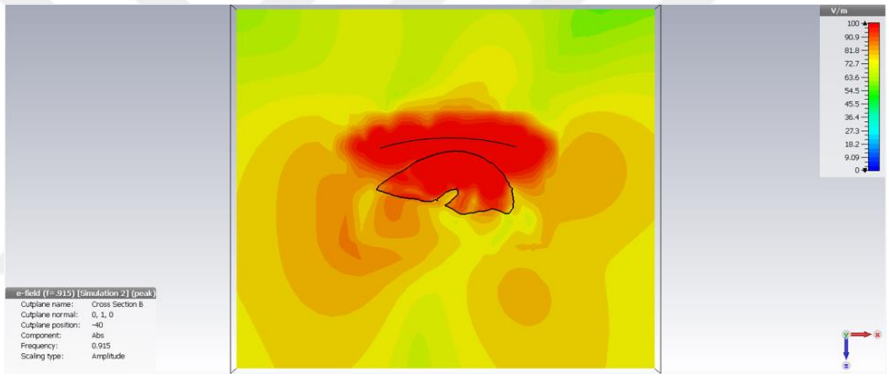

Figure 3.64 E-field simulation results of the mild HT application at 915 MHz (top view)

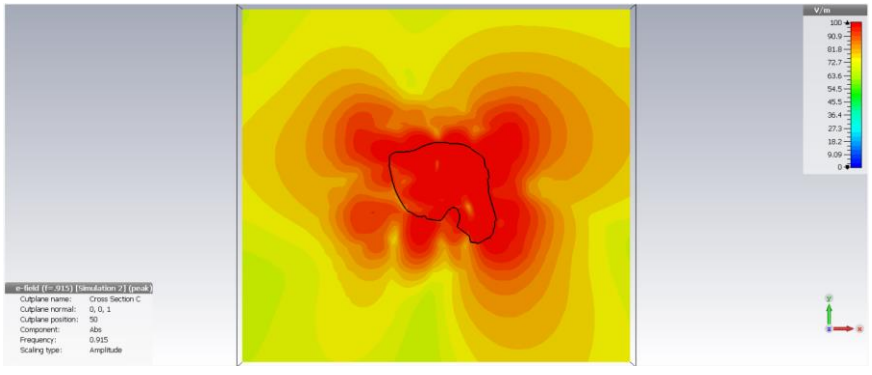

Figure 3.65 E-field simulation results of the mild HT application at 915 MHz (front view)

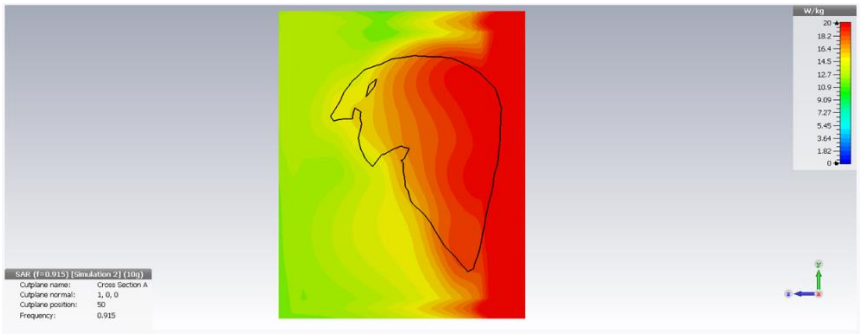

Figure 3.66 SAR results at 915 MHz (side view)

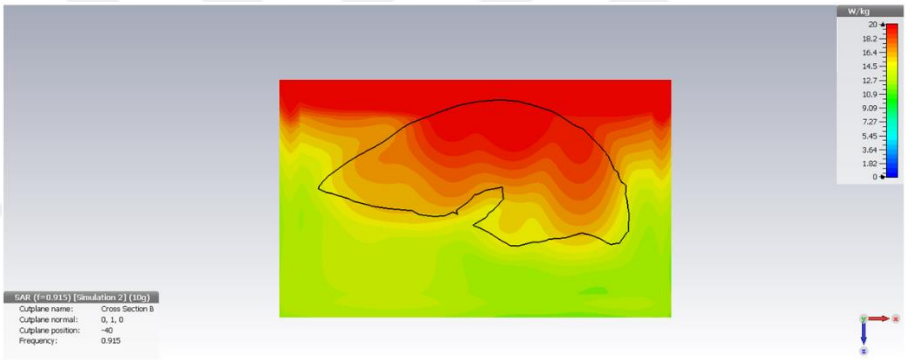

Figure 3.67 SAR results at 915 MHz (top view)

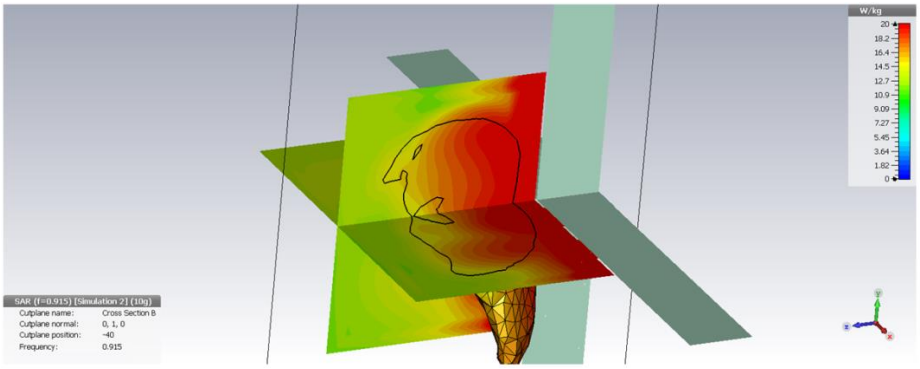

Figure 3.68 SAR results at 915 MHz

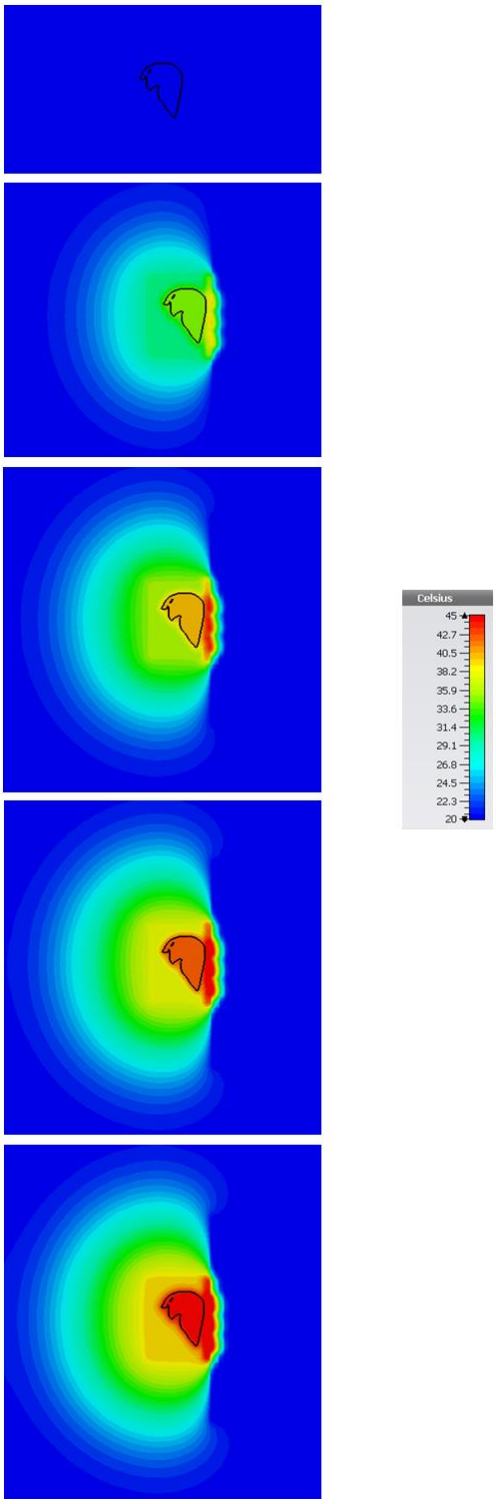

Figure 3.69 Transient temperature increase inside the liver at 915 MHz

Results at 0, 100, 200, 400, 600 seconds (from top to bottom)

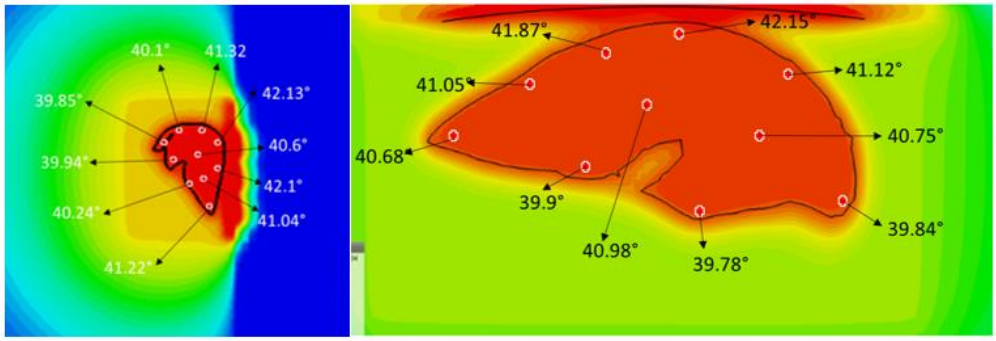

Figure 3.70 Temperature values for 915 MHz application on side and top view (with maximum skin temperature of 49.8 °C)

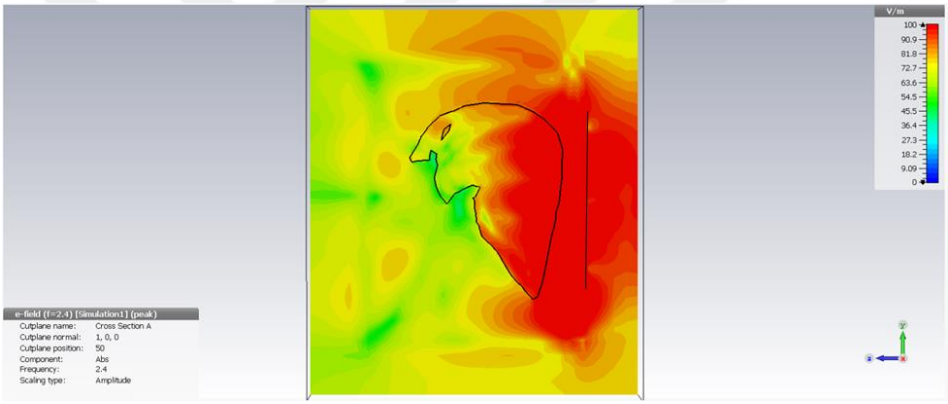

Figure 3.71 E-field simulation results of the mild HT application 2.4 GHz (side view)

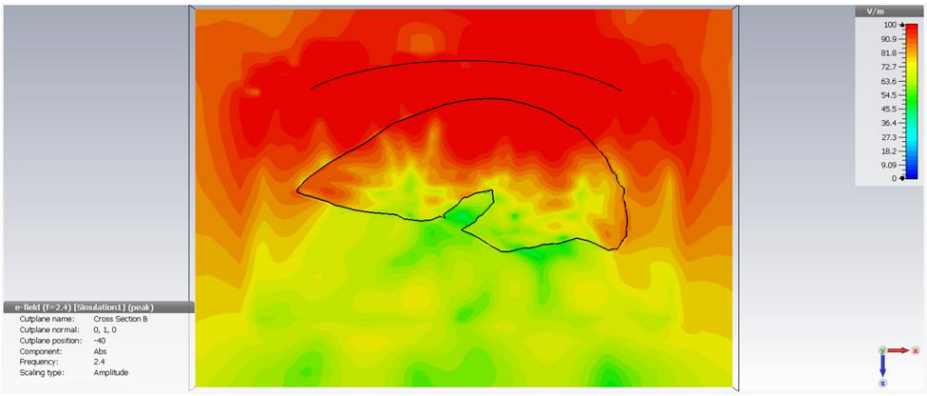

Figure 3.72 E-field simulation results of the mild HT application 2.4 GHz (top view).

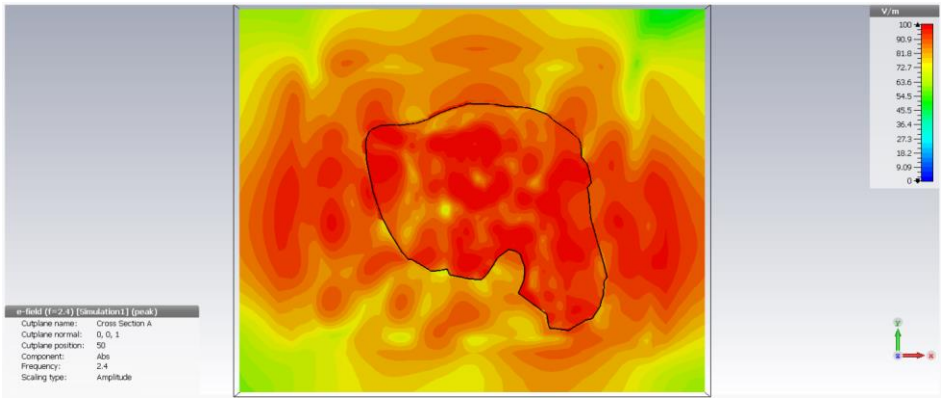

Figure 3.73 E-field simulation results of the mild HT application 2.4 GHz (front view)

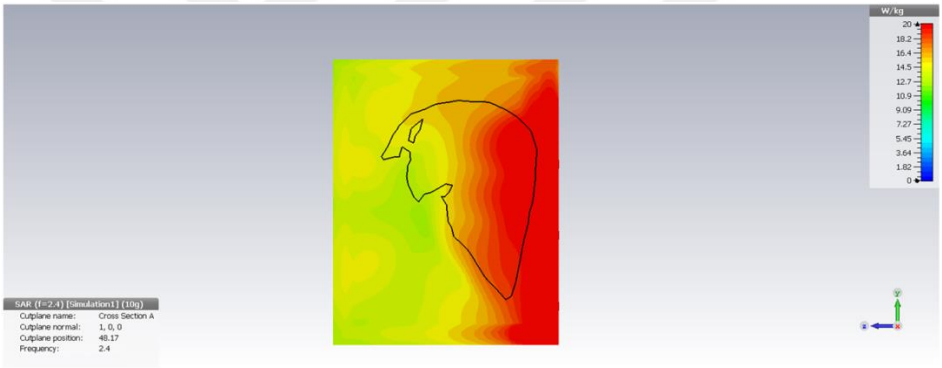

Figure 3.74 SAR results at 2.4 GHz (side view)

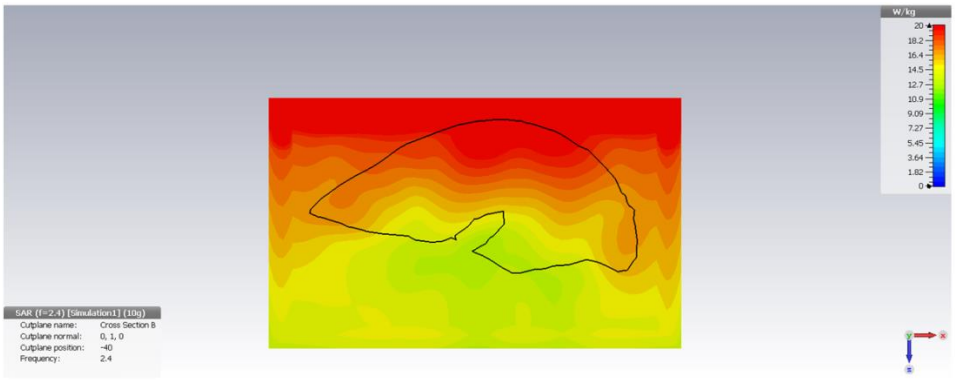

Figure 3.75 SAR results at 2.4 GHz (top view)

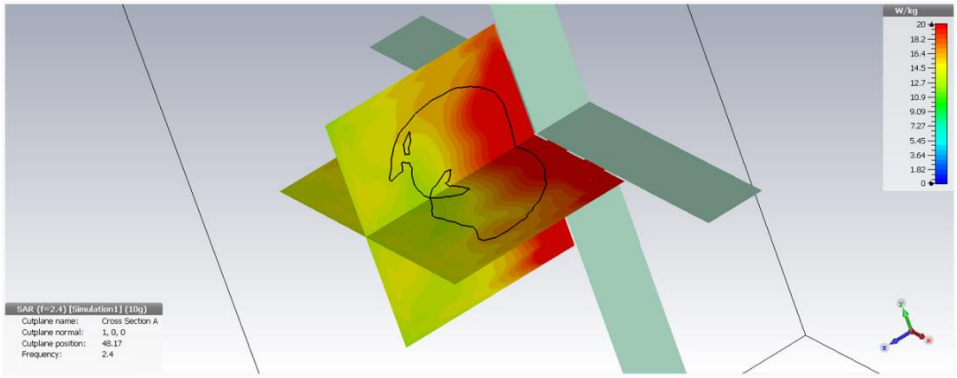

Figure 3.76 SAR results at 2.4 GHz

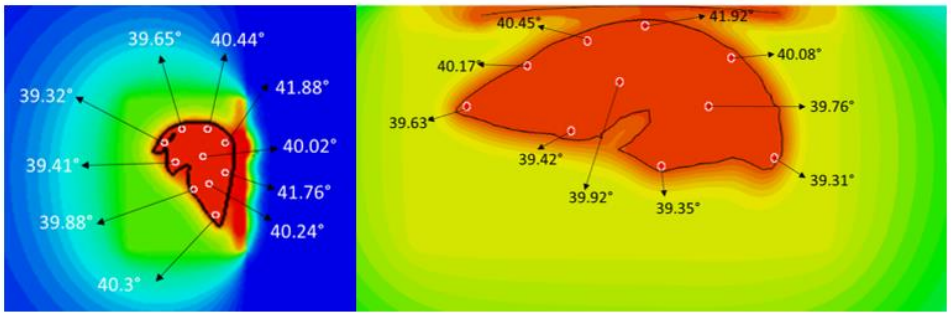

Figure 3.77 Temperature values for 2.4 GHz application on side and top view (with maximum skin temperature of 48.52 °C)

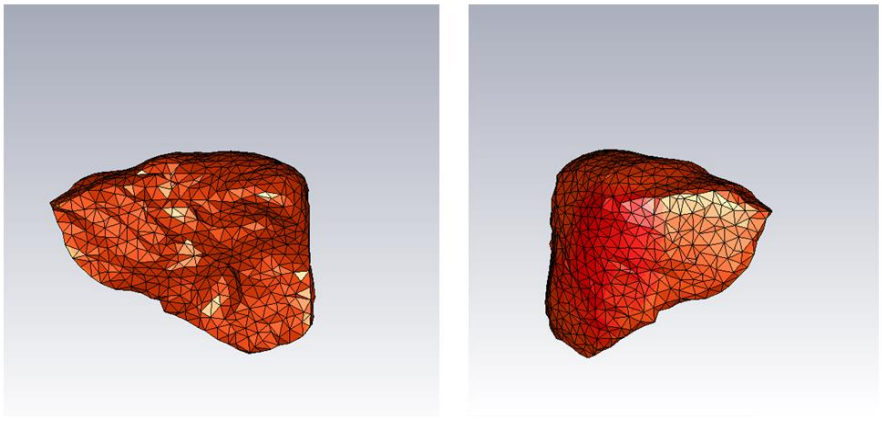

Figure 3.78 Whole liver used in human model for simulations

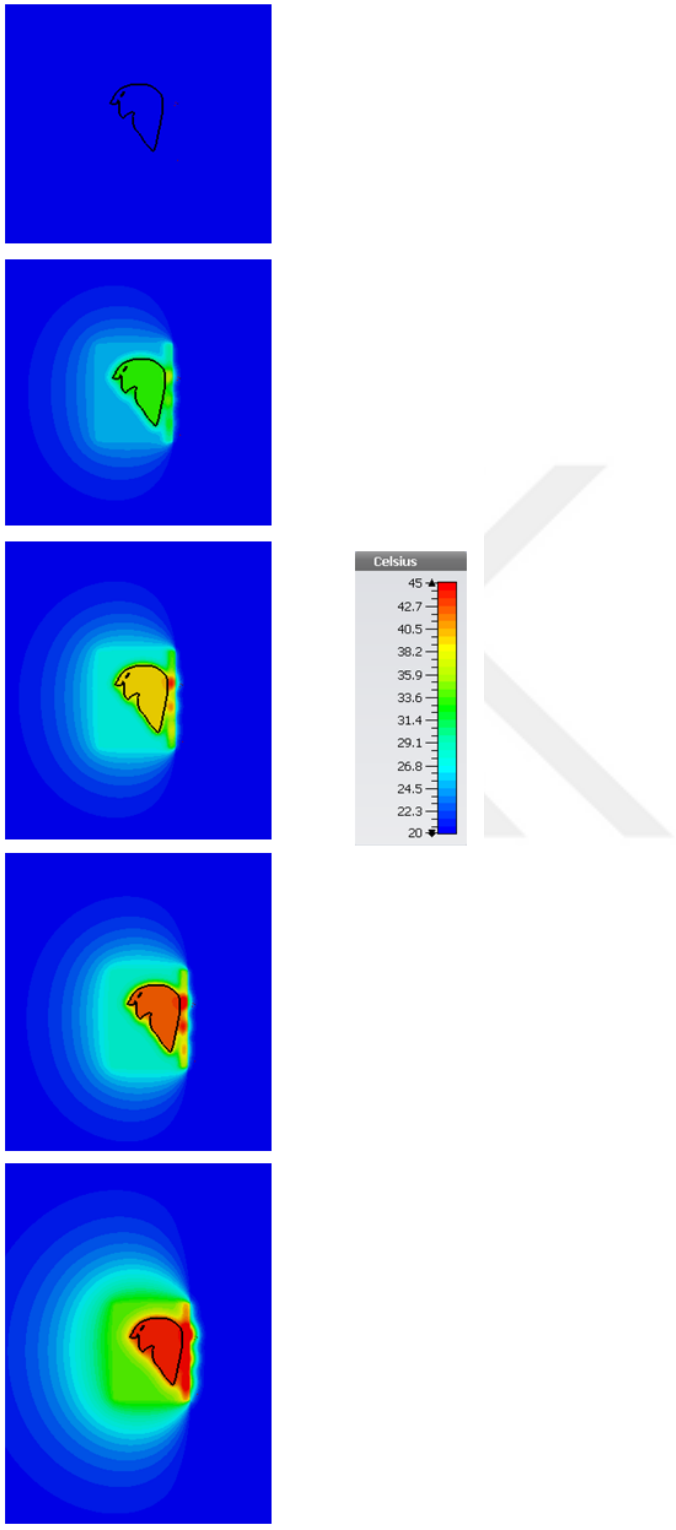

Figure 3.79 Transient temperature increase inside the liver at 2.4 GHz

Results at 0, 100, 200, 400, 600 seconds (from top to bottom)

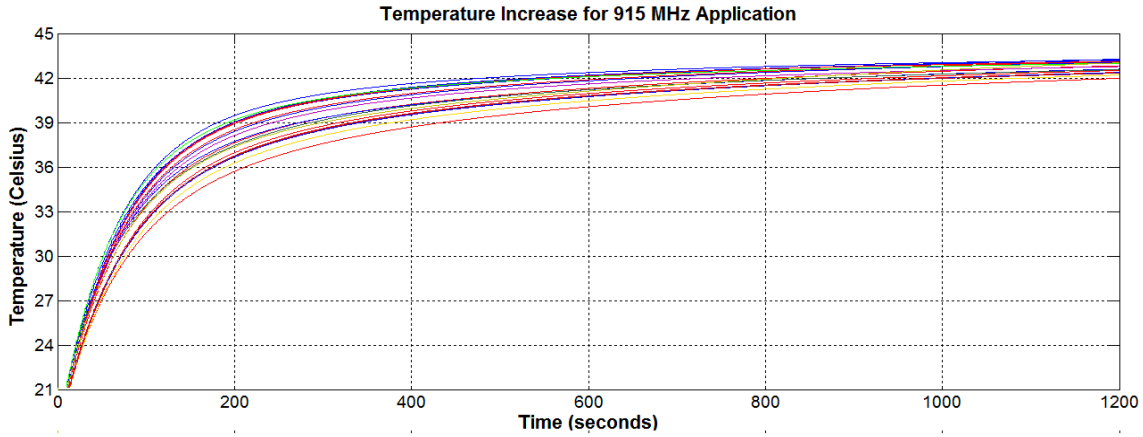

Figure 3.80 Temperature increase at 915 MHz at each selected point

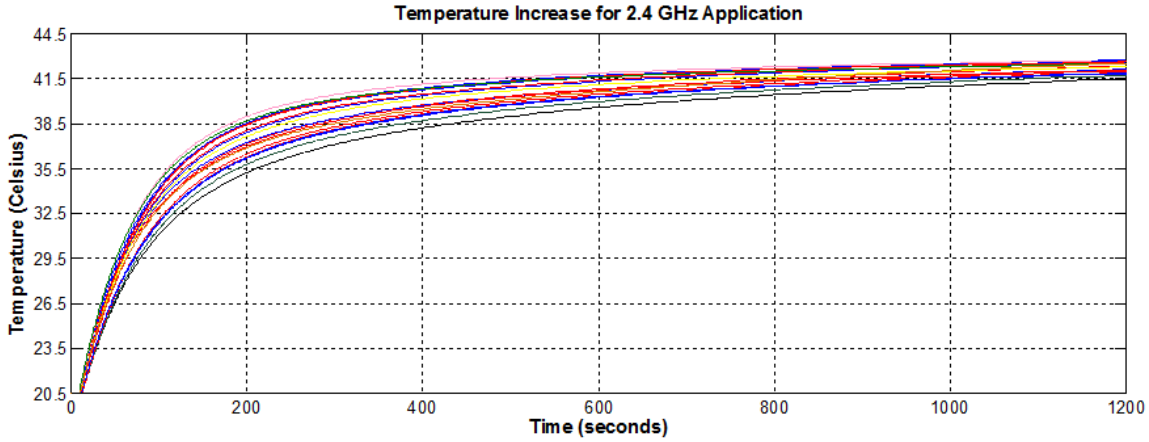

Figure 3.81 Temperature increase at 2.4 GHz at each selected point

Due to power amplifier output limitations, the overall applicator designs could not be tested in the laboratory based on the power required to heat the liver at the given

depths of penetration. An experimental measurement that required less field penetration was proposed. The whole liver model was replaced with a liver slice near the skin surface and the element power levels were replace by normalized values based on the available power in order to verify analytical results with *ex-vivo* experiments. The thickness of the slice is 2 cm, and the power amplitudes are normalized by 6.75. Normalized input powers are shown in Table 3.4. The liver slice model and the simulation results can be seen in the Figure 3.81 and Figure 3.82 – 3.83, respectively.

Table 3.4 Normalized power levels (Watt)

Antenna1	0.77	Antenna7	0.49
Antenna2	0.64	Antenna8	0.55
Antenna3	0.78	Antenna9	0.67
Antenna4	0.63	Antenna10	0.59
Antenna5	0.70	Antenna11	0.74
Antenna6	0.64	Antenna12	0.81

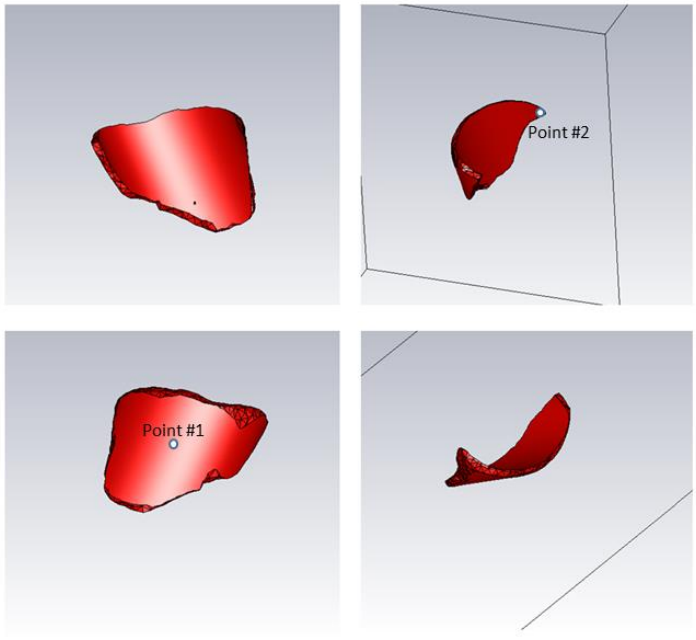

Figure 3.82 Liver slice model used in the simulations

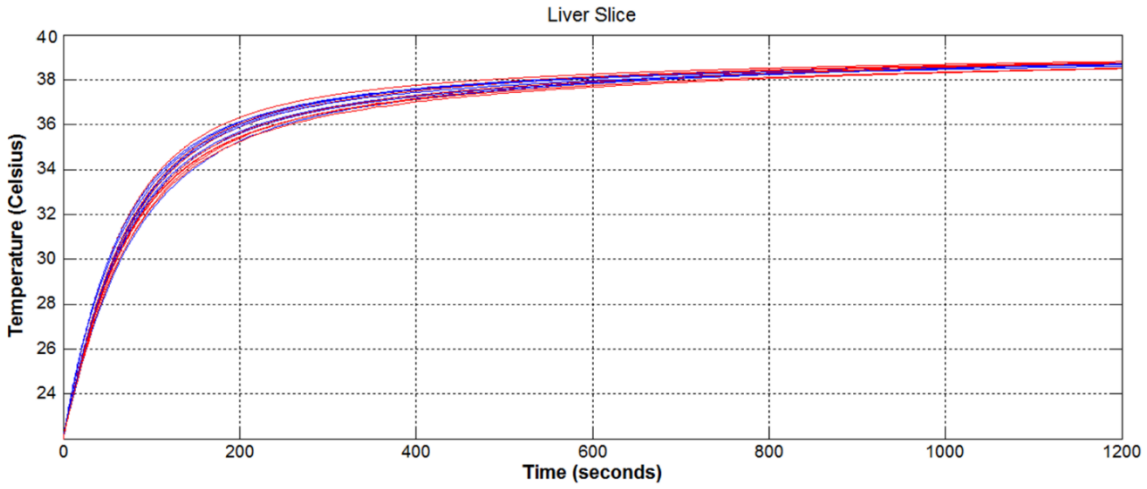

Figure 3.83 Temperature increase inside the liver slice at selected points

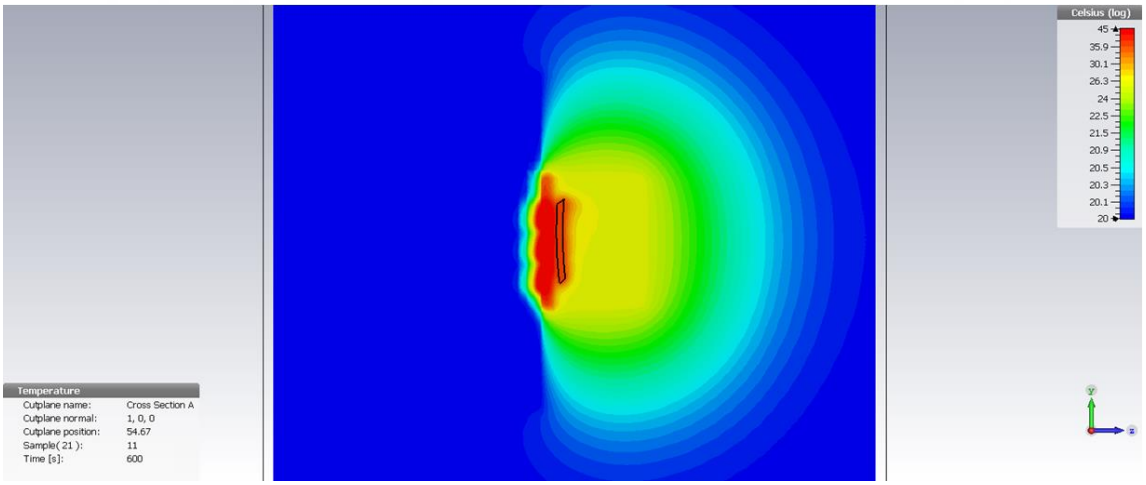

Figure 3.84 Color map for temperature increase inside the liver slice

The temperature increase with updated model and power levels is between 0.8 and 1.3 °C. The increment at the closest point - in the middle of the surface - to the skin

is 1.3°C and at the furthest point – the top right - to the skin is 0.8 °C according to the simulation results.

3.4.2 Experiment Results

Given the optimized applicator design, an applicator was fabricated (Figure 3.84) along with the power divider (Figure 3.85) using a milling machine (LPKF ProtoMat S62). A porcine liver was obtained for *ex-vivo* measurements. The experiment setup (Figure 3.88) includes a signal generator, a power amplifier, fiber-optic temperature sensors, human mimicking gels (5mm skin and 20 mm fat layers in thickness), and the porcine liver (Figure 3.86). During the experiment (~ 12 minutes), the temperature increase was observed continuously at two points. One point (Point #1 in Figure 3.81) is in the middle of the closer surface of the liver to the fat layer. The other point (Point #2 in Figure 3.81) is 2 cm away from the fat layer inside the liver. Temperature values were collected at ten different points at the end of the experiment before the power was turned off.

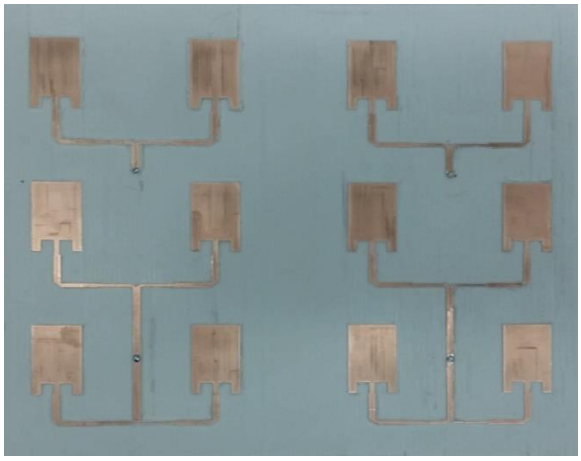

Figure 3.85 Fabricated mild HT applicator

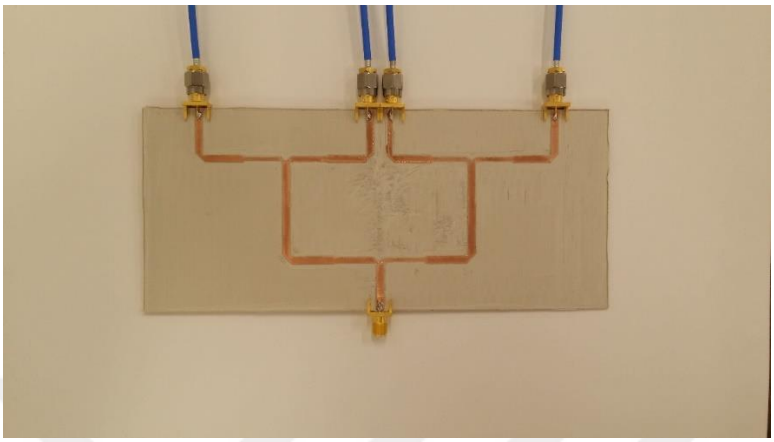

Figure 3.86 Fabricated external power divider

Figure 3.87 Porcine liver – skin mimicking gel – fat mimicking gel

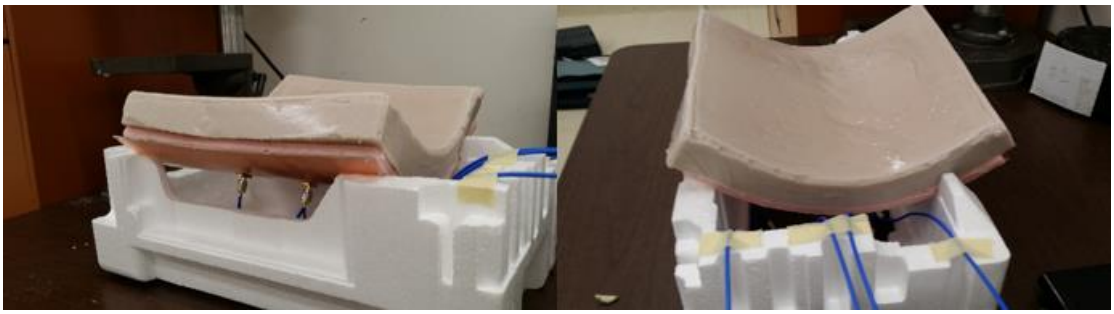

Figure 3.88 Skin and fat layers on the mild HT applicator

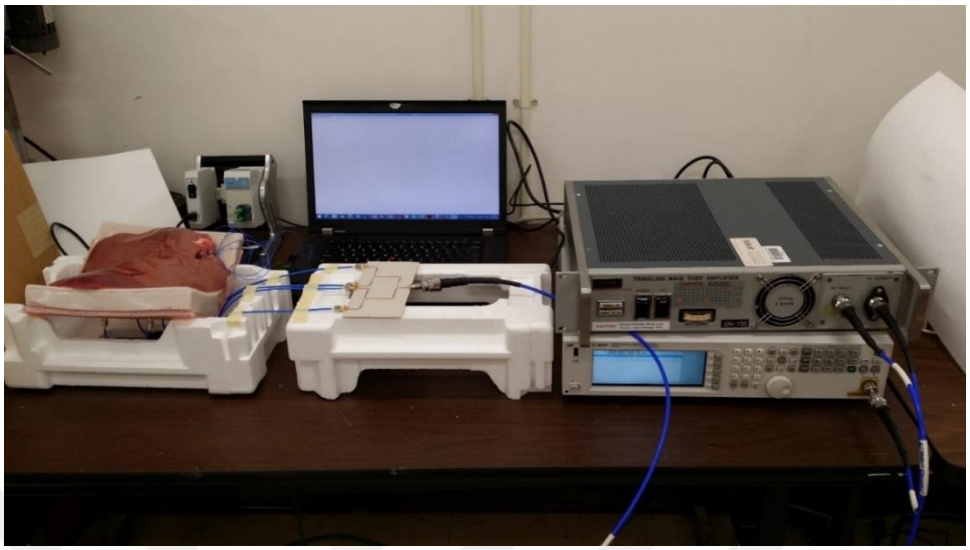

Figure 3.89 Mild HT experiment setup

The monitored temperature increment graph is provided in Figure 3.89. The results from the experiment coincide with the analytical results except for the rise in the graph at the beginning of the mild HT application. The selected ten points in simulation are also compared with experimental values and provided in Table 3.5.

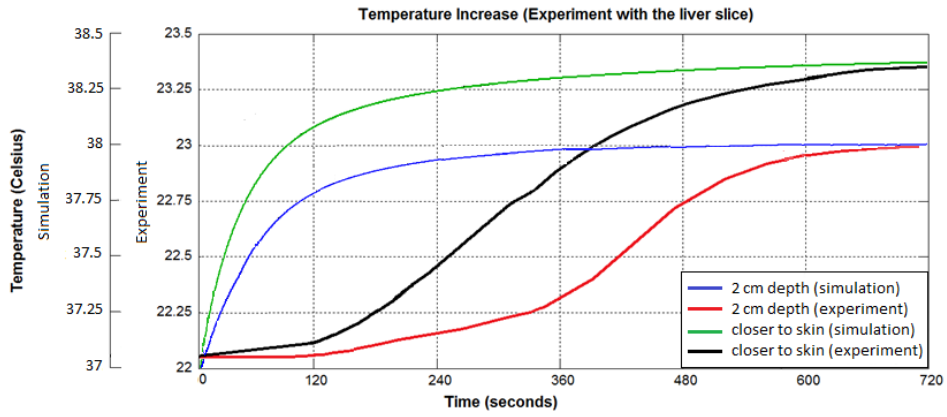

Figure 3.90 Temperature increase during the *ex-vivo* experiment

Table 3.5 Temperature Increase Inside the Liver Slice (°C)

Simulation		Experimental	
Inner Face	Outer Face	Inner Face	Outer Face
1.3	0.92	1.26	0.9
1.28	0.91	1.2	0.86
1.21	0.85	1.14	0.79
1.18	0.82	1.13	0.78
1.17	0.8	1.08	0.74

The numerical model of the mild HT applicator shows that surface temperatures could go up to 50 °C using the power levels for the required field penetration. The undesired temperature increase on the skin can be eliminated by using a cooling mechanism. There have been many cooling techniques used with HT inccluding circulating cold water, alcohol sprays, and air streams which provide rapid cooling up to 10 °C and keep the tissue at a constant temperature to a depth of 2 cm [112 – 119].

CHAPTER IV

CONCLUSIONS AND FUTURE WORK

4.1 Conclusions

The latest advances in technology make hyperthermia popular as an adjunctive treatment among thermal therapies to treat cancer in any organ or body part. The most important advantages of HT are its noninvasive and painless properties when used with an efficient cooling system, and helping to shorten the application time. Furthermore, mild HT application can make cancer treatment cheaper and more accessible for patients.

This dissertation provides MW antennas and antenna array designs as mild HT applicators through optimization. Genetic algorithm (GA) is used for the optimization of the antenna arrays due to the reference electromagnetics applications of GA in the literature. The goal of the algorithms used in this study is to provide the best temperature distribution inside the tissue compared to user defined limits.

Increasing demands for the adjuvant therapy of HT has resulted from the contributions of thermal therapy to traditional treatments. EM radiation inside the tumor provides a temperature and blood perfusion increment that helps radiation therapy and chemotherapy to be more efficient. However, existing HT systems require high input power per element on the applicators and long application time. Designing conformal and patient specific applicators with mild application can solve this issue.

The patch antenna is a good option for HT applicator design due to the ease of feeding and ground plane advantages that minimize back radiation. Therefore, two different patch antennas are optimized for 915 MHz and 2.4 GHz, and used for the array and applicator construction. The two applicators, including 12 microwave antennas, are optimized for 915 MHz and 2.4 GHz on a simplified human model. Then, optimized and simulated mild HT applicators are tested on *ex-vivo* porcine liver. According to the temperature increase inside the porcine liver, analytical results agree with *ex-vivo* experiment results. Chapter 3 shows the designs and the figures in details.

4.2 Future Work

Optimization and design of a conformal patient specific mild HT applicator is provided in this study, and further studies may provide better results. First of all, a whole human model should be used for simulations to see the effects of a more heterogeneous model. Second, animal and/or human tests with proper equipment are required to verify whole analytical model simulation results. Finally, different array configurations can be tested to see the influence of antenna placements and different antenna topologies.

REFERENCES

[1] G. Ma, and G. Jiang, "Review of tumor hyperthermia technique in biomedical engineering frontier," *International Conference on Biomedical Engineering and Informatics (BMEI)*, vol.4, no., pp.1357-1359, 16-18 Oct. 2010.

[2] M. Anbar, Thermology in the 21st century-the biomedical future of a technology based on defense oriented engineering. *Proceedings of the 16th Annual International Conference of the IEEE Engineering in Medicine and Biology Society*. Engineering Advances: New Opportunities for Biomedical Engineers, 1994. New York, USA.

[3] J. Fenn, G. L. Wolf, and R. M. Fogle, "An adaptive microwave phased array for targeted heating of deep tumours in intact breast: animal study results", *Int. J. Hyperthermia*, vol. 15, pp. 45-61, 1999.

[4] S. Fujimoto, K. Kobayashi, M. Takahashi, K. Nemoto, I. Yamamoto, T. Mutou, T. Toyasawa, T. Ashida, S. Hayashi, N. Igarashi and H. Ohkubo, "Clinical pilot studies on pre-operative hyperthermic tumour ablation for advanced breast carcinoma using an 8MHz radiofrequency heating device", *Int. J. Hyperthermia*, vol. 19, pp. 13-22, 2003.

[5] J. W. Strohbehn, Evan B. Douple, "Hyperthermia and Cancer Therapy: A Review of Biomedical Engineering Contributions and Challenges," *IEEE Transactions on Biomedical Engineering*, vol. BME-31, no.12, pp.779-787, Dec. 1984.

[6] C. C. Vernon, J. W. Hand, S. B. Field, D. Machin, J. B. Whaley, J.van der Zee, W. L. J. van Putten, G. C. van Rhoon, J. D. P. van Dijk,D. G. Gonzalez, F. F. Liu, P. Goodman, and M. Sherar, "Radiotherapy with or without hyperthermia in the treatment of superficial localized breast cancer: Results from five randomized controlled trials," *Int. J.Rad. Oncol. Biol. Phys*., vol. 35, no. 4, pp. 731-744, July 1996. National Cancer Center Singapore, "Cancer Update", vol. 2, 2006.

[7] J. W. Hand, D. Machin, C. C. Vernon, and J. B. Whaley, "Analysis of thermal parameters obtained during phase III trials of hyperthermia as an adjunct to radiotherapy in the treatment of breast carcinoma," *Int. J. Hyperthermia*, vol. 13, pp. 343-364, 1997.

[8] D. S. Kapp, "Efficacy of adjuvant hyperthermia in the treatment of superficial recurrent breast cancer: Confirmation and future directions," *Int. J. Rad. Oncol. Biol. Phys.*, vol. 35, pp. 1117-1121, 1996.

[9] H. C. Nauts, J. E. Robinson and M. J. Wisenberg, "Pyrogen therapy of cancer. A historical overview and current activities*", Proc. Int. Symp. Cancer Therapy by Hyperthermia and Radiation*, pp. 239 -250, 1976.

[10] G. M. Hahn, "Hyperthermia and Cancer," pp.1 -285, 1982.

[11] N. B. Hornbeck, "Hyperthermia and Cancer: Human Clinical Trial Experience," vol. I and II, pp. 1 -146, 1984.

[12] J. G. Short and P. F. Turner, "Physical hyperthermia and cancer therapy," *IEEE Proc*., vol. 68, pp. 133 -142, 1980.

[13] W. B. Coley, "The treatment of malignant tumors by repeated innoculations of erysipelas with a report of ten original cases", *Amer. J. Med. Sci*., vol. 105, pp. 488 -511, 1893.

[14] H. Gerhard, H. G. Klinger, E. Gabriel, "Short term hyperthermia: in vitro survival of different human cell lines after short exposure to extreme temperatures," *Streffer C., ed. Cancer Therapy by Hyperthermia and Radiation*, Baltimore: Urban & Schwarzenberg, pp. 201-3, 1978.

[15] S. A. Sapareto, W. C. Dewey, "Thermal dose determination in cancer therapy," *lnt. J. Radiat. Oncol. Biol. Phys.*, vol. 10, pp. 787-800, 1984.

[16] S. B. Field, J. W. Hand, "An Introduction to the Practical Aspects," *Clinical Hyperthermia*, New York: Taylor & Francis, pp. 293, 1990.

[17] G. C. van Rhoon, M. M. Paulides, P. Togni, R. A. M. Canters, Z. Rijnen, G. van de Velde-Verduijn, P. C. Levendag, "Challenges of the clinical application of hyperthermia for head and neck tumors," *7th European Conference on Antennas and Propagation (EuCAP)*, pp.635-637, 8-12 April 2013.

[18] Di-Xiang Yin, Meng Li, J. L. Li, "Non-invasive breast cancer thermotherapy studies using conformal microstrip antennas," in Antennas, Propagation & EM Theory (ISAPE), 2012 10th International Symposium on , pp.159-162, 22-26 Oct. 2012.

[19] C. W. Song, A. Lokshina, J. Rhee , M. Patten and S. H. Levitt "Implication of blood flow in hyperthermic treatment of tumors," *IEEE Trans. Biomed. Eng.*, vol. BME-31, pp. 9 -16, 1984.

[20] H. H. Kampinga, E. Dikomey, "Hyperthermic radiosensitization: mode of action and clinical relevance," *Int. J. Radiat. Biol.*, vol. 77, pp. 399- 408, 2001.

[21] R. Valdagni, F. F. Liu, and S. Kapp, “Important prognostic factors influencing outcome of combined radiation and HT,” *Int. J. Radiat. Oncol. Biol. Phys.*, vol. 15, pp. 959-972, 1988.

[22] R. Valdagni, and M. Amichetti, “Report of long-term follow-up in a randomized trial comparing radiation therapy and radiation therapy plus hyperthermia to metastatic lymphnodes in stage IV head and neck patients,” *Int. J. Radiat. Oncol. Biol. Phys.*, vol. 28, pp. 163-169, 1993.

[23] M. Amichetti, M. Romano, L. Busana, A. Bolner, G. Fellin, G. Pani, L. Tomio, R. Valdagni, “Hyperfractionated radiation in combination with local hyperthermia in the treatment of advanced squamous cell carcinoma of the head and neck: a phase I-II study,” *Radiother. Oncol*., vol. 45, pp. 155-158, 1997.

[24] N. G. Huilgol, S. Gupta, C.R. Sridhar, “Hyperthermia with radiation in the treatment of locally advanced head and neck cancer: a report of randomized trial,” *J. Cancer Res. Ther*., vol. 6, pp. 492-496, 2010.

[25] L. Li, T. L. ten Hagen, D. Schipper, T. M. Wijnberg, G. C. van Rhoon, A. M. Eggermont, L. H. Lindner, G. A. Koning, “Triggered content release from optimized stealth thermosensitive liposomes using mild hyperthermia*,” J. Control Release*, vol. 19, pp. 274-279, 2010.

[26] Z. Vujaskovic, D. W. Kim, E. Jones, L. Lan, L. McCall, M. W. Dewhirst, O. Craciunescu, P. Stauffer, V. Liotcheva, A. Betof, K. Blackwell, “A phase I/II study of neoadjuvant liposomal doxorubicin, paclitaxel, and hyperthermia in locally advanced breast cancer,” *Int. J. Hyperthermia*, vol. 26, pp. 514-521, 2010.

[27] W. C. Choi, K. J. Kim, H. S. Park, Y. J. Yoon, "Frequency reconfigurable applicator for superficial hyperthermia system," *International Symposium on Antennas and Propagation (ISAP)*, pp.26-29, 2012.

[28] R. A. Gardner, H. I. Vargas, J. B. Block et al., “Focused microwave phased array thermotherapy for primary breast cancer,” *Ann. Surg. Oncol*., vol. 9, pp. 326–332, 2002.

[29] C. C. Vernon, J. W. Hand, S. B. Field et al., “Radiotherapy with or without hyperthermia in the treatment of superficial localized breast cancer: results from five randomized controlled trials,” *lnt. J. Radiat. Oncol. Biol. Phys*., vol. 35, pp. 731-744, 1996.

[30] R. Valdagni, M. Amichetti, “Report of long-term follow-up in a randomized trial comparing radiation therapy and radiation therapy plus hyperthermia to metastatic lymphnodes in stage IV head and neck patients,” *lnt. J. Radiat. Oncol. Biol. Phys.*, vol. 28, pp. 163-169, 1993.

[31] J. Overgaard, D. Gonzalez, M. C. C. H. Hulshof et al., “Hyperthermia as an adjuvant to radiation therapy of recurrent or metastatic malignant melanoma. A multicentre randomized trial by the European Society for Hyperthermic Oncology,” *Int. J. Hyperthermia*, vol. 12, pp. 3-20, 1996.

[32] J. van der Zee, D. Gonzalez, G. C van Rhoon, J. D. P. van Dijk, W. L. J. van Putten, A. A. M. Hart, “Comparison of radiotherapy alone with radiotherapy plus hyperthermia in locally advanced pelvic tumors: a prospective, randomised, multicentre trial,” *Lancet*, vol. 355, pp. 1119-1125, 2000.

[33] M. Takahashi, S. Fujimoto, K. Kobayashi et al., “Clinical outcome of intraoperative pelvic hyperthermochemotherapy for patients with Dukes' C rectal cancer*,” lnt. J. Hyperthermia*, vol. 10, pp. 749-54, 1994.

[34] K. Sugimachi, H. Kuwano, H. Ide, T. Toge, M. Saku, Y. Oshiumi, “Chemotherapy combined with or without hyperthermia for patients with oesophageal carcinoma: a prospective randomized trial,” *Int. J. Hyperthermia*, vol. 10, pp. 485-493, 1994.

[35] E. J. Hall, “Radiobiology for the Radiologist,” *Philadelphia: JB Lippincott Co*, pp. 262-263, 1994.

[36] C. A. Perez, L. W. Brady, “Principles and Practice of Radiation Oncology,” *2nd ed. Philadelphia: JB Lippincott Co*, pp. 396-397, 1992.

[37] J. van der Zee, Z. Vujaskovic, M. Kondo and T. Sugahara, "The Kadota Fund International Forum 2004-clinical group consensus," *Int. J Hyperthermia*, vol. 24, pp. 111-122, 2008.

[38] N. G. Huilgol, S. Gupta, R. Dixit, 'Chemoradiation with hyperthermia in the treatment of head and neck cancer,” *Int. J. Hyperthermia*, vol. 26, pp. 21-25, 2010.

[39] Y. Hua, S. Ma, Z. Fu, Q. Hu, L. Wang, Y. Piao, “Intracavity hyperthermia in nasopharyngeal cancer: a phase III clinical study,” *Int. J. Hyperthermia*, vol. 27, pp. 180-186, 2011.

[40] M. W. Dewhirst , D. A. Sim , S. Sapareto, and W. G. Connor "The importance of minimum tumor temperature in determining early and long term responses of spontaneous canine and feline tumors to heat and radiation’” *Cancer Res.*, vol. 44, pp. 43 -50, 1984.

[41] B. Fisher, S. Anderson, C. K. Redmond, N. Wolmark, D. L. Wickerham, W. M. Cronin, “Reanalysis and results after 12 years of follow-up in a randomized clinical trial comparing total mastectomy with lumpectomy with or without irradiation in the treatment of breast cancer,” *N. Engl. J. Med.*, vol 333, pp. 1456-1461, 1995.

[42] J. R. Harris, M. E. Lippman, U. Veronesi, W. Willett, “Breast cancer,” *N. Engl. J. Med.*, vol. 327, pp. 390-398, 1992.

[43] S. J. Schnitt, A. Abner, R. Gelman et al., “The relationship between microscopic margins of resection and the risk of local recurrence in patients with breast cancer treated with breast-conserving surgery and radiation therapy,” *Cancer Res.*, vol. 74, pp. 1746-1751, 1994.

[44] Treatment of early-stage breast cancer, *NIH Consens Statement*, vol. 8(6), pp. 1-19, 1990.

[45] T. J. Eberlein, J. L. Connolly, S. J. Schnitt et al., “Predictors of local recurrence following conservative breast surgery and radiation therapy. The influence of tumor size,” *Arch. Surg.*, vol. 125, pp. 771-775, 1990.

[46] M. Lazebnik, D. Popovic, L. McCartney, C. B. Watkins, M. J. Lindstrom, J. Harter et al., "A large-scale study of the ultrawideband microwave dielectric properties of normal, benign and malignant breast tissues obtained from cancer surgeries," *Phys. Med. Biol.*, vol. 52, pp. 6093-6115, 2007.

[47] M. V. Prior , M. L. D. Lumori , J. W. Hand , G. Lamaitre , C. J. Schneider and J. D. P. van Dijk, "The use of a current sheet applicator array for superficial hyperthermia: Incoherent versus coherent operation," *IEEE Trans. Biomed. Eng.*, vol. 42, no. 7, pp. 694 -698, 1995.

[48] M. Kowalski, B. Behnia, A. Webb and J. Jin, "Optimization of electromagnetic phased-arrays for hyperthermia via magnetic resonance temperature estimation," *IEEE Trans. Biomed. Eng.*, vol. 49, pp.1229 -1241, 2002.

[49] L. Wu, R. McGough, O. Arabe, and T. Samulski, "An RF phased array applicator designed for hyperthermia breast cancer treatments," *Phys. Med. Biol.*, vol. 51, pp.1-20, 2006.

[50] M. Paulides, J. Bakker, A. Zwamborn, and G. Rhoon, "A head and neck hyperthermia applicator: Theoretical antenna array design", *Int. J. Hyperthermia*, vol. 23, pp.59-67, 2007.

[51] K. Arunachalam, S. S. Udpa, L. Udpa, "Microwave Breast Cancer Hyperthermia using Deformable Mirror," *IEEE Antennas and Propagation Society International Symposium 2006*, pp. 2191-2194, 2006.

[52] E. S. Ebbini, S. I. Umemura, S.I., M. Ibbini, C. A. Cain, "A cylindrical-section ultrasound phased-array applicator for hyperthermia cancer therapy," *IEEE Trans. Ultrason. Ferroelect. Freq. Contr*, vol. 35, pp. 561-572, 1988.

[53] M. Seebass, R Beck, J. Gellermann, J. Nadobny and P. Wust, "Electromagnetic phased arrays for regional hyperthermia: optimal frequency and antenna arrangement," *Int. J. Hyperthermia*, vol. 17, pp. 321-336, 2001.

[54] P. M. Meaney, M. W. Fanning, K. D. Paulsen, D. Li, S. A. Pendergrass, Q. Fang, K. L. Moodie, "Microwave thermal imaging: initial in vivo experience with a single heating zone," *Int. J. Hyperthermia*, vol. 19, pp. 617-641, 2003.

[55] M. C. Joiner, B. Vojnovic, "Radiofrequency diathermy for uniform heating of mouse tumours," Br. J. Cancer Suppl., vol. 5, pp. 71–76, 1982.

[56] E. L. Jones, J. R. Oleson, L. R. Prosnitz, T. V. Samulski, et al, "Randomized Trial of Hyperthermia and Radiation for Superficial Tumors", *Journal of Clinical Oncology*, Vol. 23, No. 13, pp. 3079-3085, 2005.

[57] O. A. Arabe, P. F. Maccarini, E. L. Jones, G. Hanna, T. V. Samulski, M. W. Dewhirst, D. E. Thrall, P. R. Stauffer, "A 400 MHz Hyperthermia System using Rotating Spiral Antennas for Uniform Treatment of Large Superficial and Sub-Surface Tumors", *Digest of IMS 2007*, pp. 1333-1336, 2007

[58] A. V. Vorst, A. Rosen, Y. Kotsuka, "RF/Microwave Interaction with Biological Tissues," *John Wiley and Sons*, 2006.

[59] Y. Tao, G. Wang, "Conformal Hyperthermia of Superficial Tumor With Left-Handed Metamaterial Lens Applicator," *IEEE Transactions on Biomedical Engineering*, vol.59, no.12, pp.3525-3530, 2012.

[60] C. Gabriel, S. Gabriel, and E. Corthout, "The dielectric properties of biological tissues: I. Literature survey," *Physics in Medicine and Biology*, vol. 41, pp. 2231–2249, 1996.

[61] S. Gabriel, R. W. Lau, and C. Gabriel, "The dielectric properties of biological tissues: II. Measurements in the frequency range 10 Hz to 20 GHz," *Physics in Medicine and Biology*, vol. 41, pp. 2251–2269, 1996.

[62] S. Gabriel, R. W. Lau, and C. Gabriel, "The dielectric properties of biological tissues: III. Parametric models for the dielectric spectrum of tissues," *Physics in Medicine and Biology*, vol. 41, pp. 2271–2293, 1996.

[63] E. Topsakal, M. Asili, P. Chen, U. Demirci, N. Younan, "Flexible microwave antenna applicator for chemothermotherapy of the breast," in Wireless Mobile Communication and Healthcare (Mobihealth), 2014 EAI 4th International Conference on , pp. 328-330, 3-5, 2014.

[64] M. Asili, P. Chen, A. Z. Hood, A. Purser, R. Hulsey, L. Johnson, A. V. Ganesan, U. Demirci, E. Topsakal, "Flexible Microwave Antenna Applicator for Chemo-thermotherapy of the Breast," *IEEE Antennas and Wireless Propagation Letters*, vol. PP, no. 99, pp.1-1, 2015 (early access article).

[65] A. Z. Hood, "Meta-heuristic optimization of antennas for biomedical applications," Ph.D. dissertation, Dept. ECE, MS State Univ., Mississippi State, MS, 2013.

[66] P. Wust, B. Hildebrandt, G. Sreenivasa, B. Rau, J. Gellermann, H. Riess, R. Felix, and P. M. Schlag, "Hyperthermia in combined treatment of cancer," *The Lancet Oncology*, vol. 3, pp. 487-497, 2002.

[67] B. Hildebrand, P. Wust, O. Ahlers, A. Dieing, G. Sreenivasa, T. Kerner, R. Felix, and H. Riess, "The cellular and molecular basis of hyperthermia," *Critical Reviews in Oncology/Hematology*, vol. 43, no. 1 , pp. 33-56, 2002.

[68] A.Y. Cheung and J. Al-Atrash, "Microwave hyperthermia for cancer therapy," *IEEE Proceedings*, vol. 134, no. 6, pp. 493-522, 1987.

[69] R. Colombo, L.F. Da Pozzo, A. Lev, M. Freschi, G. Gallus, and P. Rigatti, "Neoadjuvant combined microwave induced local hyperthermia and topical chemotherapy versus chemotherapy alone for superficial bladder cancer," *The Journal of Urology*, vol. 155, no. 4, pp. 1227-1232, 1996.

[70] A.G. van der Heijden, L.A. Kiemeney, O.N. Gofrit, O. Nativ, A. Sidi, Z. Leib, R. Colombo, R. Naspro, M. Pavone, J. Baniel, F. Hasner, and J.A. Witjes, "Preliminary european results of local microwave hyperthermia and chemotherapy treatment in intermediate or high risk superficial transitional cell carcinoma of the bladder," *European Urology*, vol. 46, no. 1, pp. 65-72, 2004.

[71] J. Dragovic, H.G. Seydel, T. Sandhu, A. Kolosvary, and J. Blough, "Local superficial hyperthermia in combination with low-dose radiation therapy for palliation of locally recurrent breast carcinoma," *Journal of Clinical Oncology*, vol. 7, no. 1, pp. 30-35, 1989.

[72] C.C. Vernon, J.W. Hand, S.B. Field, D. Machin, J.B. Whaley, J. van der Zee, W.L.J. van Putten, G.C. van Rhoon, J.D.P. van Dijk, D.G. Gonzalez, F. Liu, P. Goodman, and M. Sherar, "Radiotherapy with or without hyperthermia in the treatment of superficial localized breast cancer: Results from five randomized controlled trials," *International Journal of Radiation Oncology*Biology*Physics*, vol. 35, no. 4, pp. 731-744, 1996.

[73] T. M. Zagar, K.A. Higgins, E.F. Miles, Z. Vujaskovic, M.W. Dewhirst, R.W. Clough, L.R. Prosnitz, and E.L. Jones, "Durable palliation of breast cancer chest wall recurrence with radiation therapy, hyperthermia, and chemotherapy," Radiotherapy and Oncology: *Journal of the European Society for Therapeutic Radiology and Oncology*, vol. 97, no. 3, pp. 535-540, 2010.

[74] M. S. Anscher, C. Lee, H. Hurwitz, D. Tyler, L. R. Prosnitz, P. Jowell, G. Rosner, T. Samulski, and M. W. Dewhirst, "A pilot study of preoperative continuous infusion 5-fluorouracil, external microwave hyperthermia, and external beam radiotherapy for treatment of locally advanced, unresectable, or recurrent rectal cancer," *International Journal of Radiation Oncology*Biology*Physics*, vol. 47, no. 3, pp. 719-724, 2000.

[75] C.K. Chou, "Application of electromagnetic energy in cancer treatment," *IEEE Transactions on Instrumentation and Measurement*, vol. 37, no. 4, pp. 547-551, 1988.

[76] P. Wust, H. Stahl, K. Dieckmann, S. Scheller, J. Loffel, H. Riess, J. Bier, V. Jahnke, and R. Felix, "Local hyperthermia of N2/N3 cervical lymph node metastases: Correlation of technical/thermal parameters and response," *International Journal of Radiation Oncology*Biology*Physics*, vol. 34, no. 3, pp. 635-646, 1996.

[77] D. E. Thrall, D. M. Prescott, T. V. Samulski, G. L. Rosner, D. L. Denman, R. L. Legorreta, R. K. Dodge, R. L. Page, J. M. Cline, J. Lee, B. C. Case, S. M. Evans, J. R. Oleson, and M. W. Dewhirst, "Radiation plus local hyperthermia versus radiation plus the combination of local and whole-body hyperthermia in canine sarcomas," *International Journal of Radiation Oncology*Biology*Physics*, vol. 34, no. 5, pp. 1087-1096, 1996.

[78] A. Dietsch, J.-C. Camart, J.-P. Sozanski, B. Prevost, B. Mauroy, and M. Chive, "Microwave thermochemotherapy in the treatment of the bladder carcinoma - electromagnetic and dielectric studies - clinical protocol," *IEEE Transactions on Biomedical Engineering*, vol. 47, no. 5, pp. 633-641, 2000.

[79] M. D. Sapozink, F. A. Gibbs, Jr., M. J. Egger, and J. R. Stewart, "Abdominal regional hyperthermia with an annular phased array," *Journal of Clinical Oncology*, vol. 4, no. 5, pp. 775-783, 1986.

[80] R. Colombo, A. Salonia, L.F. Da Pozzo, R. Naspro, M. Freschi, R. Paroni, M. Pavone- Macaluso, and P. Rigatti, "Combination of intravesical chemotherapy and hyperthermia for the treatment of superficial bladder cancer: preliminary clinical experience," *Critical Reviews in Oncology/Hematology*, vol. 47, no. 2, pp. 127-139, 2003.

[81] J. van der Zee, D.G. Gonzalez, G.C. van Rhoon, J.D.P. van Dijk, W.L.J. van Putten, and A.A.M. Hart, "Comparison of radiotherapy alone with radiotherapy plus hyperthermia in locally advanced pelvic tumours: a prospective, randomised, multicentre trial," *The Lancet*, vol. 355, pp. 1119-1125, 2000.

[82] R. Colombo, L. F. Da Pozzo, A. Lev, M. Freschi, G. Gallus, and P. Rigatti, "Neoadjuvant combined microwave induced local hyperthermia and topical chemotherapy versus chemotherapy alone for superficial bladder cancer," *The Journal of Urology*, vol. 155, no. 4, pp. 1227-1232, 1996.

[83] A. G. van der Heijden, L. A. Kiemeney, O. N. Gofrit, O. Nativ, A. Sidi, Z. Leib, R. Colombo, R. Naspro, M. Pavone, J. Baniel, F. Hasner, and J. A. Witjes, "Preliminary european results of local microwave hyperthermia and chemotherapy treatment in intermediate or high risk superficial transitional cell carcinoma of the bladder," *European Urology*, vol. 46, no. 1, pp. 65 72, 2004.

[84] R. J. M. Lammers, J. A. Witjes, B. A. Inman, I. Leibovitch, M. Laufer, O. Nativ, and R. Colombo, "The role of a combined regimen with intravesical chemotherapy and hyperthermia in the management of non-muscle-invasive bladder cancer: a systematic review," *European Urology*, vol. 60, no. 1, pp. 81-93, July 2011.

[85] H. I. Robins, W. H. Dennis, R. A. Steeves, and P. M. Sondel, "A proposal for the addition of hyperthermia to treatment regimens for acute and chronic leukemia," *Journal of Clinical Oncology*, vol. 2, no. 9, pp. 1050-1056, 1984.

[86] P. K. Sneed, P.R. Stauffer, M. W. McDermott, C. J. Diederich, K. R. Lamborn, M. D. Prados, S. Chang, K. A. Weaver, L. Spry, M. K. Malec, S. A. Lamb, B. Voss, R. L. Davis, W. M. Wara, D. A. Larson, T. L. Phillips, and P. H. Gutin, "Survival benefit of hyperthermia in a prospective randomized trial of brachytherapy boost hyperthermia for glioblastoma multiforme," *International Journal of Radiation Oncology*Biology*Physics*, vol. 40, no. 2, pp. 287-295, 1998.

[87] Y. Kinashi, S. I. Masunaga, M. Suzuki, K. Ono, T. Ohnishi, "Hyperthermia enhances thermal-neutron–induced cell death of human glioblastoma cell lines at low concentrations of 10b," *International Journal of Radiation Oncology*Biology*Physics*, vol. 40, no. 5, pp. 1185-1192, 1998.

[88] E. L. Jones, L. R Prosnitz, M. W Dewhirst, P. K. Marcom, P. H. Hardenbergh, L. B. Marks, and D. M. Brizel, "Tumor oxygenation during concurrent hyperthermia, taxol, and radiation therapy for locally advanced breast cancer," *International Journal of Radiation Oncology*Biology*Physics*, vol. 48, no. 3, Supplement 1, p. 197, 2000.

[89] Z. Vujaskovic, J. M. Poulson, K. L. Blackwell, E. L. Jones, E. L. Rosen, T.V. Samulski, D. M. Brizel, M. W. Dewhirst, and L. R. Prosnitz, "Neoadjuvant chemotherapy and hyperthermia improve tumor reoxygenation in patients with locally advanced breast carcinoma," *International Journal of Radiation Oncology*Biology*Physics*, vol. 54, no. 2, p. 218, 2002.

[90] T. Feyerabend, G. J. Wiedemann, B. Jager, H. Vesely, B. Mahlmann, and E. Richter, "Local hyperthermia, radiation, and chemotherapy in recurrent breast cancer is feasible and effective except for inflammatory disease," *International Journal of Radiation Oncology*Biology*Physics*, vol. 49, no. 5, pp. 1317-1325, 2001.

[91] Z. Vujaskovic, E. L. Jones, L. R. Prosnitz, P. K. Marcom, P. H. Hardenbergh, L. B. Marks, T. V. Samulski, D. M. Brizel, M. W. Dewhirst, "Concurrent chemotherapy, hyperthermia and radiotherapy improve reoxygenation in locally advanced breast cancer," *International Journal of Radiation Oncology*Biology*Physics*, vol. 57, no. 2, p. S357, 2003.

[92] D. S. Yoo, Z. Vujaskovic, L. R. Prosnitz, L. B. Marks, K. L. Blackwell, M. W. Dewhirst, and E. L. Jones, "2026: Hyperthermia augments local response to doxil chemotherapy in breast cancer patients," *International Journal of Radiation Oncology*Biology*Physics*, vol. 66, no. 3, pp. S223-S224, 2006.

[93] T. M. Zagar, K. Higgins, M. Edward, Z. Vujaskovic, M. Dewhirst, R. Clough, and E. Jones, "Long-term palliation of breast cancer chestwall recurrence with radiation therapy, hyperthermia, and chemotherapy," *International Journal of Radiation Oncology*Biology*Physics*, vol. 75, no. 3, p. S505, 2009.

[94] M. Sherar, F. Liu, M. Pintilie, W. Levin, J. Hunt, R. Hill, J. Hand, C. Vernon, G. van Rhoon, J. van der Zee, D. G. Gonzalez, J. van Dijk, J. Whaley, and D. Machin, "Relationship between thermal dose and outcome in thermoradiotherapy treatments for superficial recurrences of breast cancer: Data from a phase III trial," *International Journal of Radiation Oncology*Biology*Physics*, vol. 39, no. 2, pp. 371-380, 1997.

[95] E. Jones, D. Brizel, M. Dewhirst, A. Alvarez, A. Berchuck, D. Clarke-Pearson, G. Rodriquez, J. Soper, and L. Prosnitz, "Phase I/II results using concurrent hyperthermia, radiotherapy, and chemotherapy for cervix cancer," *International Journal of Radiation Oncology*Biology*Physics*, vol. 51, no. 3, Supplement 1, pp. 63-64, Nov. 2001.

[96] M. Franckena, L. J. A. Stalpers, P. C. M. Koper, R. G. J. Wiggenraad, W. J. Hoogenraad, J. D. P. van Dijk, C. C. Warlam-Rodenhuis, J. J. Jobsen, G. C. van Rhoon, and J. van der Zee, "Long-term improvement in treatment outcome after radiotherapy and hyperthermia in locoregionally advanced cervix cancer: an update of the dutch deep hyperthermia trial," *International Journal of Radiation Oncology*Biology*Physics*, vol. 70, no. 4, pp. 1176- 1182, 2008.

[97] E. S. Correa, M. T. A. Steiner, A. A. Freitas, and C. Carnieri, "A genetic algorithm for solving a capacitated p-median problem," *Numerical Algorithms*, vol. 35, pp. 373-388, 2004.

[98] N. Mladenovic, J. Brimberg, P. Hansen, and J. A. Moreno-Perez, "The p-median problem: Survey of metaheuristic approaches*," European Journal of Operational Research*, vol. 179, pp. 927-939, 2007.

[99] N. M. Razali, J. Geraghty, "Genetic algorithm performance with different selection strategies in solving TSP," *Proceedings of the World Congress on Engineering (WCE)*, vol. 2, 2011.

[100] M. Asili, R. Green, S. Seran, E. Topsakal, "A Small implantable antenna for MedRadio and ISM bands," IEEE *Antennas and Wireless Propagation Letters*, vol.11, no., pp.1683-1685, 2012.

[101] R. L. Haupt, "Using MATLAB to control commercial computational electromagnetics software," *ACES Journal*, vol. 23, no. 1, 2008.

[102] R. L. Haupt, "Antenna design with a mixed integer genetic algorithm," *IEEE Transactions on Antennas and Propagation*, vol. 55, no. 3, pp. 577-582, 2007.

[103] http://www.albahyperthermia.com/

[104] "Diagram of RFA procedure," [online]. Available: http://www.upmc.com/services/liver-cancer/treatments/radiofrequency/pages/rfa-images.aspx

[105] R.L. Haupt, "An Introduction to Genetic Algorithms for Electromagnetics," *IEEE Antennas and Propagation Magazine*, vol. 37, no. 2, Apr. 1995.

[106] D.S. Weile and E. Michielssen, "Genetic Algorithm Optimization Applied to Electromagnetics: A Review," *IEEE Transactions on Antennas and Propagation*, vol. 45, no. 3, pp. 343-353, Mar. 1997.

[107] J.M. Johnson and Y. Rahmat-Samii, "Genetic Algorithms in Engineering Electromagnetics," *IEEE Antennas and Propagation Magazine*, vol. 39, no. 4, Aug. 1997.

[108] T. Karacolak, A.Z. Hood, and E. Topsakal, "Design of a dual-band implantable antenna and development of skin mimicking gels for continuous glucose monitoring," *IEEE Transactions on Microwave Theory and Techniques,* vol.56, no.4, pp.1001-1008, April 2008.

[109] T. Karacolak and E. Topsakal, "Electrical properties of nude rat skin and design of implantable antennas for wireless data telemetry," *2008 IEEE MTT-S International Microwave Symposium Digest*, pp. 907-910, 15-20 June 2008.

[110] T. Yilmaz, T. Karacolak, and E. Topsakal, "Characterization and testing of a skin mimicking material for implantable antennas operating at ISM band (2.4 GHz-2.48 GHz)," *IEEE Antennas and Wireless Propagation Letters,* vol.7, pp.418-420, 2008.

[111] H. J. Visser, "Array and phased array antenna basics," John Wiley and Sons, New York, 2006.

[112] W. Hobbins, "Thermal assessment of breast health," *MTP Press Ltd. Lancaster*, pp. 40, June 1983.

[113] M. Gauthier et al., "Long term assessment of breast cancer risk by liquid crystal thermal imaging," *Biomedical Thermology, Alan R. Liss Inc.*, pp. 279-301, New York , NY, 1982

[114] M. Gauthier M., "Temperature and blood flow patterns in breast cancer during natural evolution and following radiotherapy," *Biomedical Thermology, Alan R. Liss Inc.*, New York, NY pp. 21-64, 1982.

[115] T. Love, "Thermography as an indicator of blood perfusion. school of aerospace, mechanical and nuclear engineering," *Annals New York Academy of Science*, University of Oklahoma, pp 429-437, 1980.

[116] J. DeLarve, J. Mignot, T. Caulet, "Modifications vasculaires de la poche jugal du hamster dore au cours de greffes melanique," *CR Seances Soc Biol Paris*, vol. 157, pp. 69, 1963.

[117] R. L. Kane, "Considerations in the application of various cooling methods during breast thermography stress studies," *International Academy of Clinical Thermology*, 2002.

[118] W. Hobbins, "The initial," *Wisconsin Breast Cancer Detection Foundation*, vol. 7, pp. 158-161, 1986.

[119] E. Ring, "Thermal assessment of breast health," *MTP Press Ltd. Lancaster*, pp. 32, 1983.

[120] Z. Michalewicz, “Genetic algorithms + data structures = evolution programs,” *Springer*, 3rd edition, New York, 1996.

[121] A. C. Balanis, “Antenna theory: analysis and design,” *John Wiley*, NJ, 2005.

[122] Z. Ji and C. L. Brace, “Expanding modeling of temperature-dependent dielectric properties for MW thermal ablation,” *Phys Med Biol*, vol. 16, no. 52, pp. 5249 – 5264, 2011.

[123] C. L. Brace, “Radiofrequency and microwave ablation of the liver, lung, kidney and bone: what are the differences?” *Curr. Probl. Diagn. Radiol.*, vol.38, pp. 135-143, May 2009.